NUREG/CR-3148
BNL-NUREG-51645

INDEPENDENT ASSESSMENT OF TRAC-PD2 AND RELAP5/MOD1 CODES AT BNL IN FY 1981

P. Saha, J.H. Jo, L. Neymotin,
U.S. Rohatgi, and G. Slovik

Date Published: December 1982

DEPARTMENT OF NUCLEAR ENERGY, BROOKHAVEN NATIONAL LABORATORY
UPTON, LONG ISLAND, NEW YORK 11973

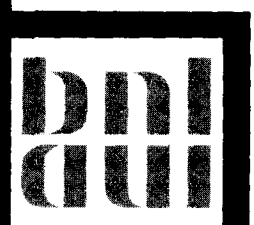

Prepared for
U.S. Nuclear Regulatory Commission
Washington, D.C. 20555

DISCLAIMER

NUREG/CR-3148
BNL-NUREG-51645
AN, R-4

NUREG/CR--3148

DE83 013653

INDEPENDENT ASSESSMENT OF TRAC-PD2 AND RELAP5/MOD1 CODES AT BNL IN FY 1981

P. Saha, J.H. Jo, L. Neymotin
U.S. Rohatgi, and G. Slovik

Manuscript Completed - November 1982
Date Published - December 1982

LWR CODE ASSESSMENT AND APPLICATION GROUP
DEPARTMENT OF NUCLEAR ENERGY
BROOKHAVEN NATIONAL LABORATORY
UPTON, LONG ISLAND, NEW YORK 11973

PREPARED FOR
U.S. NUCLEAR REGULATORY COMMISSION
WASHINGTON, D.C. 20555
UNDER INTERAGENCY AGREEMENT DE-AC02-76CH00016
NRC FIN A-3215

EDB

Available from
GPO Sales Program
Division of Technical Information and Document Control
U.S. Nuclear Regulatory Commission
Washington, D.C. 20555
and
National Technical Information Service
Springfield, Virginia 22161

ABSTRACT

This report documents the independent assessment calculations performed with the TRAC-PD2 and RELAP5/MOD1 codes at Brookhaven National Laboratory (BNL) during Fiscal Year 1981. A large variety of separate-effects experiments dealing with (i) steady-state and transient critical flow, (ii) level swell, (iii) flooding and entrainment, (iv) steady-state flow boiling, (v) integral economizer once-through steam-generator (IEOTSG) performance, (vi) bottom reflood and (vii) two-dimensional phase separation of two-phase mixtures were simulated with TRAC-PD2. In addition, the early part of an overcooling transient which occurred at the Rancho Seco nuclear power plant on March 20, 1978 was also computed with an updated version of TRAC-PD2.

Three separate-effects tests dealing with (i) transient critical flow, (ii) steady-state flow boiling, and (iii) IEOTSG performance were also simulated with RELAP5/MOD1 code.

Comparisons between the code predictions and the test data are presented. A number of areas where further modeling improvements are necessary have been identified for both codes. Several suggestions have also been made to aid the code developers in making further improvements.

EXECUTIVE SUMMARY

A large variety of separate-effects and basic thermohydraulic tests have been simulated at BNL with the TRAC-PD2 code in FY 1981. These include experiments dealing with (i) steady-state and transient critical flow, (ii) level swell during depressurization, (iii) countercurrent flow limitation (CCFL) and entrainment, (iv) flow boiling in a heated rod bundle, (v) internal economizer once-through steam generator (IEOTSG) performance during load changes, (vi) bottom reflood, and (vii) two-dimensional phase separation of two phase mixtures. In addition, the early part of an overcooling transient which occurred at the Rancho Seco nuclear power plant on March 20, 1978 was simulated with an updated version of TRAC-PD2.

In general, TRAC-PD2 behaved more smoothly than its predecessor, namely TRAC-P1A. TRAC-PD2 was able to yield at least a near steady-state solution for several cases where TRAC-P1A had failed to reach a steady-state. The RPI phase separation test with high inlet quality was the only exception. In addition, for the cases where direct comparisons between the TRAC-P1A and TRAC-PD2 predictions were performed, the TRAC-PD2 code generally yielded slightly better results than TRAC-P1A. Therefore, TRAC-PD2 is a definite improvement over the TRAC-P1A code.

The RELAP5/MOD1 (cycle 1) code, on the other hand, received only a limited review at BNL during FY 1981. Experiments dealing with (i) transient critical flow, (ii) flow boiling in a heated rod bundle, and (iii) steam generator (IEOTSG) performance during load change, were simulated with this code. The results were comparable to the TRAC-PD2 results, and no clear technical superiority of either code emerged. The computer running times for the two codes were also comparable. Further assessment of RELAP5/MOD1 is, of course, needed.

The major conclusions drawn from the BNL assessment calculations are listed below. They are arranged according to the phenomenon studied.

a) Critical Flow: TRAC-PD2, in general, underpredicts the critical flow rate when subcooled liquid condition exists upstream of a nozzle or pipe. RELAP5/MOD1 appears to do slightly better in a similar situation.

b) Level Swell: TRAC-PD2 appears to overpredict the rate of level swell during a depressurization. Lack of a flashing delay model, along with a possible higher interfacial shear, seems to be the reason. (RELAP5/MOD1 was not applied to similar situations).

c) CCFL and Entrainment: TRAC-PD2 appears to underpredict the gas velocity at the onset of entrainment and overpredict the entrainment ratio. These cause the gas velocity at the flooding onset to be underpredicted by TRAC-PD2. (RELAP5/MOD1 was not applied to similar situations.)

d) Flow Boiling: The subcooled boiling model of TRAC-PD2 is rather poor. RELAP5/MOD1, on the other hand, does not have any subcooled boiling model at all. The interfacial shear in TRAC-PD2 seems to be adequate for bulk boiling, whereas the same in RELAP5/MOD1 needs further investigation.

e) Steam Generator (IEOTSG) Performance: Both TRAC-PD2 and RELAP5/MOD1 results are highly dependent on nodalization even though they can predict the trend of the data. Also, large magnitude oscillations were observed in the code results. For RELAP5/MOD1, the magnitude of oscillations did not necessarily decrease as a finer nodalization was used.

f) Bottom Reflood: TRAC-PD2 appears to predict the peak cladding temperature quite well. With proper nodalization, the code can be expected to predict the quench front propagation reasonably well at the lower and middle part of a rod bundle. However, it can be expected to predict an earlier quench at the upper part due to enhanced precursory cooling. (RELAP5/MOD1 was not applied to similar situations).

g) 2-D Phase Separation: TRAC-PD2 did not reach a stable solution for some of the RPI 2-D phase separation tests. Even when a stable solution was obtained, the code overpredicted the lateral void migration at the intermediate elevation of the test channel. This may be caused partially by the lack of a turbulent mixing model in TRAC. The code, however, did calculate the observed recirculation pattern. (RELAP5/MOD1 cannot simulate such two-dimensional situations.)

h) Overcooling Transient: TRAC-PD2 is capable of calculating the trend of loss-of-feedwater transient with subsequent overcooling of the primary side in the event of injection of excessive cold feedwater. However, the results should improve with the appropriate modeling of the aspirator and downcomer in a once-through steam generator, finer nodalization and correct relief and safety valve characteristics, etc. (RELAP5/MOD1 was not applied to such transients.)

Based on the above conclusions, the following modeling changes are recommended for future versions of TRAC-PWR:

a) Efforts should continue towards developing and/or implementing an improved critical flow model which will predict the subcooled blowdown rate more accurately. Inclusion of a flashing delay correlation or its equivalent seems to be desirable. The interfacial area, momentum and heat transfer correlations may also need modification.

b) The TRAC-PD2 entrainment model should be replaced by a better model. The model of Ishii and Mishima (1981) should be considered. Also, two liquid fields, one for the film and the other for the droplets, should be considered for the annular-mist flow.

c) The TRAC-PD2 subcooled boiling model should be improved either by reducing the condensation effects or implementing a new model. The model suggested by Saha (1981) may be considered.

d) The numerical algorithm and/or modeling in the TRAC steam generator component should be improved so that the fluctuations in the calculated variables are reduced. The feasibility of inserting finer hydraulic cells within a fixed coarse mesh should be explored. Also, an aspirator model should be included in the once-through steam generator component.

e) Introduction of a turbulent mixing model should be considered. This may improve the code prediction for radial (or lateral) fluid mixing and void dispersion.

Although only a limited assessment of RELAP5/MOD1 has been performed so far, the following recommendations are in order for future versions of RELAP5:

a) RELAP5 should include a subcooled boiling model. The model suggested by Saha (1981) may be considered.

b) The numerical algorithm and/or modeling pertinent to the steam generator thermal performance should be improved so that the numerical oscillations are reduced.

ACKNOWLEDGEMENTS

The authors would like to thank Dr. Fuat Odar of USNRC for his comments and suggestions on the code assessment activity at BNL. Discussions with several LANL and INEL staff members are gratefully acknowledged. Special thanks are to Dr. L. E. Hochreiter of Westinghouse Electric Corporation for providing the detailed data on FLECHT-SEASET reflood experiments, and to Professor G. Birkhoff of Harvard University for reviewing and improving the manuscript. Finally, the fine typing by Mrs. Ann C. Fort is highly appreciated.

TABLE OF CONTENTS

TABLE OF CONTENTS (CONTD)

TABLE OF CONTENTS (CONTD)

TABLE OF CONTENTS (CONTD)

LIST OF TABLES

LIST OF FIGURES

LIST OF FIGURES (CONTD)

LIST OF FIGURES (CONTD)

LIST OF FIGURES (CONTD)

LIST OF FIGURES (CONTD)

LIST OF FIGURES (CONTD)

1. INTRODUCTION

1.1 Background

TRAC and RELAP5 are the two best-estimate, advanced systems codes that are being developed under the sponsorship of the U. S. Nuclear Regulatory Commission (USNRC) for analyzing various accidents and transients in the Light Water Reactor (LWR) systems. TRAC for the Pressurized Water Reactors (PWRs) is being developed at the Los Alamos National Laboratory (LANL) whereas the same for the Boiling Water Reactors (BWRs) is being developed at the Idaho National Engineering Laboratory (INEL). INEL is also responsible for developing the RELAP5 code.

It was decided by the USNRC that after a code is released, it should go through an independent assessment by groups not involved in its development or developmental assessment. Such an effort began with the TRAC-P1A code released by LANL in March, 1979. A summary of the TRAC-P1A independent assessment results can be found in the NRC Research Information Letter No. 115 (Minogue, 1981).

TRAC-PD2 was the next released version of the TRAC-PWR series of codes, and the independent assessment of this code began in November, 1980. The RELAP5/ MOD1 code was also released in November, 1980. However, the independent assessment effort for this code is not yet as extensive as that for TRAC.

Brookhaven National Laboratory (BNL) is involved in the independent assessment of both TRAC-PD2 and RELAP5/MOD1. Emphasis at BNL is to assess the basic thermohydraulic models that are used in these codes. With this in mind, several basic and separate-effects tests have been simulated in FY 1981 with the TRAC-PD2 and RELAP5/MOD1 codes. Table 1.1 shows the experiments simulated, the code used and the thermal-hydraulic effects assessed. The main purpose of this report is to present the results of these calculations, compare them with the experimental data, and to indicate the areas where further improvements are needed.

1.2 Brief Description of TRAC-PD2 and RELAP5/MOD1

Detailed description of the TRAC-PD2 and RELAP5/MOD1 codes can be found in the respective code documentations (Liles, 1981 and Ransom, 1980). However, a few words on these codes may help to better understand the assessment calculations that follow this introduction.

1.2.1 TRAC-PD2

It was mentioned earlier that the TRAC-PD2 code was developed at LANL to calculate the thermal-hydraulic responses in the Pressurized Water Reactors (PWRs) for various accident and transient conditions. The code has several modules, namely VESSEL, PIPE, TEE, PRESSURIZER, STEAM GENERATOR, PUMP, VALVE, etc. to represent various components in a PWR system. By suitably connecting these modules, one may model a reactor system or a wide spectrum of test facilities ranging from LOFT to a simple round tube test section. There are two special components, namely BREAK and FILL which are used to provide the boundary conditions. In addition, models for structural heat transfer and point-reactor kinetics are included in the code.

TABLE 1.1 BNL Independent Assessment Matrix for FY 1981

Experiment	Code Used		Phenomena Studied
	TRAC-PD2	RELAP5/MOD1	
1. Moby-Dick Steam-Water Tests (Run Nos 401, 406 455)	X		1-D steady-state critical flow.
2. BNL Nozzle tests (Run Nos. 291, 309, 318, and 339)	X		Same as above.
3. Super-CANON Blowdown test	X		1-D transient critical flow.
4. Marviken Critical Flow Tests (Run No. 24)	X	X	Large scale 1-D transient critical flow for small length-to-diameter ratio.
5. Battelle-Frankfurt Top Blowdown Experiment (Test SWR-2R)	X		Level swell and 1-D transient critical flow.
6. University of Houston Flooding Experiment	X		Basic countercurrent flow limitation in a a vertical round tube.
7. FRIGG-Loop Tests			
Run No. 313020	X	X	Steady-state axial void distribution in a heated rod bundle.
Run No. 313007	X		
8. B&W Steam Generator Tests			Performance of integral economizer once-through steam generator during load change.
Series 68,69,70	X		
Series 74,75,76	X	X	

TABLE 1.1 (Cont'd)

Experiment	Code Used		Phenomena Studied
	TRAC-PD2	RELAP5/MOD1	
9. FLECHT-SEASET Reflood Experiment Run No. 31504	X		Heat transfer and quench front propagation during bottom reflood.
10. RPI (1 x 3) Phase-Separation Experiment	X		Lateral void migration and phase separation for air/water flow in a 2-D rectangular channel.
11. Rancho Seco Overcooling Transient of March 1978	X		Transient response of the B&W plant to a feedwater trip and subsequent injection of HPI and auxiliary feedwater.

NOTE: Simulation of BCL downcomer tests with the TRAC-PD2 code began in FY 1981, but continued in FY 1982. Results of these calculations are presented in a separate report.

The VESSEL module represents the reactor vessel of a PWR. By suitable partitioning and nodalization, one can model the upper and lower plena, the downcomer and the core within this module. The module is based on a six-equation, two-fluid, three-dimensional formulation of two-phase flow. Conservation of mass and energy for the two-phase mixture and the vapor phase are employed. Also, two phasic equations of motion, one for the liquid and the other for the vapor, are used. These two equations are then resolved into three co-ordinates, namely the axial, radial and azimuthal, to calculate the phasic velocities in three directions. Furthermore, many constitutive relations for the interfacial and wall-to-fluid momentum and heat transfer are needed and used to close the formulation. These constitutive relations play a major role in the code predictions, and the assessment activities at BNL are directed at verifying their adequacy or reliability in various situations pertinent to the LWR safety.

Although the VESSEL module is based on a three-dimensional formulation, one may degenerate it into a one- or two-dimensional module by proper choice of an input parameter. The formulation is, of course, still based on a two-fluid model. This approach was used for the calculation of the Battelle-Frankfurt top blowdown test, University of Houston flooding tests, FRIGG-loop tests, FLECHT-SEASET reflood test and the RPI phase separation tests.

All the other TRAC-PD2 modules are based on a one-dimensional, five-equation, drift-flux formulation of two-phase flow. Like the VESSEL module, these components also use the conservation of mass and energy for the mixture and the vapor phase. However, they use only one equation of motion for the center of mass of the mixture. Therefore, a constitutive relation for the relative velocity between the phases is specified to determine the two phasic velocities. Furthermore, as in the two-fluid model, constitutive relations for the interfacial heat and mass transfer and the wall-to-fluid heat and momentum transfer are added to close the formulation. It should be stressed that all the components of TRAC are based on nonhomogeneous and nonequilibrium formulation of two-phase flow. In addition, since TRAC uses two energy equations, it does not restrict either phase at saturation.

1.2.2 RELAP5/MOD1

This code was developed at the Idaho National Engineering Laboratory (INEL) with the objective of producing an economic and user-convenient computer code for best-estimate analyses of the light water reactor accidents and transients. The code includes component models for pipes, branches, abrupt flow area changes, pumps, valves, control systems, etc. to represent a reactor system or a test facility. Special components such as time-dependent volumes and time-dependent junctions are used to provide boundary conditions. Heat structures are available to model heat transfer to or from the fluid. The code also includes a point-reactor kinetics model with reactivity feedback.

The basic hydrodynamic model is based on a one-dimensional, five-equation, two-fluid formulation of two-phase flow. It consists of two phasic conservation of mass equations, two phasic conservation of momentum equations, and one

mixture energy equation. Since only one energy equation is used, an additional specification regarding one-phase (liquid or vapor) being at the local saturation temperature has to be made. Furthermore, constitutive relations for the nonequilibrium phase change rate, interfacial momentum transfer, and the correlations for wall friction and wall heat transfer are needed to close the formulation. As such, RELAP5 is based on a nonhomogeneous and nonequilibrium (at least, partial) description of two-phase flow. However, it does not have a three-dimensional capability as available in TRAC.

It is worth mentioning that RELAP5 has a separate choking model so that a fine nodalization is not required near a break, which reduces the computer running time. TRAC-PD2, however, relies on the natural choking (or self-choking), and usually requires a fine nodalization near the break. There are many other differences between these two codes, and some of them will be discussed during the description of the RELAP5 assessment calculations.

1.3 Report Outline

The TRAC-PD2 assessment calculations are described in Chapter 2. They are discussed in the order shown in Table 1.1. Notice that the experiments simulated range from very basic air-water tests (e.g., Univerisity of Houston flooding tests) to more involved separate-effects tests such as FLECHT-SEASET reflood experiments. In addition, an actual primary side overcooling incident that occurred in the Rancho Seco Power Plant was calculated with an updated version of TRAC-PD2.

The RELAP5/MOD1 assessment calculations are presented in Chapter 3. Only three experiments as indicated in Table 1.1 have been simulated with RELAP5. However, the same experiments were also simulated with TRAC-PD2. Thus, some quantitative comparisons between these two code predictions are available in Chapter 3.

The assessment results are summarized and the conclusions are drawn in Chapter 4. Finally, the recommendations for further improvements are presented in Chapter 5.

2. TRAC-PD2 ASSESSMENT CALCULATIONS

This chapter presents the TRAC-PD2 assessment calculations performed at BNL during FY 1981. TRAC calculations for each series of experiments are discussed separately and each presentation includes: (i) Objective, (ii) Test description, (iii) TRAC input model description, (iv) Code prediction and comparison with data, (v) Discussion, and (vi) Conclusions.

2.1 Moby-Dick Steam-Water Experiment

2.1.1 Objective

Moby-Dick steam-water experiment (Reocreux, 1977) was simulated with TRAC-PD2 to determine the code's capability in predicting the steady-state steam-water critical flow rate through a pipe or nozzle. Accurate prediction of critical flow rate is of great importance for the best-estimate analyses of large and small break LOCAs in LWRs.

Since the code does not have a separate choking model and it relies on the natural choking through the solution of the basic hydrodynamic equations, the predicted critical flow rate depends significantly on the thermal-hydraulic models used in the code. Thus, the combined effects of the wall friction, slip (or relative velocity) and the nonequilibrium vapor generation on the critical flow rate can be evaluated through the following calculations.

2.1.2 Test Description

Steady-state steam-water critical flow tests at low pressures ($p < 3$ bar) were conducted in the Moby-Dick loop at Grenoble (Reocreux, 1977). Experiments were run in glass as well as metallic channel. Only the tests conducted in the metallic channel are considered here since the vapor nucleation characteristic in the glass test section could be very different from that in the prototypic reactor system.

The metallic test section had three parts. The first part was a vertical round tube with 0.02m inside diameter and approximately 2.4m long. This was followed by a 7° diverging nozzle 0.327m long. The final section was another round tube with 0.06m inside diameter and approximately 0.2m long. Subcooled water entered at the bottom of the test section and flowed upwards. As the pressure dropped, flashing began and a two-phase mixture flowed through the remainder of the test section. The vapor was condensed in the exit tank by spraying cold water and the water from the exit tank was pumped back to the test section entrance.

Experimental measurements included the axial pressure and the diametrical void fraction distribution in the test section. However, the accuracy of these measurements could not be found in the test documentation (Reocreux, 1977). In addition, the pressure, temperature and the water flow rate at the test section inlet and the pressure and temperature at the exit tank were measured. The water flow rate was measured with an accuracy of $\pm$ 1%.

.Run Nos. 401, 406 and 455 were simulated with TRAC-PD2. For the first two runs, i.e., 401 and 406, the critical or throat pressure was approximately 1.5 bar, inlet water temperature was approximately 116°C and the mass-fluxes at the throat were approximately 6500kg/m^2s and 8700 kg/m^2s, respectively. For the last run, i.e., Run 455, the critical pressure was 2 bar, inlet water temperature was 125°C, and the mass-flux at the throat was approximately 10,300 kg/m^2s. These three tests effectively represent the range of the Moby-Dick steam-water experiments, although over a hundred tests were conducted

2.1.3 TRAC Input Model Description

Figure 2.1.1 illustrates the nodalization for the entire test section which was modeled by a PIPE component. After a nodalization study, 50 cells were used for the best-estimate calculations. As shown in Figure 2.1.1, cells with different lengths were employed with greater resolution in the throat area. Two BREAK components, one at the entrance and the other at the exit of the test section, were used to impose the boundary conditions. The center of the inlet BREAK component coincided with the pressure tap A and the experimental values of pressure and water temperature were specified. The center of the exit BREAK component coincided with the tap number 35, and the experimental value of pressure was specified. The nodalization shown in Figure 2.1.1 was used for Runs 401 and 406. However, for Run 455, the pressure recorded at Tap A was in error (Reocreux, 1977). Therefore, for the TRAC calculation, the test section was shortened to make the center of the inlet BREAK component coincide with the pressure tap B.

The official version of TRAC-PD2 (Version 26.0) was used to reach a steady-state for each test run. Both the homogeneous (NFF = 1) and the annular (NFF = 4) wall friction factor options were used for Run 401 to study the sensitivity of the predicted mass flow rate to the friction factor options still available in TRAC-PD2. However, only the annular friction factor option (NFF = 4) was used for Runs 406 and 455. No additive loss coefficient was used in any calculations. These calculations took 130 to 350 CPU seconds in the BNL CDC-7600 for 2 seconds of problem time before an approximate steady-state was reached.

2.1.4 Code Prediction and Comparison with Data

The code predictions of the simulated tests are shown in Figures 2.1.2 through 2.1.4 and are summarized in Table 2.1.1.

Although Figure 2.1.2 shows that TRAC-PD2 does not yield an exact steady state for these tests, it predicts a considerably more stable behavior than the TRAC-P1A code which produced large amplitude oscillations in the outlet flow rate for a similar experiment (Saha, 1979). Ignoring the small amplitude fluctuations in the flow variables, one can now compare the TRAC-PD2 predictions with the tests.

The predicted mass flow rates for the three runs are presented in Figure 2.1.2. The predictions with the annular friction factor option are lower than the experimental flow rates by 39, 29 and 33 percent for Runs 401, 406 and 455, respectively.

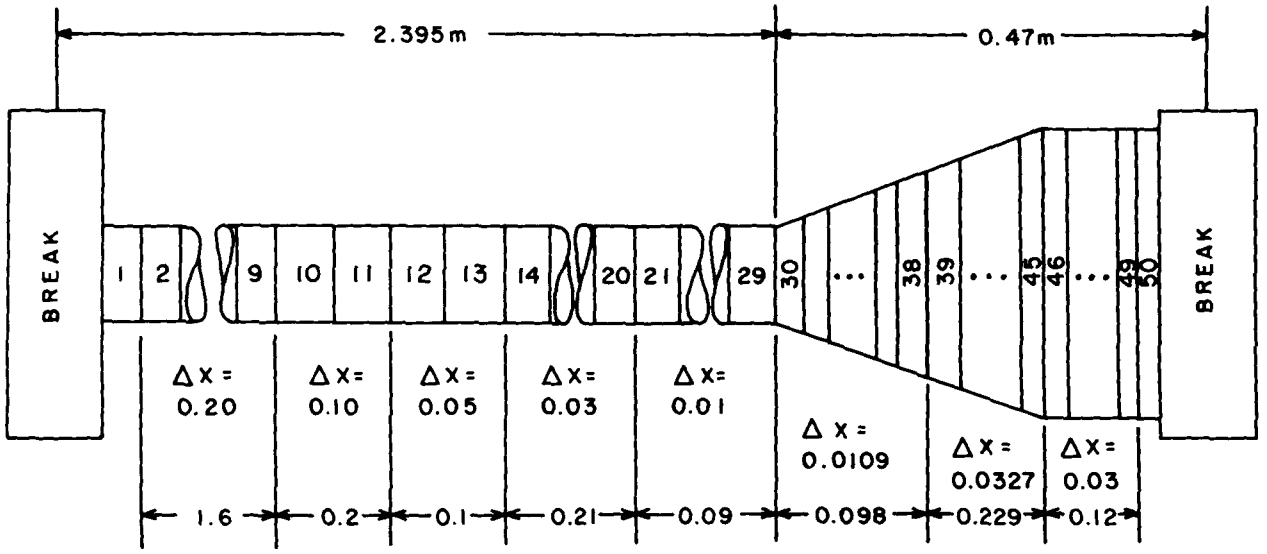

Figure 2.1.1 TRAC Noding For The Moby-Dick Test Section (BNL Neg. No. 2-891-82).

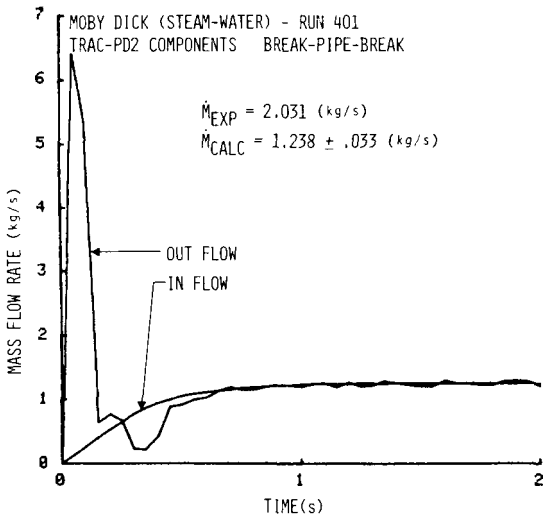

(a)

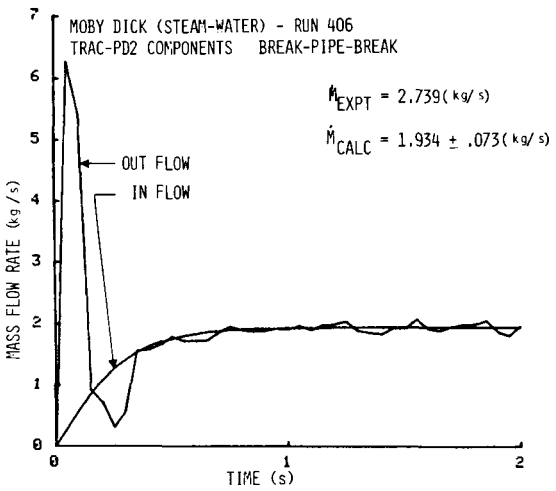

(b)

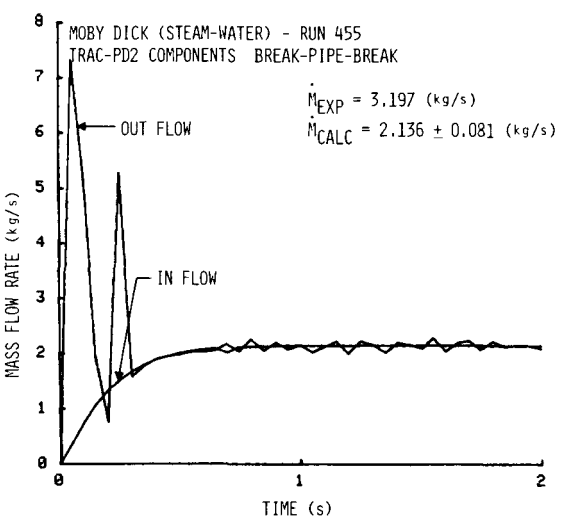

(c)

Figure 2.1.2 TRAC-PD2 Prediction of the Mass Flow Rate for Moby-Dick Run: a) 401, b) 406, c) 455 (BNL Neg. Nos. 5-228-81, 5-232-81, 5-229,81).

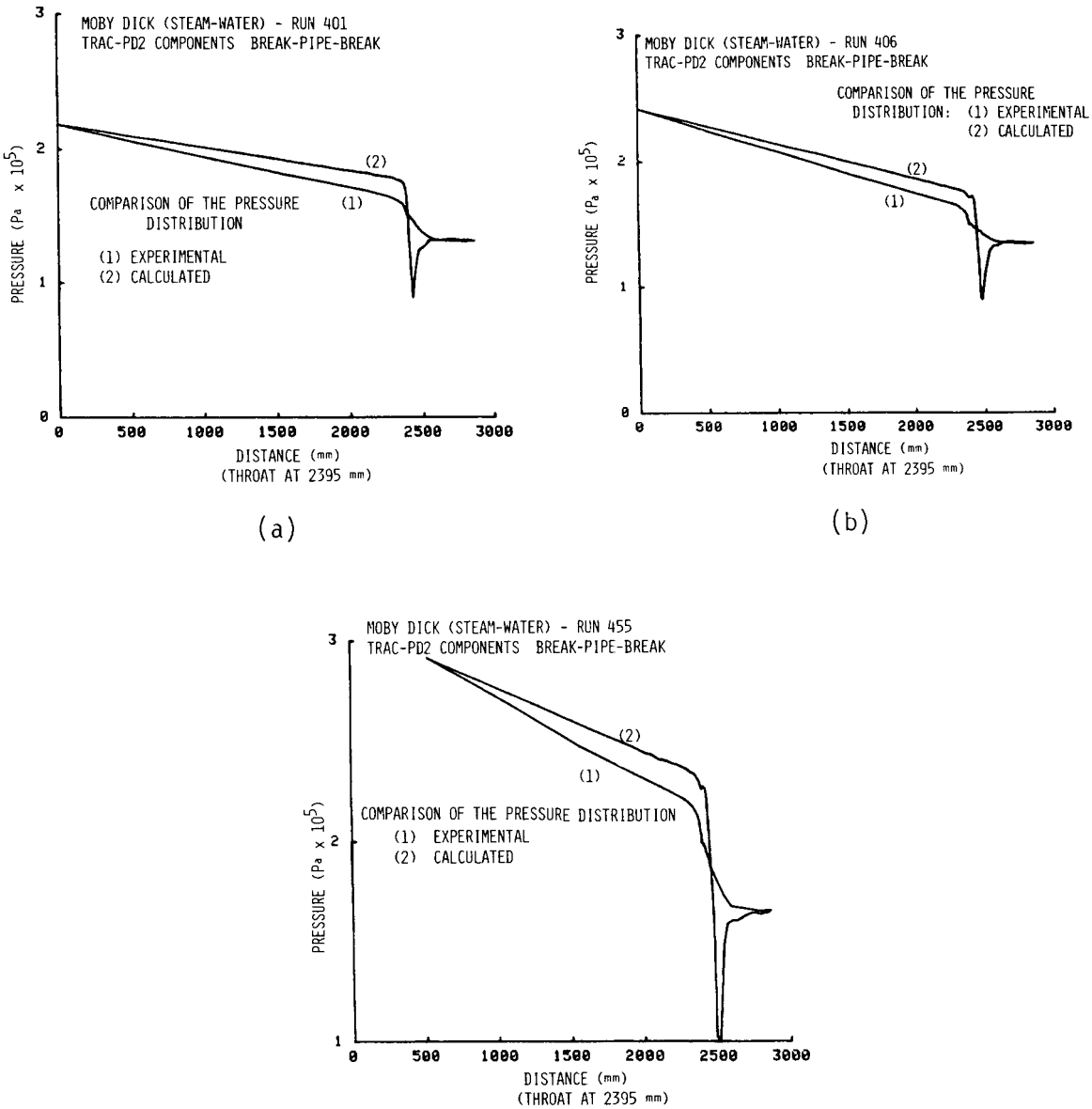

Figure 2.1.3 Comparison Between the Computed and the Measured Pressure Distribution for Moby-Dick Run: a) 401, b) 406, c) 455 (BNL Neg. Nos. 5-203-81, 5-234-81, 5-233-81).

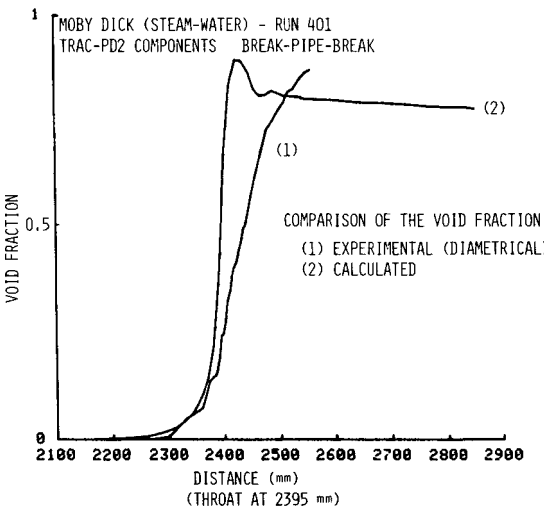

(a)

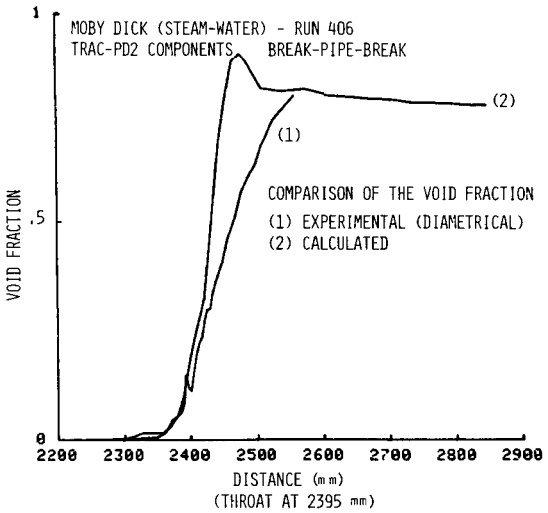

(b)

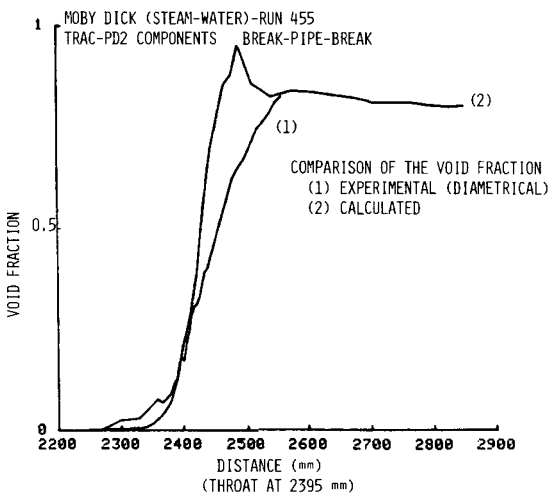

(c)

Figure 2.1.4 Comparison Between the Computed and the Measured Void Fraction Data for Moby-Dick Run: a) 401, b) 406, c) 455 (BNL Neg. Nos. 5-227-81, 5-231-81, 5-226-81).

Table 2.1.1 Summary of the Moby-Dick Test Simulations With Annular Wall Friction Factor Option

Run No.	Inlet		Exit Pressure (kPa)	Experimental Mass Flow (kg/s)	TRAC-PD2 Mass Flow (kg/s)	Relative Error (%)
	Pressure (kPa)	Temperature (°C)				
401	218.6	116.6	131.8	2.031	1.238±0.033	-39.0±2.0
406	241.9	116.3	134.9	2.739	1.934±0.073	-29.4±3.0
455	291.8	125.1	165.5	3.197	2.136±0.081	-33.2±2.5

The predicted mass flow rate for run 401 with the homogeneous friction factor options is 1.285±0.064 kg/s. This is only 4% higher than that obtained by using the annular flow friction factor, and still 36.7% lower than the experimental value. Moreover, the calculation with the homogeneous friction factor showed more fluctuations than that with the annular flow friction factor option. In view of this, only the annular flow friction factor was used for the other two runs, i.e., Runs 406 and 455. The pressure and void fraction distribution along the length of the test section are compared in Figures 2.1.3 and 2.1.4. Since pressure boundary conditions were imposed, the pressure predictions at the two ends of the test section agree with the data. However, the pressure prediction is rather poor along the length of the test section. This is due to the possible overprediction of the vapor generation rate, as discussed below.

Figure 2.1.4 seems to show that the onset of vapor generation predicted by TRAC-PD2 occurred simultaneously with the data. This similarity is quite accidental. The underprediction of the mass flow rate decreased the calculated pressure drop that caused a delay for the onset of vapor generation. However, the experimental data showed that flashing began in a superheated liquid state (by $\sim$2K) while the code begins flashing approximately at the saturation point. Hence, these two different delays somehow converged at the same location to yield the agreement, as seen in Figure 2.1.4. Also, one may infer from Figure 2.1.4 that the vapor generation rate is much higher in the code than what was found experimentally for all three tests. This overproduction of vapor caused the mass flow rate to be highly underpredicted. It also increased the acceleration pressure drop that caused the pressure dip in Figure 2.1.3. The pressure returned to the correct pressure in all three predictions because it was a boundary condition.

2.1.5 Discussion

Several key parameters calculated by TRAC-PD2 did not demonstrate the physical trends observed in the experiment. The code underpredicted the mass flow rate for all three runs by 25 to 40 percent. This is caused by several factors. First, the vapor generation rate calculated in the code is presumably higher than that in the actual experiment. Secondly, the code does not have a flashing delay model although a liquid superheat of about 2K at the flashing inception was observed in the tests. Finally, the correlations for the relative velocity as used in the PIPE component or the drift-flux formu-

lation may not be valid in the diverging section just downstream of the throat. The code always uses a positive value for the relative velocity, $V_g - V_\ell$ where V_g and V_ℓ are the velocity of the vapor and the liquid phase, respectively. However, it has been shown through a two-fluid model calculation that in the diverging section, V_g could be smaller than V_ℓ (Van der Welle, 1981). Therefore, further model improvements would be needed to obtain a better agreement between the TRAC results and the Moby-Dick steam-water tests.

2.1.6 Conclusions

The following conclusions can be drawn from the simulation of the Moby-Dick steam-water tests:

a) TRAC-PD2 exhibited a more stable behavior than the TRAC-P1A code. TRAC-PD2 almost reached a steady-state whereas TRAC-P1A did not.

b) TRAC-PD2 underpredicted the steady-state critical mass flow rates as measured in the Moby-Dick test facility by 25 to 40%.

c) Significant modeling improvements in the area of interfacial mass and momentum transfer seem to be required to obtain a better agreement with the data. Addition of a flashing delay model should also help.

d) The predicted critical mass flow rates seem to be insensitive to the wall friction factor option. However, as in the TRAC-P1A code, the annular flow friction factor in the TRAC-PD2 code always results in a lower mass flow rate than that obtained with the homogeneous flow friction factor.

2.2 BNL Nozzle Tests

2.2.1 Objective

Since the BNL nozzle tests (Abuaf, 1981) are similar to the Moby-Dick steam-water tests discussed earlier, simulation of these tests complements the assessment objectives presented in Section 2.1.1.

2.2.2 Test Description

Steady-state steam-water flashing tests at low pressures ($p < 7$ bar) were conducted in a vertical converging-diverging nozzle. The test section was made of stainless steel and it was symmetric about the throat. The throat inside diameter was 0.0254 m and the inside diameter at the inlet and outlet of the test section was 0.0508 m. The length of the converging-diverging portion of the test section was approximately 0.57 m. The total angle of convergence and divergence was approximately 5°. Subcooled water entered at the bottom of the test section and flowed upwards. As the pressure dropped, flashing began at or near the throat, and a two-phase mixture flowed through the diverging part of the test section. The vapor was condensed in the exit tank by spraying cold water and the water from the exit tank was pumped back to the test section entrance.

Experimental measurements included the axial pressure and area-averaged void fraction distribution along the test section. In addition, the pressure, temperature and the water flow rate at the test section inlet and the pressure and temperature at the exit tank were measured. The measurement accuracies were:

Temperature:	$\pm$	0.1°C
Pressure:	$\pm$	1% of reading
Flow rate:	$\pm$	0.5% of reading
Void fraction:	$\pm$	0.05

Four tests have been simulated with TRAC-PD2. These are Run Nos. 291-295, 309-311, 318-321 and 339-342. Earlier they were simulated with TRAC-P1A; however, satisfactory agreement between the code calculations and the data were not obtained (Abauf, 1981).

2.2.3 TRAC Input Model Description

Figure 2.2.1 shows the nodalization for the BNL test section which was represented by a 94-cell PIPE component. All the cell lengths were 0.00635 m. The same nodalization was used for the TRAC-P1A calculations. The center of the inlet BREAK component coincided with the pressure tap 1 and the experimental values of pressure and water temperature were supplied as boundary conditions. The center of the exit BREAK component coincided with the pressure tap 49 and the experimental value of pressure was supplied there.

The official version of TRAC-PD2 (Version 26.0) was used to reach a steady-state solution for each of the tests simulated. The homogeneous friction factor option (NFF=1) was used for all the simulations mainly because this option was used for the TRAC-P1A calculations. However, for Run Nos. 339-342, the annular flow friction factor option (NFF=4) was also used for sensitivity study. No additive loss coefficient was used in any calculations. These calculations took 60 to 100 CPU seconds in the BNL CDC-7600 to reach steady-states.

2.2.4 Code Prediction and Comparison with Data

Steady-states were reached for all the test runs attempted. The predicted mass flow rates for both the TRAC-P1A and TRAC-PD2 codes are compared with the experimental values in Table 2.2.1. It can be seen that like TRAC-P1A, the TRAC-PD2 also underpredicts the mass flow rate by a significant amount. Moreover, for Runs Nos. 291-295, the TRAC-PD2 prediction became worse than that of TRAC-P1A.

In general, the use of annular flow friction factor option would lead to a slightly lower value of the predicted mass flow rates. This was confirmed by recalculating the Run Nos. 339 - 342 with the annular flow friction factor option, and the TRAC-PD2 predicted value of the mass flow rate was 7.626 kg/s. This was less than 1% lower than the value (7.69 kg/s) predicted with the homogeneous friction factor option.

Figures 2.2.1 through 2.2.5 depict the pressure and area-averaged void fraction distributions along the length of the test section as predicted by the TRAC-PD2 and TRAC-P1A codes, and the comparisons with the experimental

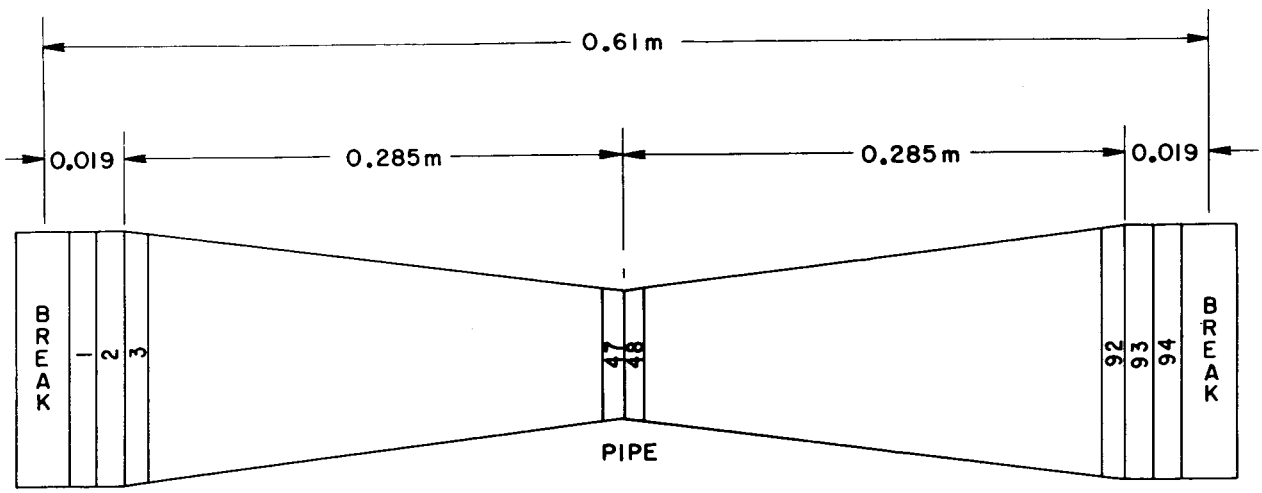

Figure 2.2.1 TRAC Nodalization for the BNL Nozzle. (BNL Neg. No. 9-38-81)

Table 2.2.1 Summary of the BNL Test Simulations with Homogeneous Friction Factor Option.

Nos.	Inlet Pressure (kPa)	Inlet Temp. (°C)	Exit Pressure (kPa)	Experimental Mass Flow Rate (kg/s)	TRAC-P1A		TRAC-PD2	
					Mass Rate (kg/s)	% Error	Mass Rate (kg/s)	% Error
291-295	502	148.9	471	6.43	5.68	-11.7	5.08	-21.0
309-311	556	149.1	397	8.79	7.37	-16.2	7.28	-17.2
318-321	322	121.1	167	8.98	7.56	-15.9	7.79	-13.2
339-342	320	121.3	252	8.97	7.48	-16.6	7.69	-14.3

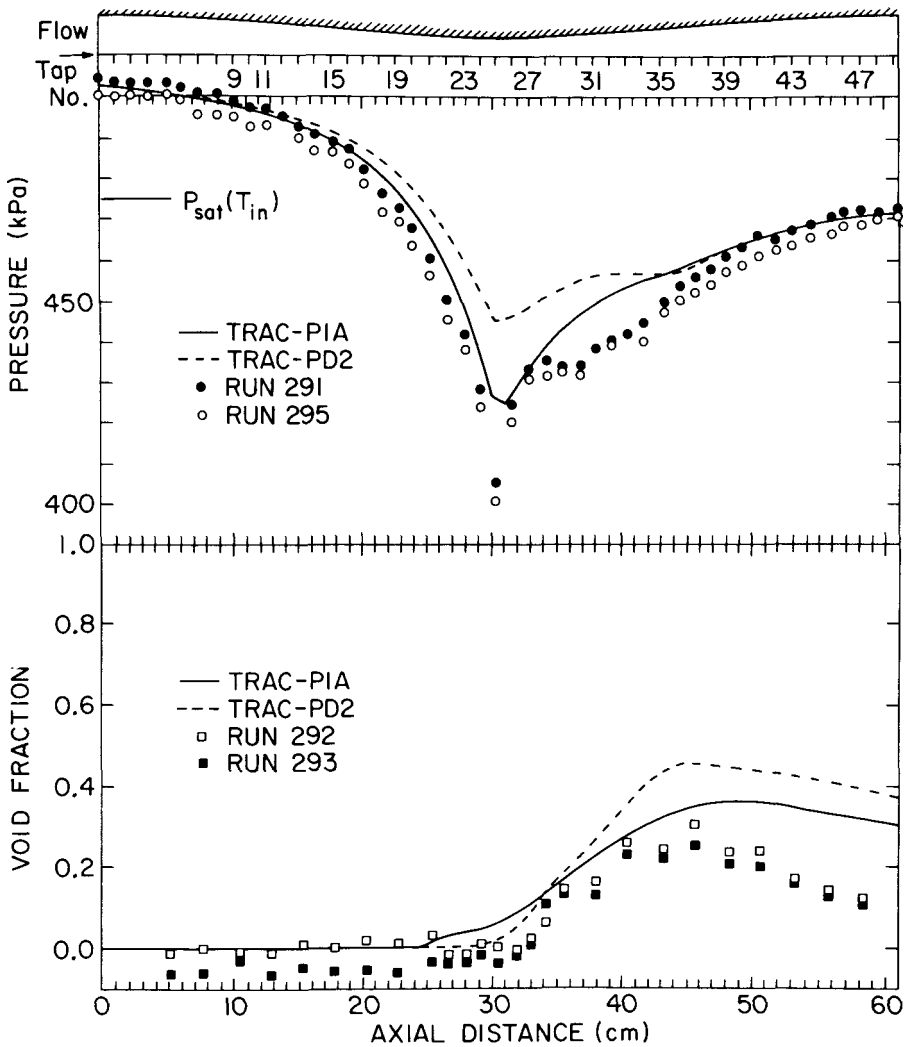

Figure 2.2.2 Comparison Between the TRAC Predictions and the Experimental Data for Run Nos. 291 - 295. (BNL Neg. No. 9-37-81)

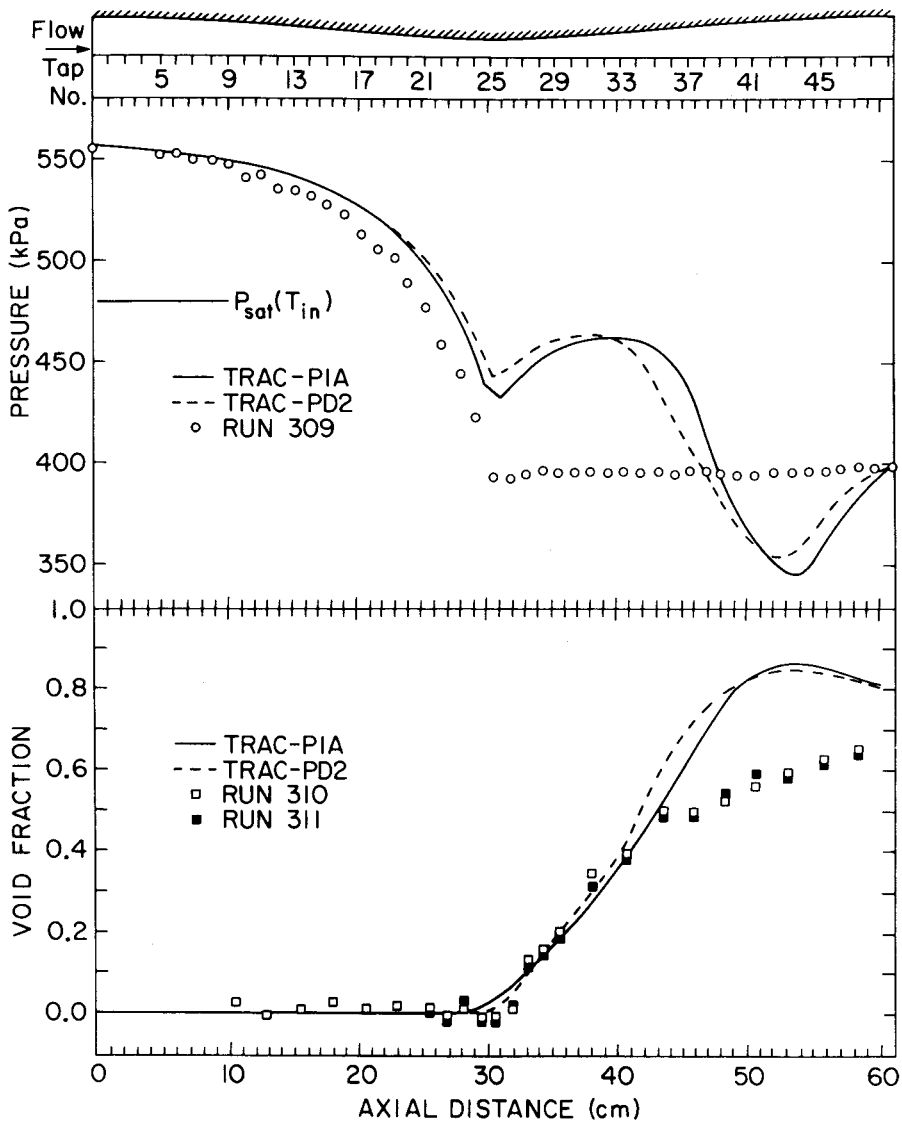

Figure 2.2.3 Comparison Between the TRAC Predictions and the Experimental Data for Run Nos. 309 - 311. (BNL Neg. No. 9-36-81)

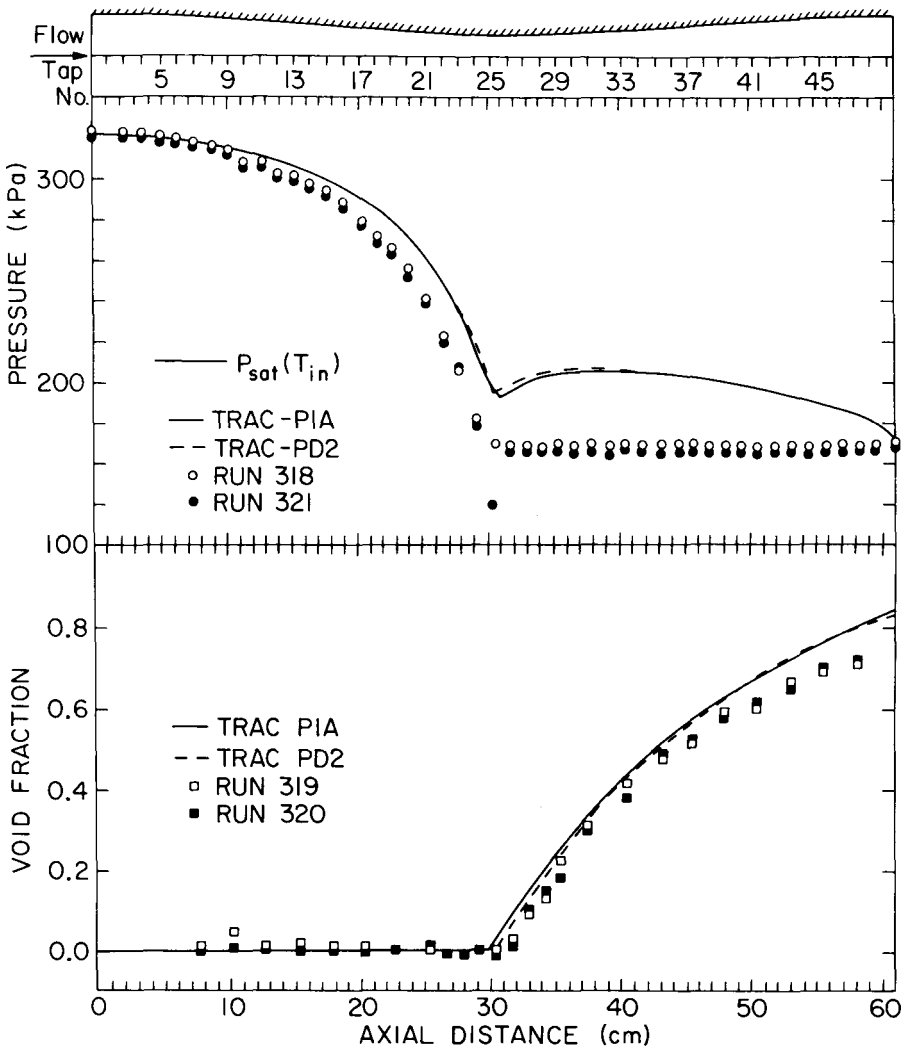

Figure 2.2.4 Comparison Between the TRAC Predictions and the Experimental Data for Run Nos. 318 - 321. (BNL Neg. No. 9-35-81)

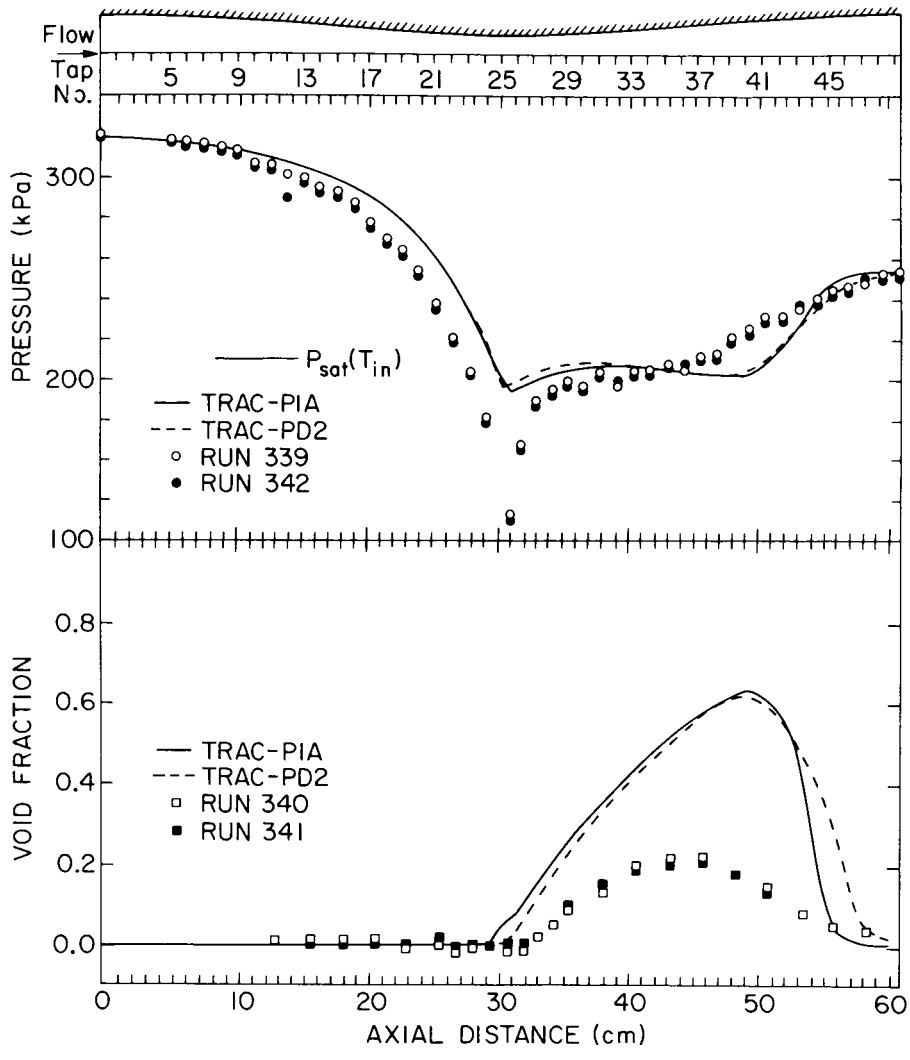

Figure 2.2.5 Comparison Between the TRAC Predictions and the Experimental Data for Run Nos. 339 - 342. (BNL Neg. No. 9-34-81)

data. In general, the predictions for both the pressure and the void fraction are poor. This is to be expected in view of the poor mass flow rate predictions as shown in Table 2.2.1.

A few calculational trends are worth-noting. First, with the exception of Runs 291 - 295, the predictions of the TRAC-PD2 were very close to those of TRAC-P1A. Secondly, the codes overpredicted pressure in the converging section for all runs. This is consistent with the fact that the codes underpredicted the mass flow rates. Thirdly, the predicted void fractions in the diverging section were usually much higher than the data. This presumably caused the mass flow rates to be underpredicted like in the Moby-Dick test simulations discussed in Section 2.1.

2.2.5 Discussion

Simulation of BNL tests with TRAC-PD2 showed results very similar to those obtained for the Moby-Dick steam-water test discussed in Section 2.1. In both cases, the code underpredicted the mass flow rate significantly. The most probable explanation for this anomaly seems to be the overproduction of vapor in the diverging part of the test sections. In addition, the modeling changes (Rohatgi, 1982) that were made in the area of interfacial heat and mass transfer between the TRAC-P1A and TRAC-PD2 codes did not improve the code predictions for this type of experiments. It should be noted that the relative velocity or slip correlations were not changed between TRAC-P1A and TRAC-PD2.

It is clear that further model improvements must be done to achieve better prediction of the BNL and Moby-Dick steam-water tests. The key item seems to be the modeling in the diverging part, i.e., for the decelerating two-phase flow. Since the inertia of each phase is important in such situations, a two-fluid model may be more appropriate than the drift-flux model which uses relative velocity correlations developed from the steady-state two-phase flow in constant area channels. Furthermore, a model for flashing delay should also improve the code predictions. The experiments did show significant amount of liquid superheat (2 - 6°K) at the throat where flashing began.

2.2.6 Conclusions

The following conclusions can be drawn from the simulation of the BNL flashing tests:

a) TRAC-PD2 predictions were very similar to those of the TRAC-P1A code. Both codes underpredicted the mass flow rates by significant amounts. The predictions for pressures and area-averaged void fractions were also poor.

b) The predictions were rather insensitive to the friction factor option. This is to be expected since the frictional pressure drop component was a small fraction of the total pressure drop in the converging-diverging test section.

c) Further model improvements in the area of interfacial mass and momentum transfer, particularly for the decelerating flow, seem to be required to obtain a better agreement with data. Addition of a flashing delay model should also help.

2.3 Super-CANON Blowdown Test

2.3.1 Objective

The Super-CANON blowdown test (Riegel, 1979) was simulated with TRAC-PD2 (Version 26.0) to assess the code's capability to predict the transient critical flow rate from a horizontal pipe, initially filled with high pressure subcooled water. Since the initial pressure was 150 bar, the typical PWR operating pressure, this test may be representative of what could happen during the early stage of a hypothetical PWR loss-of-coolant accident.

2.3.2 Test Description

The test section consisted of a horizontal pipe with 0.1 m inside diameter and 4.389 m long. The pipe was closed at one end and fitted with a rupture disc assembly at the other. By varying the diameter of the rupture disc one could create various break diameters ranging from 0.1 m (full open) to 0.03 m. Initially the pipe was filled with subcooled water at 150 bar. The transient was initiated by rupturing the disc assembly. Pressure and temperature histories were recorded at various stations as shown in Figure 2.3.1. The area-averaged void fraction was also measured at one location, shown in Figure 2.3.1, by using a neutron scattering technique (Rousseau, 1976).

Twelve blowdown tests were conducted. The initial pressure in all tests was 150 bar. However, all combinations of three different initial water temperatures, i.e., 280°C, 300°C, and 320°C, and four different break diameters, i.e., 0.03 m, 0.05 m, 0.07 m and 0.1 m, were tested. In the BNL TRAC-PD2 assessment effort only one test, i.e., the test with full opening (break diameter of 0.1 m) and the initial temperature of 280°C (a subcooling of approximately 62°C) has been calculated. Earlier the same test along with three other tests was computed with the TRAC-P1A code (Saha, 1980).

2.3.3 TRAC Input Model Description

The test section was represented by a PIPE component with 104 cells. Starting from the closed end, there were 84 cells each 0.05 m in length, 18 cells each 0.01 m in length and two 0.0045 m long cells near the open end. A zero-velocity FILL component represented the closed end and a BREAK component with ambient pressure of 1 bar modeled the discharge end. The initial conditions were the same as the experimental values. They were:

Initial pressure:	150 bar
Initial temperature:	280° C
Initial void fraction:	0.0
Initial velocity:	0 m/s

The annular friction factor option (NFF=4) was used mainly because the same option was employed in the TRAC-P1A calculation. In addition, this option results in a slightly lower critical flow rate and provides a slightly better agreement with the data. However, it must be stressed that the wall friction factor option plays a very minor role in this calculation. Also, no additive friction factor was used in any cell. The calculation took 73 CPU seconds in the BNL CDC-7600 for 0.51 second of transient.

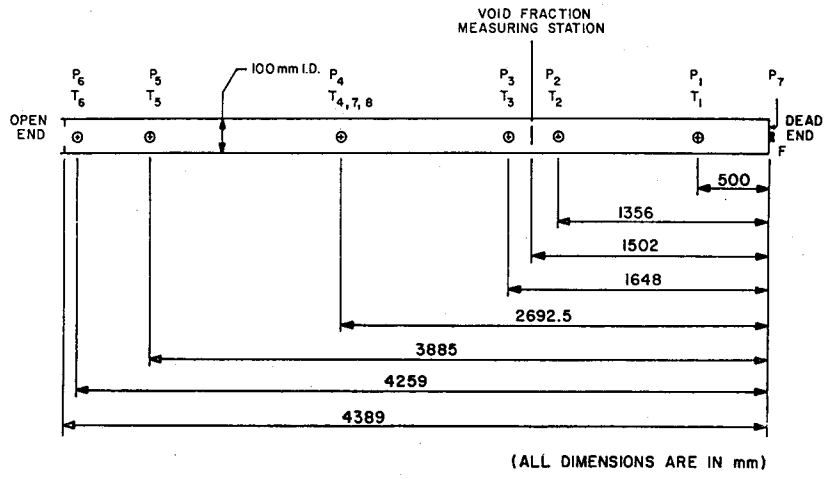

Figure 2.3.1 Schematic of the Super-CANON Test Section. (BNL Neg. No. 9-599-81)

2.3.4 Code Prediction and Comparison with Data

Figure 2.3.2 shows the comparison between the measured and the predicted pressure histories at P3. This location was chosen because it was near the void fraction measurement station which would enable one to check the consistency between the pressure and void fraction measurement and prediction. Predictions of both TRAC-P1A and TRAC-PD2 are shown in all figures presented in this section.

It can be seen from Figure 2.3.2 that the TRAC-PD2 pressure prediction is slightly better than that of TRAC-P1A. However, the code (TRAC-PD2) still overpredicts the pressure at the early part ($t < 0.05$s) by approximately 7 bar (or 14%). After that, the predicted pressure drops rather sharply and the pressure is underpredicted during the later stage of the transient ($t > 0.1$s). From this pressure history one may infer that like TRAC-P1A, TRAC-PD2 also overpredicts the integrated mass and energy discharge rate at least during the early part of the transient. A comparison between the TRAC-PD2 and TRAC-P1A results showed that the TRAC-PD2 discharge flow rate was only slightly lower than that of TRAC-P1A. Since the discharge flow rate was not measured, no direct comparison of the break flow rate was possible.

Figure 2.3.3 shows the predicted and measured void fraction at 1.5 m from the closed end. The TRAC-PD2 result was in better agreement with the data during the early stage of the transient. Thereafter, as the predicted pressure dropped sharply the predicted void fraction rose faster than the data, and there was no significant difference between the predictions of TRAC-P1A and TRAC-PD2.

Figures 2.3.4 and 2.3.5 show the axial distributions of pressure, void fraction and mixture velocity at two different time levels ($t = 0.02$ second and $t = 0.087$ second, respectively). Although the predictions of TRAC-P1A and TRAC-PD2 were very similar, some differences do exist. These were caused by the modeling changes that were made between the TRAC-P1A and TRAC-PD2 codes. Specifically, in TRAC-PD2, the vapor generation rate in the bubbly flow regime was lowered by decreasing the interfacial area density by as much as thirty times than that in TRAC-P1A. Consequently, the predicted liquid superheat in the bubbly flow regime increased in TRAC-PD2. On the other hand, the liquid film heat transfer coefficient for the annular flow regime was increased by a factor of three in TRAC-PD2. This along with the increased rate of liquid entrainment may have led to a very small liquid superheat (~ 0.1°C) in TRAC-PD2 at the exit end of the pipe. For TRAC-P1A, this liquid superheat was in the range of 10 to 15°C.

2.3.5 Discussion

The prediction of TRAC-PD2 for the Super-CANON test with full opening and an initial water temperature of 280°C is slightly better than that of TRAC-P1A. However, significant disagreement between the TRAC-PD2 prediction and the experimental data still exists. Meaningful comparisons could be made only with the pressure measurements and the area-averaged void fraction at one

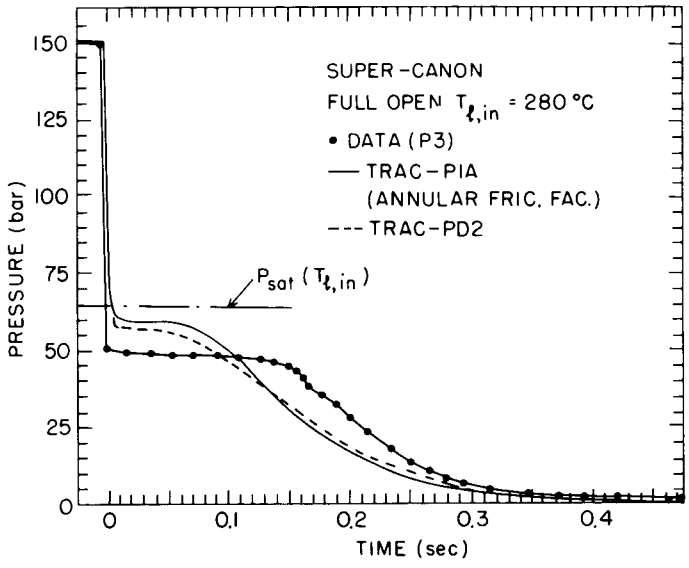

Figure 2.3.2 Comparison of TRAC Predictions for Pressure at P3 With Data. (BNL Neg. No. 9-597-81)

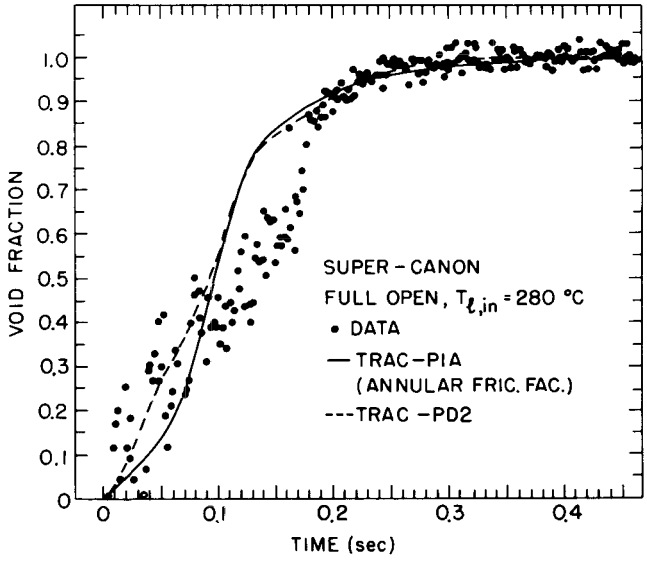

Figure 2.3.3 Comparison of TRAC Predictions for Void Fraction With Data. (BNL Neg. No. 9-598-81)

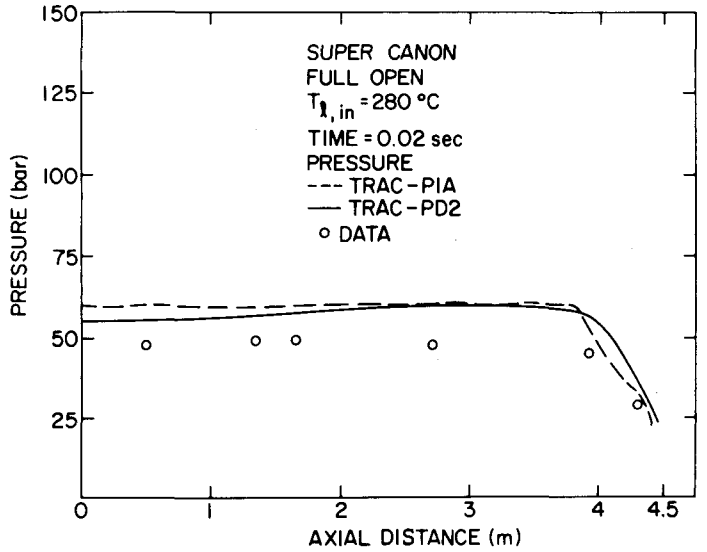

(a)

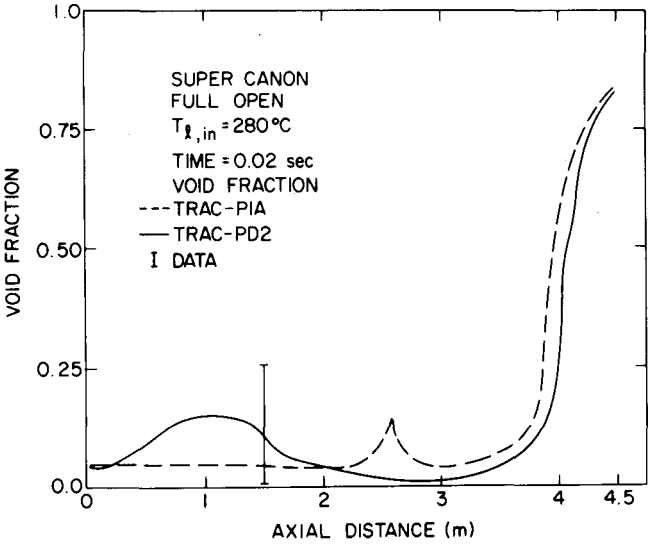

(b)

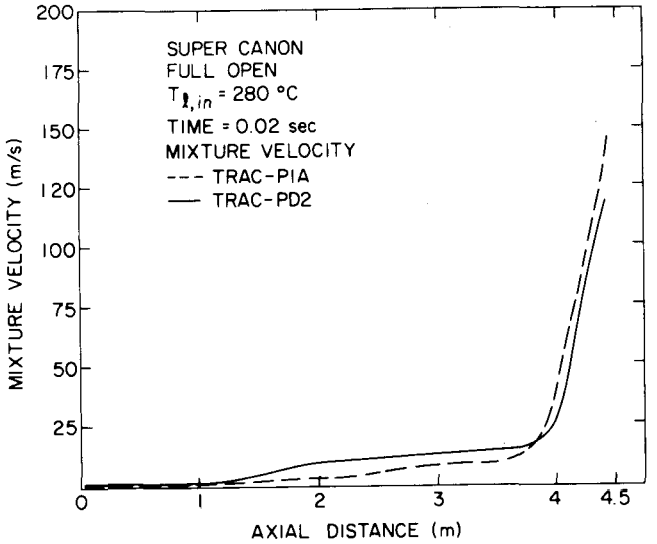

(c)

Figure 2.3.4 Comparison of Predicted and Measured Axial Pressure (a), Void Fraction (b), and Mixture Velocity (c), Distribution at 0.02 Second. (BNL Neg. Nos. 9-595-81, 2-800-81 and 2-792-81)

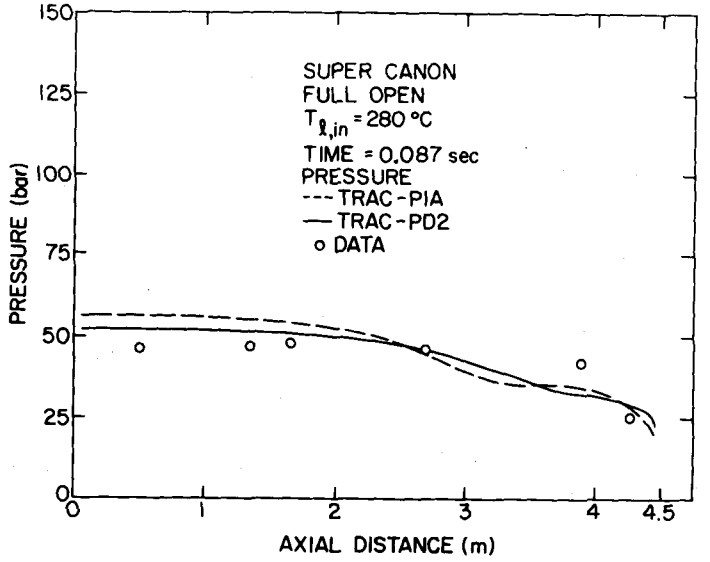

(a)

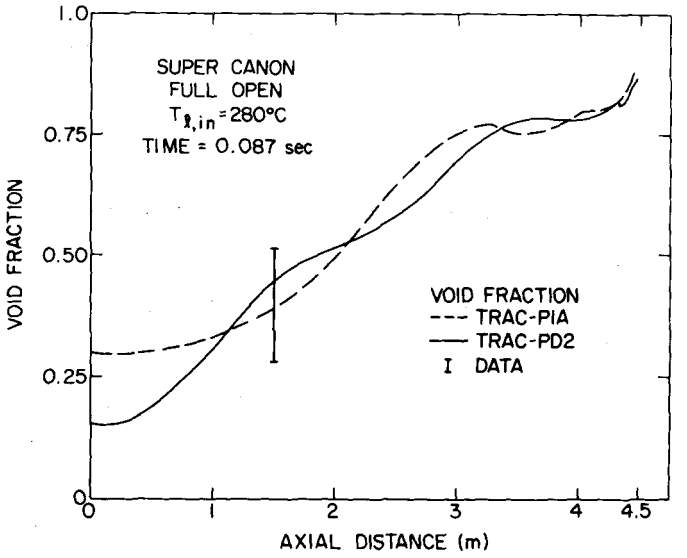

(b)

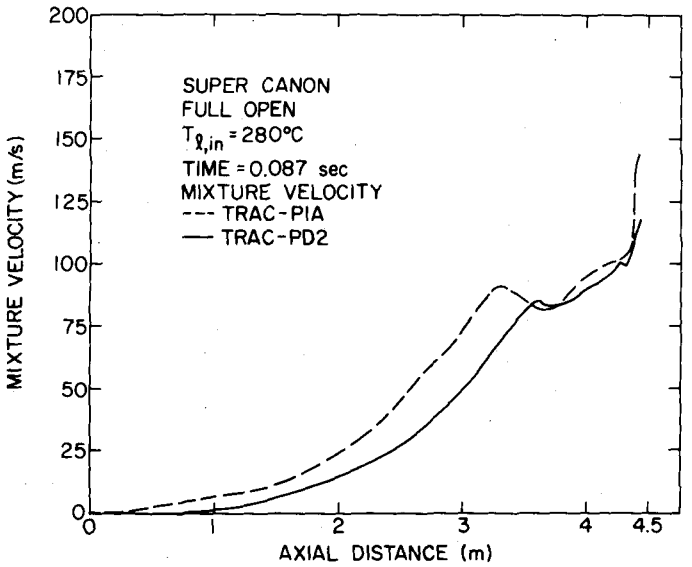

(c)

Figure 2.3.5 Comparison of Predicted and Measured Axial Pressure (a), Void Fraction (b), and Mixture Velocity (c) Distribution at 0.087 Second. (BNL Neg. Nos. 9-593-81, 9-596-81, and 5-594-81)

location. From these comparisons, it appears that like TRAC-P1A, TRAC-PD2 also tends to overpredict the integrated discharge flow rate during the early stage of the transient. In other words, the code tends to empty the pipe sooner than the experiment suggests. The modeling changes that were made in TRAC-PD2 with regard to the vapor generation rate appear to be in the correct direction. However, these were not sufficient to obtain a total agreement with the data.

No sensitivity studies were done with TRAC-PD2 for this test. However, one can still draw from the sensitivity studies conducted with the TRAC-P1A code (Saha, 1980). As with the TRAC-P1A, it can be expected that if the relative velocity for the horizontal flow is reduced in TRAC-PD2, the pressure prediction during the later part of the transient would improve. A better prediction during the early part of the transient appears to be a more challenging task. Addition of a flashing delay model, although seems necessary, may not be sufficient as found from the TRAC-P1A calculation.

2.3.6 Conclusions

The following conclusions may be drawn from the TRAC-PD2 prediction of the above-mentioned Super-CANON test:

a) The TRAC-PD2 code prediction is similar to but slightly better than that of TRAC-P1A. However, the code still tends to empty the pipe sooner than the experiment suggests.

b) A reduction in relative velocity would most likely improve the prediction in the later stage of the transient. However, further studies seem to be necessary to obtain a better agreement for the entire transient.

2.4 Marviken Critical Flow Test

2.4.1 Objective

The Marviken critical flow test No. 24 (Ericson, 1979) was simulated with TRAC-PD2 in order to assess the code's capability to predict the transient critical flow rate through a large diameter (0.5 m) vertical pipe with small length-to-diameter ratio (0.33). A good prediction of this test would greatly enhance one's confidence in applying the code to calculate the break flow rate during a hypothetical large break LOCA in light water reactor systems.

2.4.2 Test Description

The Marviken critical flow tests (Ericson, 1979) were conducted to study the blowdown of initially subcooled water from a full-scale reactor vessel through large diameter pipes. The test apparatus consisted of a vessel with an inside diameter of 5.22 m and a height of 23.14 m. A vertical discharge pipe with 0.76 m inside diameter and 6.3 m long was attached to the vessel bottom. The same vessel and the discharge pipe were used for all tests. However, various-size vertical nozzles were attached to the bottom of the discharge pipe to study the effect of break diameters and nozzle lengths. A rupture disc assembly was installed at the downstream end of the test nozzle and

it was burst to initiate the blowdown. Initially the apparatus was partially filled with water at medium pressure ($\sim$ 50 bar) with a vapor region at the top of the vessel. The liquid level in the vessel, the amount of water subcooling and the initial water temperature profile were varied from one test to another. For the current assessment effort, test 24 was selected. This test utilized a short nozzle with 0.5 m inside diameter. The nozzle had a rounded entrance section followed by a constant diameter (0.5 m) section 0.166 m in length. Thus the length-to-diameter ratio of the nozzle was only 0.33. The average liquid subcooling in the vessel was 33°C. This test provides a formidable challenge to the code to predict the transient critical flow rate accurately through full-scale short pipes. Besides, the TRAC-P1A prediction of this test was not satisfactory (Rohatgi, 1980a).

The experimental measurements included pressures, differential pressures and fluid temperatues at many locations in the test apparatus. A three-beam gamma densitometer was employed to measure the fluid density in the discharge pipe, approximately 3.18 m above the nozzle entrance. The mass flow rate out of the nozzle was evaluated mainly by two methods. The first method was by calculating the vessel mass inventory from the differential pressure measurements. The second method used the pitot-static and fluid density measurements in the discharge pipe. Both the methods produced reasonably close values of the mass flow rates. The errors in the measurements were as follows (Ericson, 1979):

Pressure:	$\pm$ 9 to $\pm$ 90 kPa
Temperature:	$\pm$ 0.6 to $\pm$ 2°C
Fluid density:	$\pm$ 50 kg/m^3 or more
Mass flow rate:	
a) Vessel inventory method:	$\pm$ 6 to $\pm$ 12%
b) Pitot-static method:	$\pm$ 3 to $\pm$ 10% in subcooled water region $\pm$ 8 to $\pm$ 15% in two-phase region

2.4.3 TRAC Input Model Description

The test was simulated by using the one-dimensional component with drift flux formulation such as PIPE, BREAK and FILL of TRAC-PD2 (Version 26.0). The vessel and the discharge pipe together was modeled by a PIPE component with 40 cells. The test nozzle was also modeled by a PIPE component with 40 cells. The nodalization for the vessel and discharge pipe is shown in Figure 2.4.1. The cell lengths in the vessel and the discharge pipe varied from 0.02 m to 1.0 m. The cell lengths in the nozzle were smaller. The sixteen cells near the break were 0.002875 m long, while fifteen cells in the middle were 0.008 m and nine cells near the discharge pipe were 0.025 m long. Finer nodalizations were used around the vapor-liquid interface in the vessel, the area changes and the nozzle exit where steep gradients in flow parameters could be expected.

A zero flow boundary condition at the top of the vessel was provided by a FILL component and a pressure boundary condition of 1.0 bar at the exit of the nozzle was provided by a BREAK component. Initially there was no flow in the test apparatus and the pressure and the temperature conditions were provided

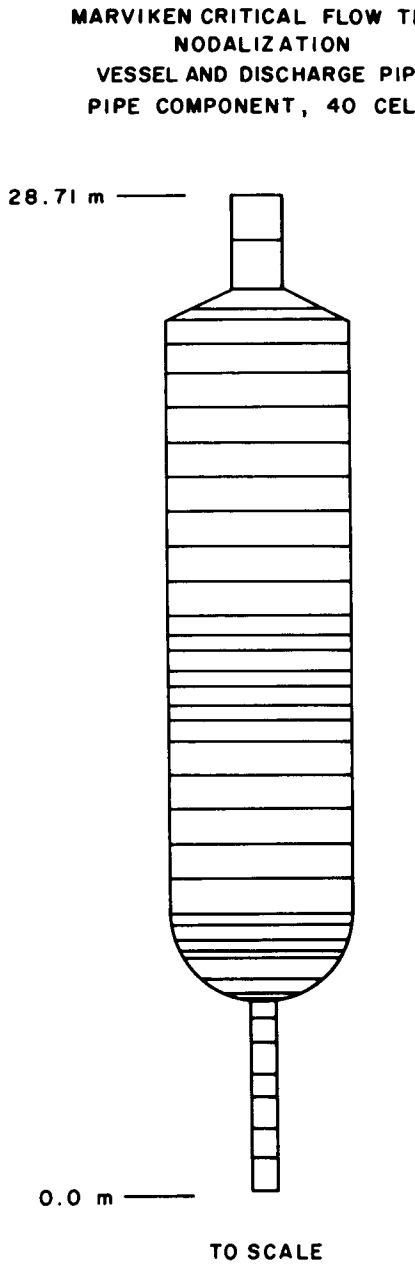

Figure 2.4.1 TRAC Nodalization for the Marviken Vessel and Discharge Pipe.
(BNL Neg. No. 2-890-82)

from the data. The initial condition will not be given here due to the proprietary nature of the data. It was found that the wall friction factor options did not affect the large diameter system. Therefore, the annular friction factor option was used. Furthermore, no additive friction factor was used in any cell.

The semi-implicit numerical option was used for the top PIPE which represented the vessel and the discharge pipe. However, to achieve a higher computing speed, the implicit numerical option was employed for the bottom PIPE representing the test nozzle. The calculation took 269 CPU seconds in the BNL CDC 7600 for 70 seconds of transient.

2.4.4 Code Prediction and Comparison with Data

The TRAC-PD2 prediction of Test No. 24 has been compared with the data and the TRAC-P1A calculation. Figure 2.4.2 shows the pressure at the top of the vessel. Since TRAC does not have a flashing delay model, neither TRAC-PD2 nor TRAC-P1A predicted the initial pressure undershoot observed in the experiment. Furthermore, TRAC-PD2 underpredicted this pressure for the first 15 seconds and then overpredicted the same for the remainder of the transient. Figure 2.4.3 shows the comparison between the measured and the predicted exit mass flow rates. It can be seen that the TRAC-PD2 prediction is slightly better than that of TRAC-P1A. However, the code (TRAC-PD2) still underpredicts the discharge flow rate during the subcooled blowdown period by as much as 25%, whereas the error in the measured (evaluated) mass flow rate was not more than 12%. During the saturated blowdown period ($t > 25$ seconds), both TRAC-PD2 and TRAC-P1A showed reasonable agreement with the data.

Figure 2.4.4 shows the comparison between the measured and predicted values of fluid density in the discharge pipe. The ball valve in the discharge pipe was starting to close at 55 second when steam appeared. The data shows a sharp decrease in density which implies that a sharp interface leaves the densitometer location while none of the codes predicted emptying even until 70 seconds which is consistent with the flow rate predictions.

2.4.5 Discussion

From Figures 2.4.2 and 2.4.3 it is evident that TRAC-PD2 predicts the exit mass flow rate slightly better than TRAC-P1A. However, as a consequence, the TRAC-PD2 pressure prediction is slightly lower than that of TRAC-P1A during the entire transient. Still both the codes underpredict the mass flow rate significantly while the pressure predictions are relatively close to the data. This seems to be a general problem with all the present codes. Both TRAC-PD2 and TRAC-P1A seem to compute higher vapor generation rates in the bubbly and bubbly-slug regimes, which presumably cause the underprediction of the choked flow rate. Intuitively this should have resulted in a higher pressure in the vessel. But that is not the case. This discrepancy between the data and the calculation could be due to underestimation of vapor generation in the upper level of the vessel, among other things.

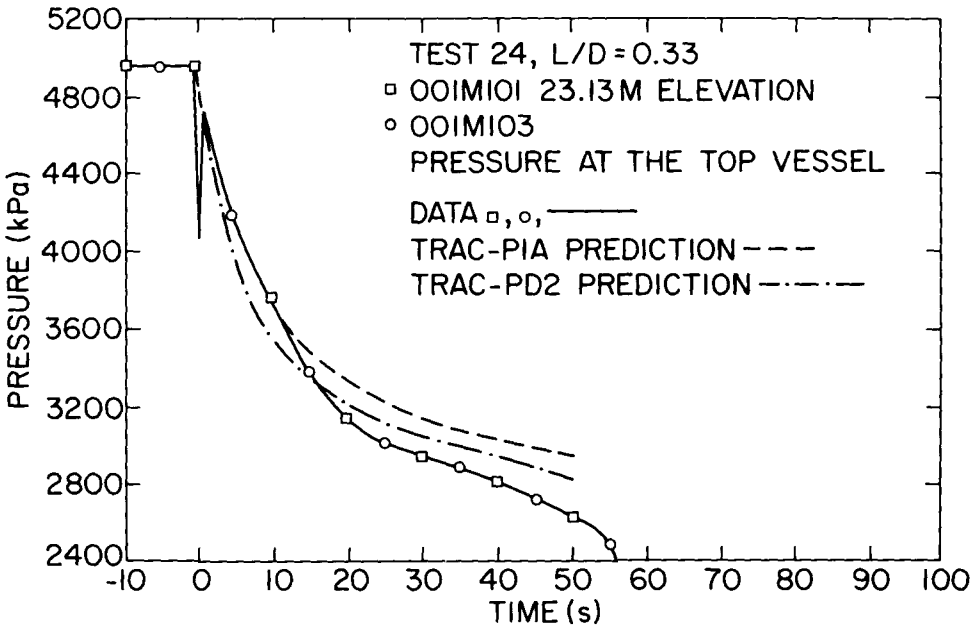

Figure 2.4.2 Comparison Between the Predicted and Measured Pressure at the Vessel Top.
(BNL Neg. No. 3-71-82)

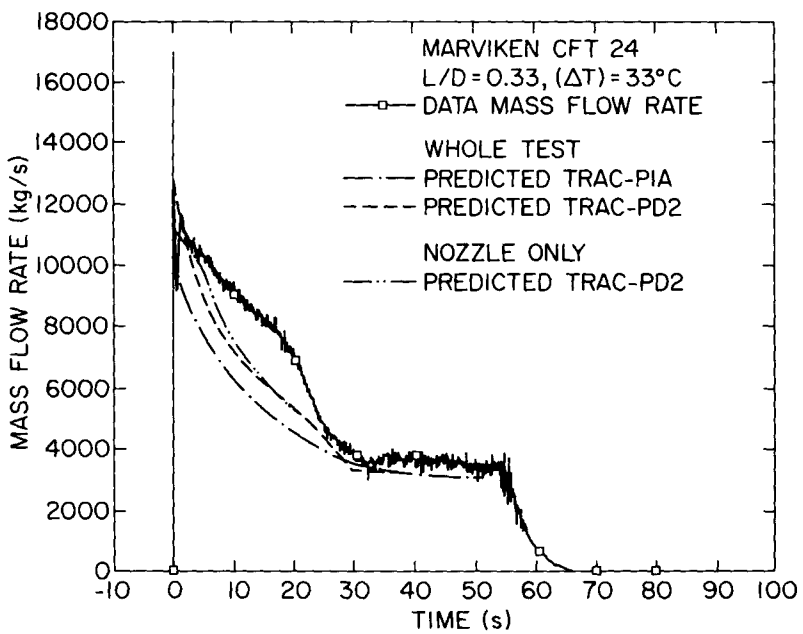

Figure 2.4.3 Comparison Between the Predicted and Measured Discharge Flow Rate.
(BNL Neg. No. 3-70-82)

There have been many model changes in the one-dimensional formulation of TRAC-PD2 from TRAC-P1A in the area of interfacial mass and energy transfer although the same drift-flux correlations have been used. This has direct bearing on the critical flow prediction. Figure 2.4.5 shows the predicted void fraction and liquid superheat at the exit of the nozzle. In the case of TRAC-P1A calculation the liquid superheat was small at the beginning of the transient where the bubbly and bubbly-slug regime existed and it suddenly increased as the flow regime changed to the annular-mist flow. However, in the TRAC-PD2 calculation the predicted superheat was higher in the bubbly and bubbly-slug regime, which reflects a more nonequilibrium situation than in TRAC-P1A, and thereafter the liquid superheat decreased as the flow regime changed to the annular-mist flow. The increased nonequilibrium in the case of TRAC-PD2 for bubbly and bubbly-slug flow resulted in the slightly higher discharge flow rate in TRAC-PD2 during the subcooled blowdown period. Thus the changes in the interfacial transfer terms seem to be in the correct direction.

In order to eliminate the effect of the vessel, only the nozzle was simulated separately by supplying inlet boundary conditions from the experiment. As shown in Figure 2.4.6, the inlet pressure used (Data table) was slightly higher than that predicted by TRAC-PD2 for the whole test. The driving pressure drop across the nozzle was higher and this led to improved mass flow rate prediction as shown in Figure 2.4.3. However, there is still a large discrepancy in the prediction. TRAC-PD2 is not accurately computing the critical flow for very small length-to-diameter ratio nozzle and further investigation of the constitutive relationships used in the code is required.

2.4.6 Conclusions

The following conclusions may be drawn from the TRAC-PD2 prediction of the Marviken Test 24:

a) The TRAC-PD2 prediction is similar to but slightly improved over that of TRAC-P1A. The model changes in TRAC-PD2, therefore, seem to be in the correct direction. However, the code still significantly underpredicts the discharge flow rate for small length-to-diameter ratio nozzle during the subcooled blowdown period.

b) There seems to be an inherent discrepancy between the code prediction and the test data. During most of the subcooled blowdown period, the code underpredicted both the exit mass flow rate and the vessel pressure. This should be investigated further.

c) A flashing delay model must be incorporated if the initial dip in pressure and break flow rate is to be predicted. However, this may not be sufficient to achieve good agreement with data for the entire transient.

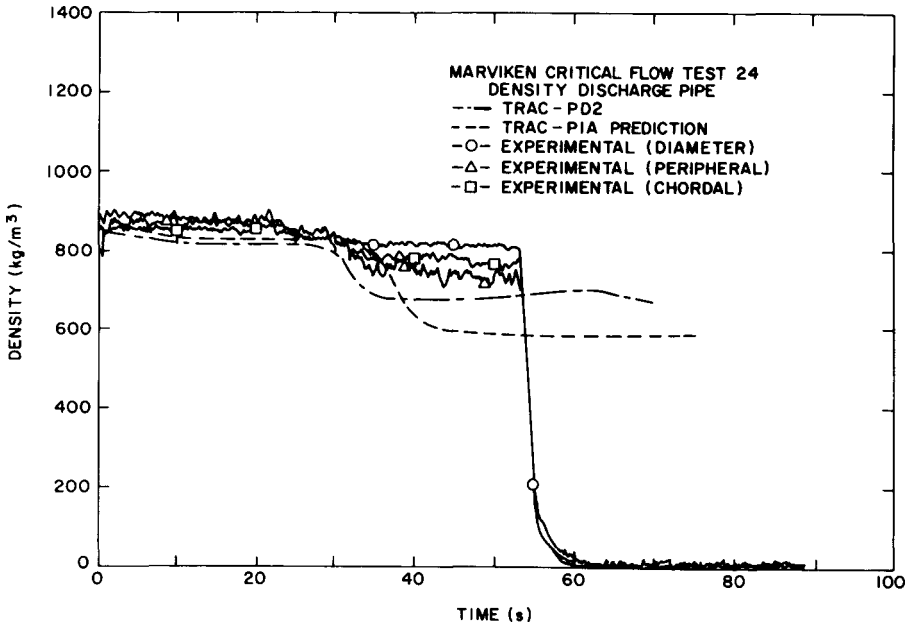

Figure 2.4.4 Comparison Between the Predicted and Measured Fluid Density at the Discharge Pipe. (BNL Neg. No. 2-886-82)

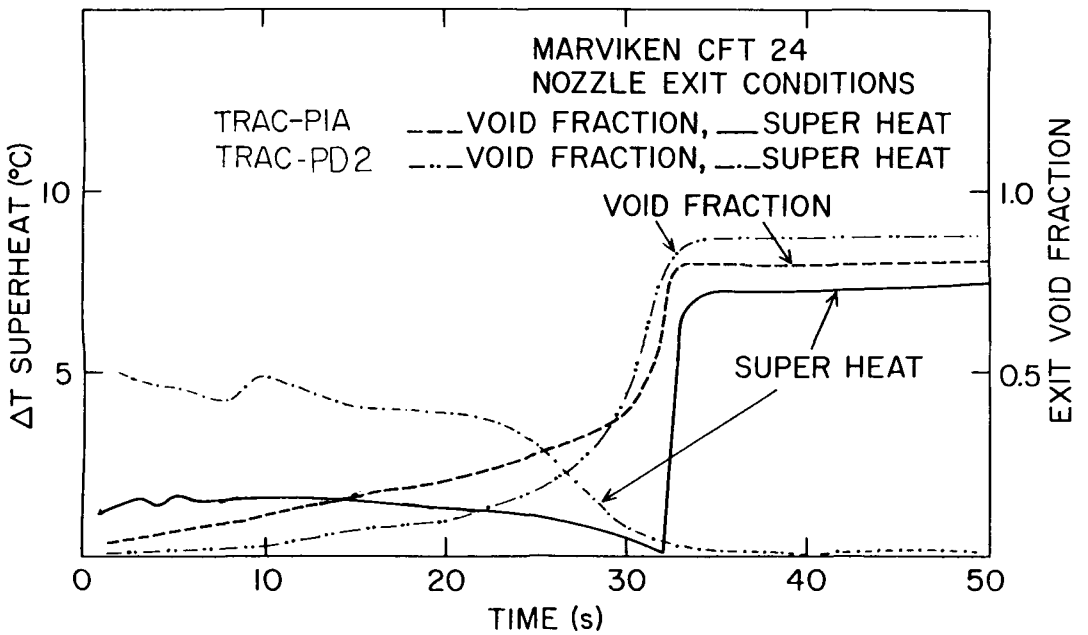

Figure 2.4.5 Predicted Void Fraction and Liquid Superheat at the Nozzle Exit. (BNL Neg. No. 1-828-81)

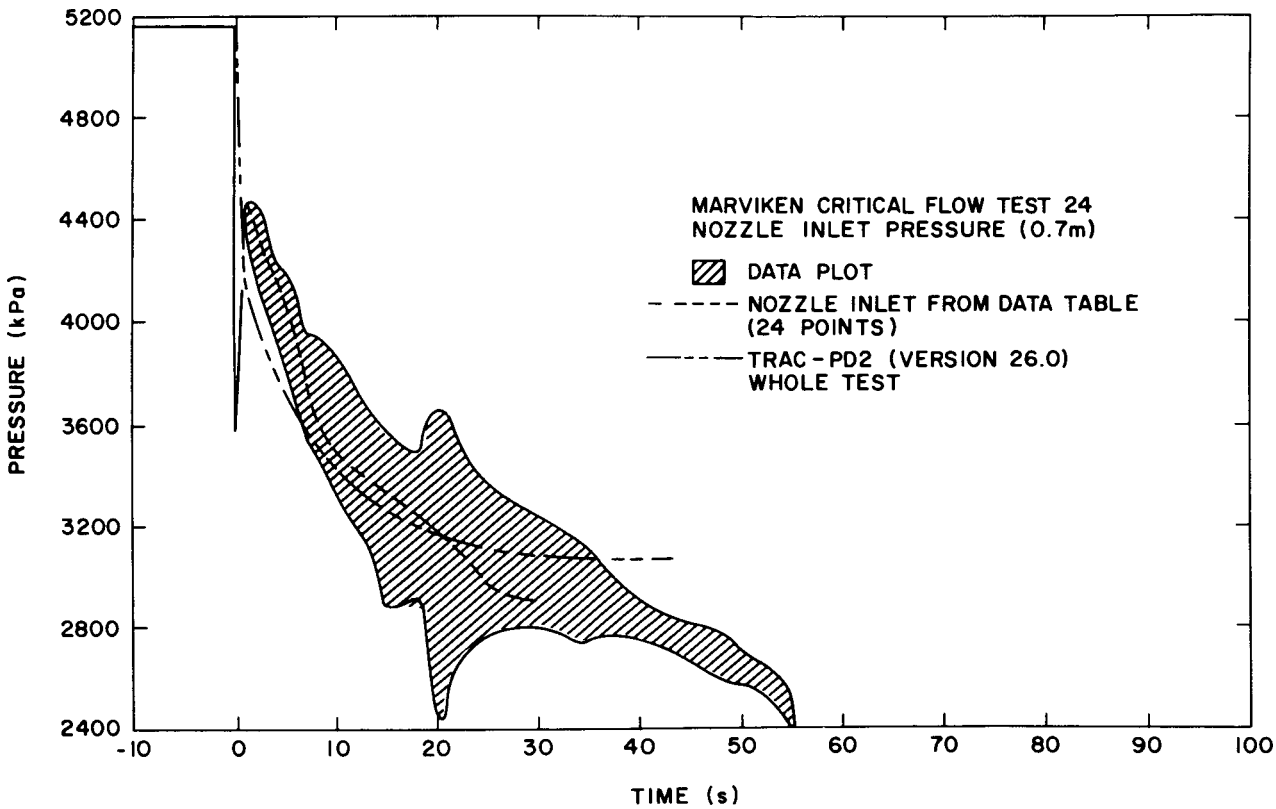

Figure 2.4.6 Comparison Between the Predicted and the Measured Pressure at the Nozzle Inlet. (BNL Neg. No. 2-895-82)

2.5 Battelle-Frankfurt Top Blowdown and Level Swell Test

2.5.1 Objective

The SWR-2R test (Holzer, 1977) conducted at the Battelle-Institute in Frankfurt was simulated with TRAC-PD2 to assess the code's capability to predict the discharge flow rate and track the two-phase mixture level during the initial blowdown stage. The test was designated as the OECD-CSNI Standard Problem No. 6, and it provided valuable data pertinent to blowdown and level swell (or phase separation) during a hypothetical loss-of-coolant accident in LWR systems.

2.5.2 Test Description

The test apparatus was a vertically oriented steel vessel of 0.776 m in inside diameter and 11.18 m in height. The vessel was fitted with a rod bundle heater located between 2.69 m and 5.19 m from the bottom of the vessel. This was used to achieve and maintain the chosen thermodynamic conditions before the blowdown began. A horizontal discharge pipe of 0.143 m in inside diameter and 0.47 m in length was connected to the vessel sidewall at an elevation of 9.94 m from the bottom of the vessel. A square-edged orifice plate of 0.064 m in inside diameter was mounted at the end of the discharge pipe. Finally a rupture disc assembly was installed at the downstream of the orifice. Blowdown was initiated by destroying this rupture disc assembly by the electrical ignition of a fuse.

Initially the vessel was filled with subcooled water up to a level of 7.07 m from the bottom. After the appropriate thermodynamic condition inside the vessel was attained (which in this particular test was an average water temperature of 558 °K and a pressure of 70.6 bar), the heater was turned off and the blowdown was initiated. At the beginning, pure steam was discharged through the break. Later, the flow regime changed to a two-phase regime when the mixture level reached the discharge pipe entrance.

Several pressure taps and thermocouples were placed at different vessel levels as well as in the discharge pipe to monitor the pressure and fluid temperature during the transient. The errors in the pressure and temperature measurements were approximately 1% and 2°K, respectively.

The fluid density at the discharge nozzle was measured by a two-beam gamma densitometer. The accuracy of this measurement was approximately 12%. There were also two drag bodies to measure the fluid momentum at the discharge nozzle. The break mass flow rate was determined from the fluid density and the drag body measurements. The error in the measured discharge flow rate was estimated to be between 10 and 15%.

The time history of the water (or mixture) level was measured by a stack equipped with electrical contacts at many axial locations. The accuracy of the mixture level measurement was $\pm$ 0.02 m.

2.5.3 TRAC Input Model Description

Two separate calculations were performed in order to compare the TRAC-PD2 results of the drift-flux formulation and the two-fluid model. Therefore, in

the first calculation, the test vessel along with the discharge pipe was modeled as a TEE component which employs the drift-flux formulation. For the second calculation, the test vessel was represented by the one-dimensional VESSEL module (i.e., one cell per level) which uses the two-fluid model. The discharge pipe, however, had to be modeled by a PIPE component which uses the drift-flux equations.

The schematic of the test apparatus and the TRAC input model for the first calculation is shown in Figure 2.5.1. The test vessel was modeled as the primary pipe of a TEE component whereas the discharge pipe was represented by the secondary pipe of the same TEE component. There were 120 cells in the primary pipe, i.e., the test vessel, and the cell lengths varied from 0.055 m to 0.248 m. This is shown in Figure 2.5.2. Notice that finer nodalization was utilized between the initial water level and the discharge pipe level to better "track" the two-phase mixture level during the transient. The effect of the rod bundle heater inside the test vessel was taken into account by decreasing the flow area by 22% and the hydraulic diameter by a factor of ten (10) compared to those for the vessel without heater. The discharge pipe had eight cells with finer nodalization near the orifice or the break where the diameter was reduced to 0.064 m.

Two zero-velocity FILL components were attached to the top and bottom of the test vessel or the primary pipe of the TEE component. A BREAK component was connected to the free end of the secondary pipe of the TEE component, and the ambient pressure of 1 bar was used as the boundary condition. Incidentally, the same nodalization and boundary conditions were also used for the TRAC-P1A calculation for this test (Neymotin, 1980a).

The homogeneous friction factor option (NFF=1) was used in all cells; but, no additive friction was employed in any cell. The fully implicit numerical option was used, and this calculation with the drift-flux model took 134 seconds on the BNL CDC-7600 for a transient of 3 seconds.

In the second calculation, the test vessel was represented by the one-dimensional VESSEL module with 23 levels. The nodalization is shown in Figure 2.5.3. The cell lengths varied from 0.205 m to 1.345 m with finer nodalization between the initial water level and the discharge pipe level. The effect of the rod bundle inside the test vessel was taken into account in the same way as was done in the drift-flux model calculation. Also, the same PIPE component with the same nodalization as the secondary pipe in the first calculation was used to model the discharge pipe. The only boundary condition was the ambient pressure imposed at the BREAK component attached to the free end of the discharge pipe. (The VESSEL module takes care of the zero-flow boundary condition at the top and bottom of the test vessel.) This calculation took 151 seconds on the BNL CDC-7600 for 3 seconds of transient.

2.5.4 Code Prediction and Comparison with Data

Figure 2.5.4 shows the comparison of the pressure predictions by both the drift-flux and two-fluid models with the data at 6.35 m elevation. Both models were in reasonable agreement with the data except for the initial undershoot which was missed by both of them. This is to be expected since TRAC starts vapor generation at saturation condition, while in the test there was some delay at the onset of flashing. Moreover, there was almost no difference

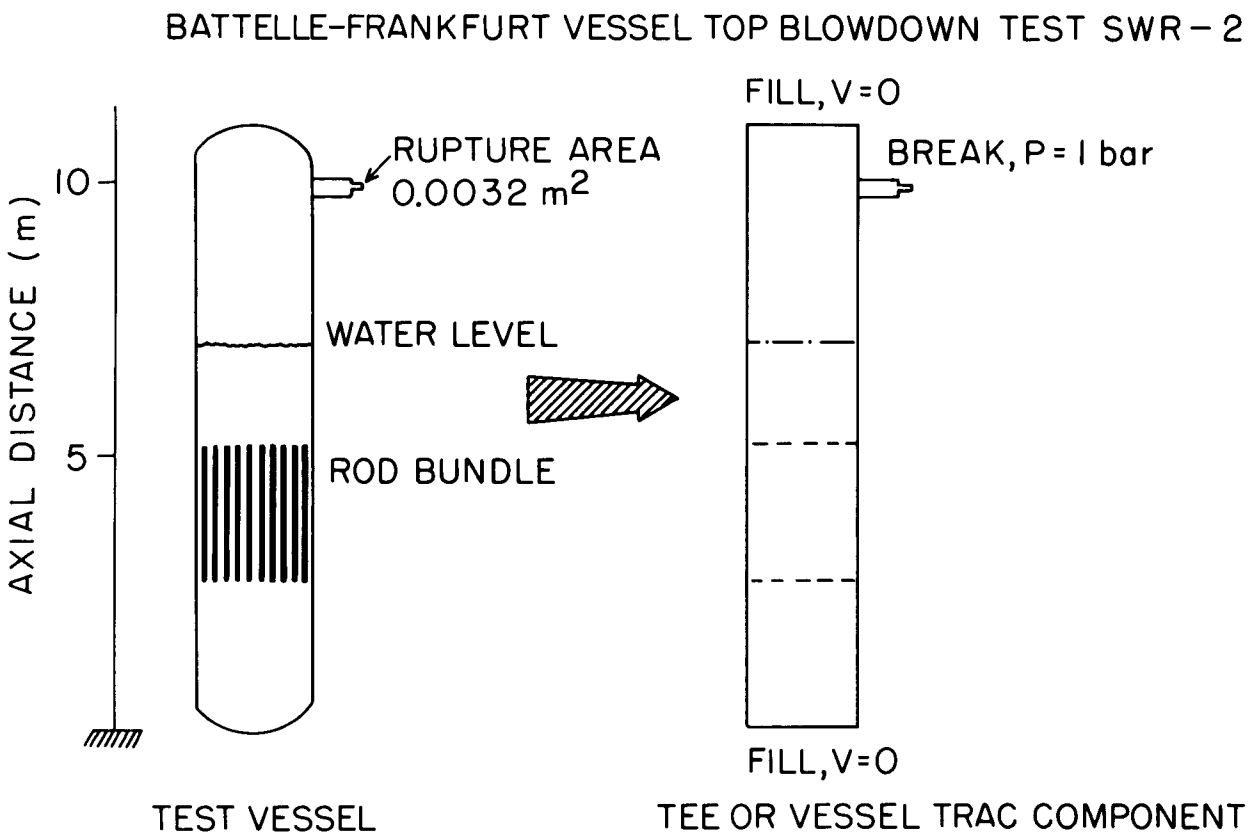

Figure 2.5.1 Configuration of Test Vessel for TRAC Calculations (BNL Neg. No. 2-798-81).

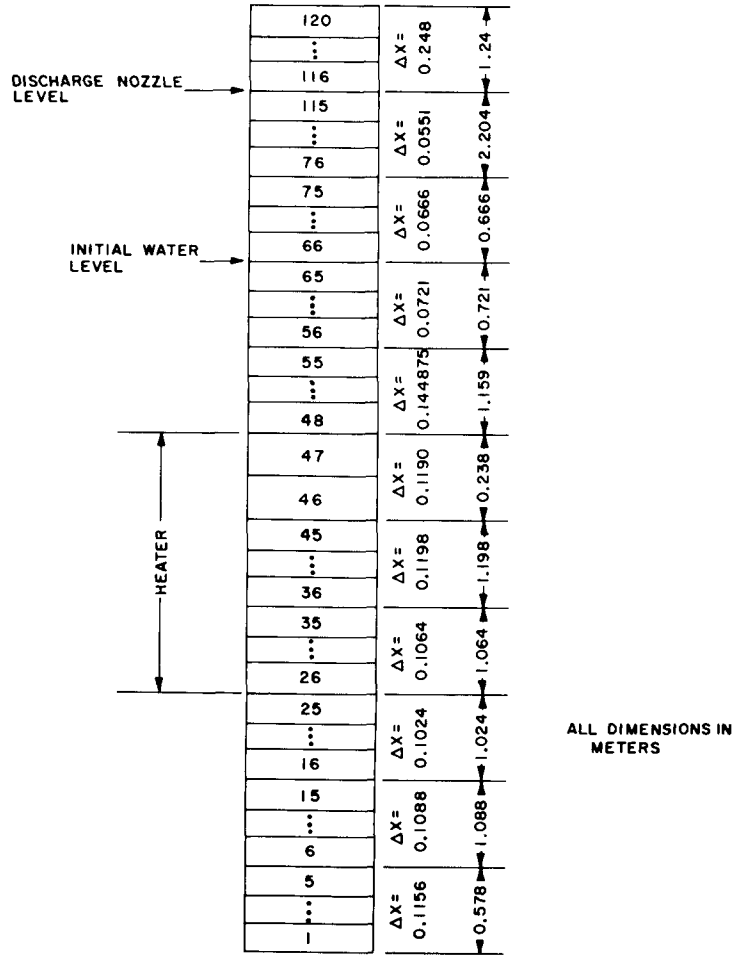

Figure 2.5.2 TRAC Nodalization of the Test Vessel for Drift-Flux Model. (BNL Neg. No. 2-883-82)

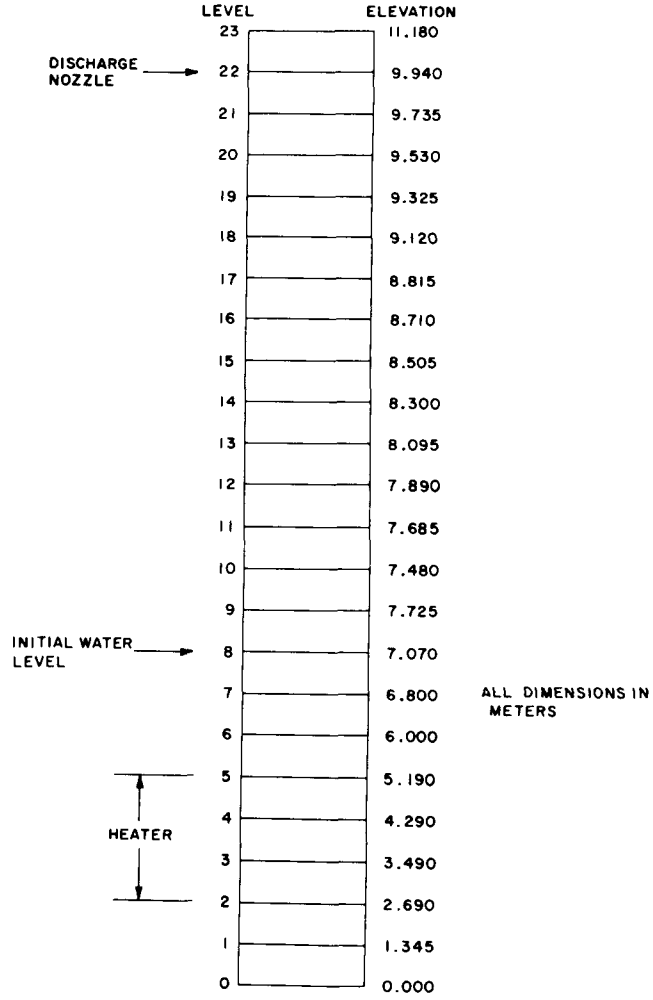

Figure 2.5.3 TRAC Nodalization of the Test Vessel for Two-Fluid Model. (BNL Neg. No. 2-884-82)

between the TRAC-P1A and TRAC-PD2 results for the drift-flux model.

Figure 2.5.5 shows the mass flow rate through the break. During the early part of the transient ($t \leq 2$ seconds), only steam flowed through the discharge pipe. Surprisingly both the TRAC-PD2 calculations yielded approximately 30% higher flow rate than the experimental value even during this stage. A hand calculation indicated that a discharge coefficient of 0.725 would produce the break flow rate close to the experimental value. This appears to be consistent with the LANL calculation (Knight, 1980) with TRAC-P1A where an additive friction was used to obtain close agreement with the data. In the BNL calculations no additive friction was used. (A subsequent BNL calculation with a 30% reduction in the orifice area produced good agreement with the experimental break mass flow rate before the mixture level arrived at the discharge pipe. However, the vessel pressure and the time of level arrival at the discharge pipe were overpredicted significantly.)

As the transient progressed, the two-phase mixture level in the test vessel swelled. When the mixture level arrived at the discharge pipe, the break mass flow rate increased sharply because of a sudden increase in the fluid density. This happened at approximately 2.3 seconds in the test. However, as shown in Figure 2.5.5, both of the TRAC-PD2 models predicted an early arrival of this mixture level at the discharge pipe. The break mass flow rates were also overpredicted by both of the TRAC models. As for the predicted values of the mass flow rate, they have been calculated using identical one-dimensional PIPE components. Therefore, quantitative discrepancies in the results for $t > 2$ seconds, as shown in Figure 2.5.5, are mainly due to differences in the specific thermohydraulic properties of the two-phase mixture delivered to the PIPE by the two models. For example, the void fraction at the break level predicted by the drift-flux formulation was considerably higher than in the case of the two-fluid prediction (0.73 and 0.62, respectively, when the two-phase mixture reached the break level).

Figure 2.5.6 shows the direct comparison between the measured and the predicted location of the mixture level. Since the code does not "track" the mixture level rigorously, the cell boundary across which the largest rise in void fraction is calculated, has been taken as the predicted mixture level. (This is why finer nodalization was employed between the initial water level and the discharge pipe level). It is clear from Figure 2.5.6 that both the TRAC-PD2 models overpredicted the speed of the mixture level. It is important to note that during the first 0.3 seconds, the water level did not rise in the experiment. This coincided with the time of pressure undershoot as shown in Figure 2.5.4. Therefore, inclusion of a flashing delay model would most likely improve both the pressure and the mixture level predictions.

Figure 2.5.7 shows the axial void fraction distribution at various times during the transient, as computed by the drift-flux approach. The void distribution has shown some unusual behavior at the heater boundaries. This can be explained in terms of code description of relative velocity in the void fraction range of 0.1 to 0.75. The relative velocity computed in the constitutive relations package is a function of $(D_h)^{0.5}$, and there is a large decrease in the hydraulic diameter in the rod bundle or heater region, leading to a discontinuity in relative velocity and, as a result, also in void fraction. This was verified by computing a hypothetical case without the rod bundle, and the void distribution did not have any peculiar behavior as seen

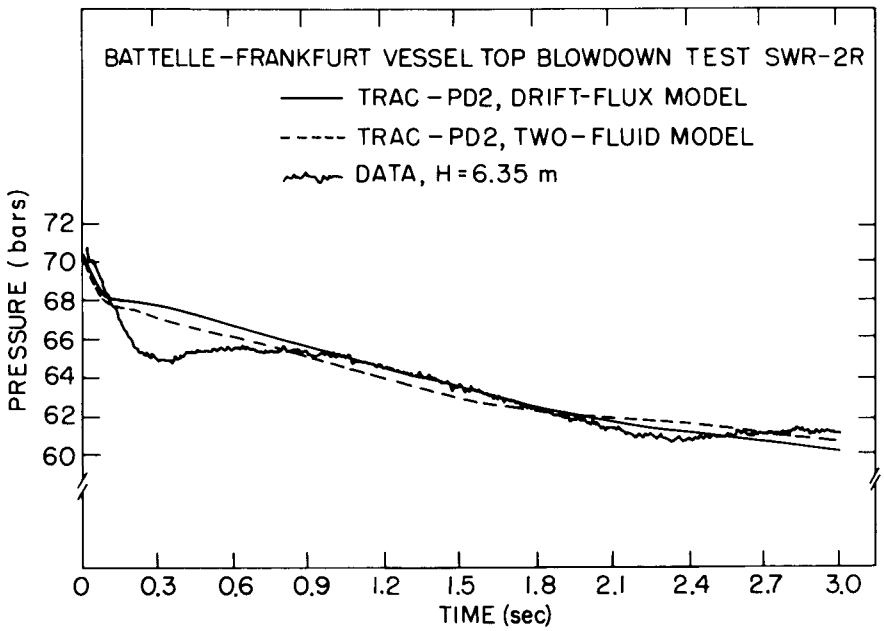

Figure 2.5.4 Comparison Between the Measured and Predicted Pressure in the Test Vessel at 6.35 m Elevation. (BNL Neg. No. 2-799-81)

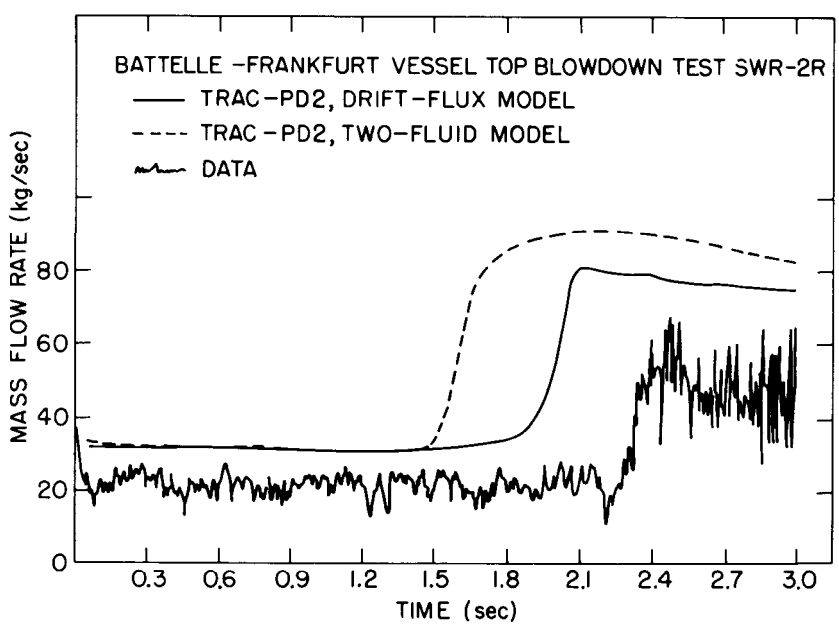

Figure 2.5.5 Comparison Between the Measured and Predicted Mass Flow Rate at the Break. (BNL Neg. No. 2-790-81)

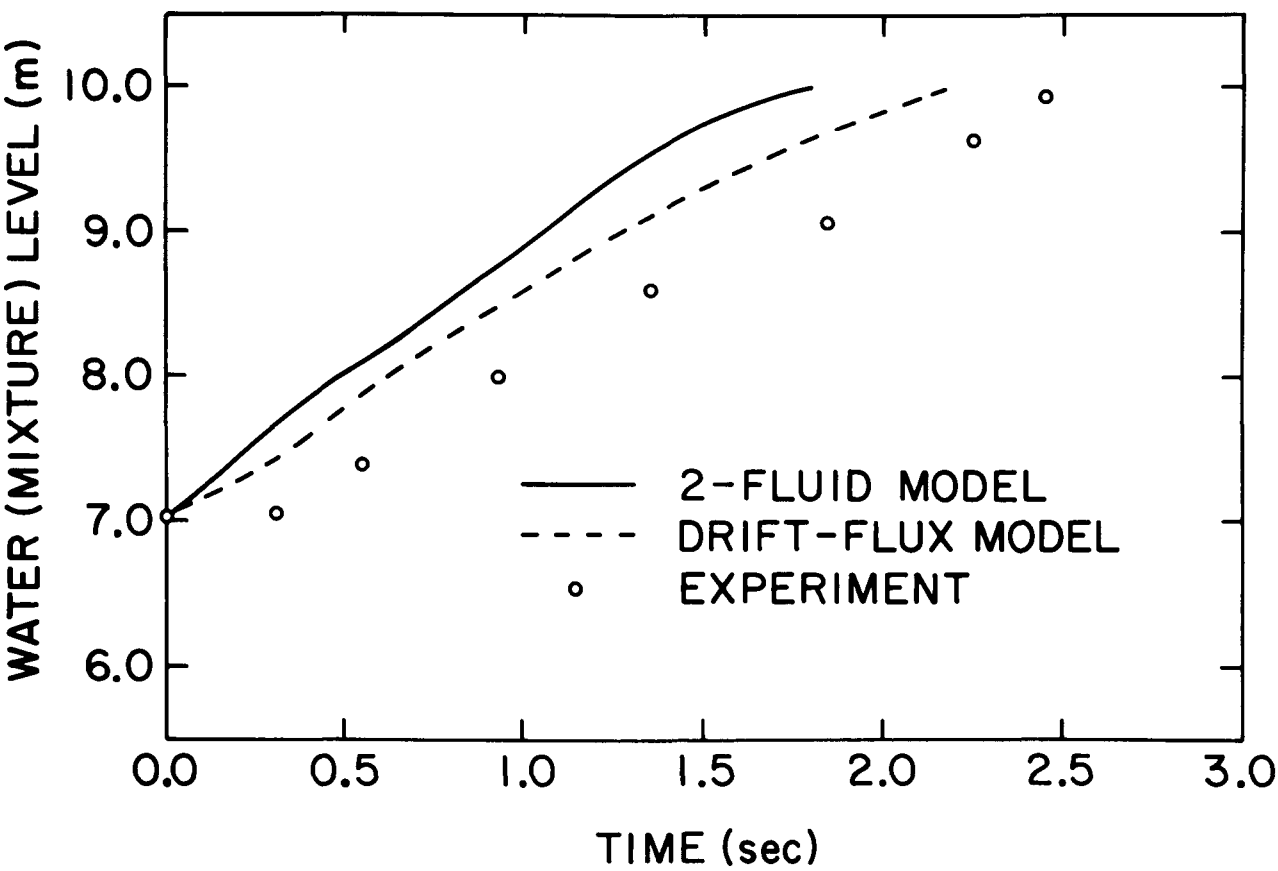

Figure 2.5.6 Comparison Between the Measured and Predicted Mixture Level. (BNL Neg. No. 2-888-82)

in Figure 2.5.7. Figure 2.5.8 shows the axial void distribution as computed by the two-fluid formulation. The original TRAC-PD2 (Version 26.0) had some errors in the constitutive package for interfacial momentum transfer, which were corrected at BNL and will be discussed in Section 2.7. Figure 2.5.8 shows a solution with the corrected version of the code, and the void fraction distribution obtained at this time appears to be of more reasonable shape. Unfortunately, no measurements of void fraction distributions in the vessel were performed so only qualitative comments on the code prediction of void fraction are made.

2.5.5 Discussion

The TRAC-PD2 prediction with the drift-flux model, i.e, the TEE component was very similar to that of the TRAC-P1A code. This is not surprising since the level swell phenomenon greatly depends on the phase separation or the relative velocity correlations which are the same in the TRAC-PD2 and TRAC-P1A. Also, it was found that the two-fluid model predicted a faster level rise than the drift-flux model. This means that the interfacial momentum transfer is higher in the two-fluid model than in the drift-flux model. In other words, the relative velocity is less in the two-fluid model. Thus as the vaporization takes place, the vapor drags the liquid along and the level rises faster than the experiment or the drift-flux model indicates. It was found earlier with TRAC-P1A drift-flux model (Neymotin, 1980a) that an increase of 25% in the relative velocity could yield the correct mixture arrival time at the discharge nozzle.

Omission of a flashing delay model in TRAC is also responsible for some discrepancies between the code predictions and the experimental data. This is clear from Figures 2.5.4 and 2.5.6 where a pressure undershoot and an insignificant level rise, respectively, can be seen during the early part of the transient ($t < 0.3$ second). Therefore, inclusion of a flashing delay model is strongly recommended in the future versions of TRAC.

Finally, the reason for the apparent overprediction of discharge flow rate particularly for the single-phase vapor regime could be due to inconsistency between the pressure and the break mass flow rate measurements. An attempt to match the break mass flow rate resulted in significant overprediction of vessel pressure and arrival time of the mixture level at the discharge pipe. From the experimental data report (Holzer, 1977), it appears that the vessel pressure and the mixture level arrival time were measured more accurately than the break mass flow rate. Therefore, attempts to match the break flow rate by either reducing the orifice area or increasing the frictional loss coefficient are not justified.

2.5.6 Conclusions

The following conclusions can be drawn from the TRAC-PD2 prediction of the Battelle-Frankfurt level swell test (SWR-2R):

1. Both the drift-flux and two-fluid models of TRAC-PD2 tend to overpredict the interfacial momentum transfer or underpredict the relative velocity in the bubbly and bubbly-slug flow regimes. The discrepancy is more for the two-fluid model than for the drift-flux model.

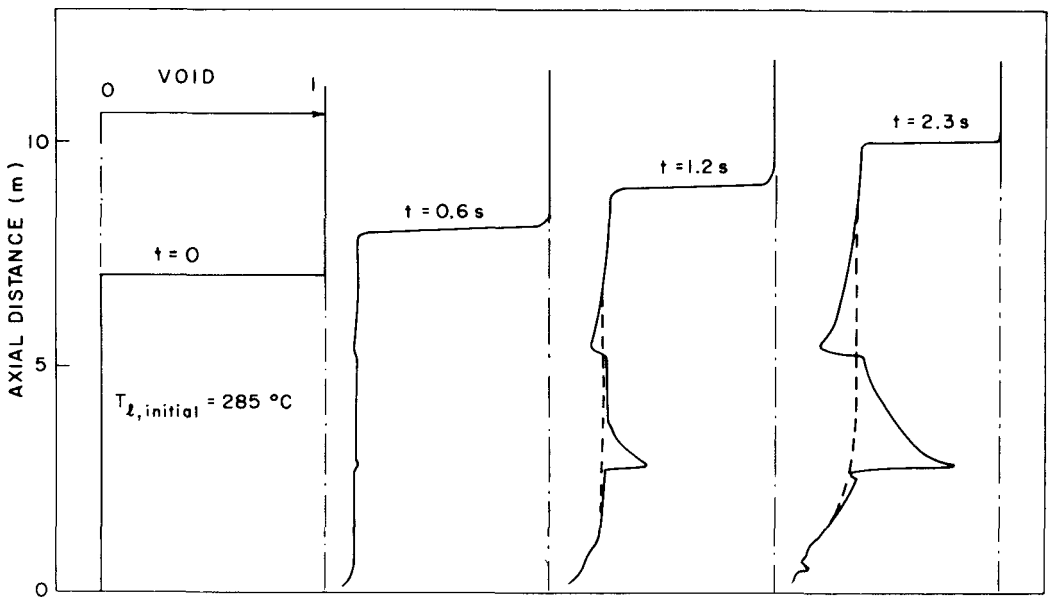

Figure 2.5.7 Axial Void Distribution in the Test Vessel as Predicted by TRAC-PD2 Drift-Flux Formulation (— With Heater, ---Without Heater) (BNL Neg. No. 6-979-80)

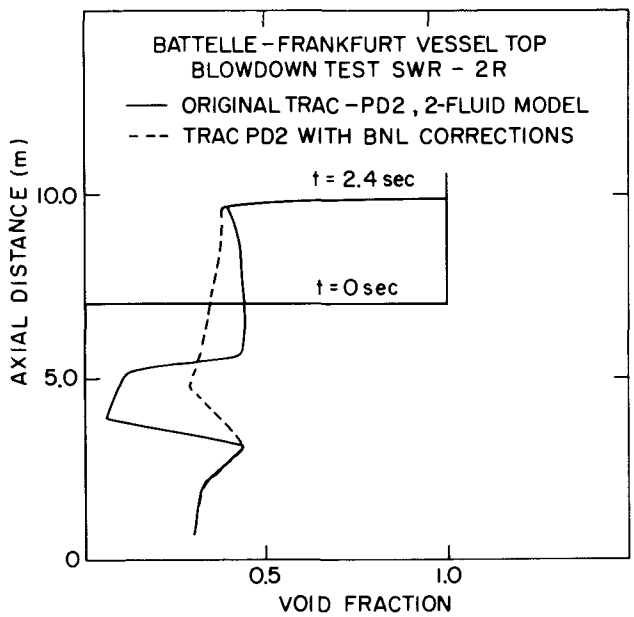

Figure 2.5.8 Axial Void Distribution in the Test Vessel as Predicted by TRAC-PD2 Two-Fluid Formulation. (BNL Neg. No. 2-791-81)

2. Inclusion of a flashing delay model is necessary for the accurate prediction of pressure at the early stage of blowdown. This should also help in the prediction of the mixture level location.

3. The reason for the apparent overprediction of steam discharge flow rate could be due to inaccuracy in the break mass flow rate measurement, and not due to any deficiency in the TRAC-PD2 code.

2.6 University of Houston Flooding Tests

2.6.1 Objective

The University of Houston flooding tests (Dukler and Smith, 1979) were simulated with TRAC-PD2 in order to assess the code's ability to predict the liquid downflow rate for a given upward gas flow rate. Since the liquid downflow rate depends highly on the interfacial shear and liquid entrainment rate, these tests also provide data to assess the TRAC-PD2 models and correlations for the interfacial momentum transfer and the liquid entrainment fraction in the gas core. It is needless to say that the counter-current flow limitation (CCFL) or "flooding" is an important phenomenon which must be predicted accurately in best-estimate analyses of LWR loss-of-coolant accidents.

2.6.2 Test Description

The test section was a 4.11 m long, 0.05 m I.D. vertical tube. Water at ambient pressure and temperature was injected into the middle of the test section through a 0.225 m long porous section surrounded by a jacket. Air at ambient pressure and temperature was supplied at the bottom through a collecting chamber. This chamber was also used to collect and measure the water downflow rate. The top of the test section was connected to another chamber in which the liquid film was separated from the air-droplet mixture and the upward film flow rate was measured. The air-droplet mixture was passed through a separator and the entrained liquid flow rate was measured. There were four stations on the test section for film thickness measurements and four more stations for pressure measurements. Further details of the test section and instrumentation can be found in the data report (Dukler and Smith, 1979).

Four different water feed rates were used. They were: 100 lb/hr (0.0126 kg/s), 250 lb/hr (0.0315 kg/s), 500 lb/hr (0.063 kg/s) and 1000 lb/hr (0.126 kg/s). In each series of tests the air flow rate was gradually increased from 120 lb/hr (0.01512 kg/s) to 300 lb/hr (0.0378 kg/s). The air flow rate at the flooding point or the onset of liquid upflow increased as the water feed flow rate was decreased.

For the current assessment effort, the test series with water feed rates of 100 lb/hr and 1000 lb/hr were chosen. These two water feed rates produced two distinctly different flooding situations.

2.6.3 TRAC Input Model Description

In principle, the test could be simulated with either the one-dimensional PIPE component (drift-flux formulation) or the VESSEL module with one cell per

level (two-fluid formulation). However, it was discovered during a preliminary assessment that the relative velocity correlation as used in the PIPE component of TRAC-PD2 (or TRAC-P1A) could not predict a counter-current flow situation in the annular-mist flow regime (Rohatgi, 1980b). Since this was the flow regime of interest for the present tests, the two-fluid formulation or the VESSEL module was used.

The test section was represented by the VESSEL module with 25 levels with one cell in each level. The nodalization is shown in Figure 2.6.1. The axial cell lengths varied from 0.05 m to 0.35 m. Longer cells were used at the bottom to collect the water which flowed down. The measured air flow rate was introduced at the third cell from the bottom through a FILL component. Similarly, the water feed rate was introduced at the sixteenth cell from the bottom through another FILL component. The bottom end of the VESSEL was connected to a zero-velocity FILL component whereas the top end was connected to a BREAK component where the (system) pressure boundary condition was imposed. With a given water feed rate and an air flow rate the code was run until a stable solution was obtained. Each calculation produced one point of the flooding curve, and a typical run took 127 CPU seconds in the BNL CDC-7600 computer.

2.6.4 Code Prediction and Comparison with Data

2.6.4.1 Water Feed Rate of 100 lb/hr

As mentioned earlier, calculations were performed for various air flow rates by keeping the water feed rate constant at 100 lb/hr. As shown in Figure 2.6.2, according to the TRAC-PD2 (Version 26.0) calculations (labeled by open circles) all the water flowed down until an air flow rate greater than 200 lb/hr was used. Thereafter, even at the air flow rate of 205 lb/hr, air carried all the injected water upwards and no water flowed through the bottom of the test section. In the experiment, however, no water flowed upwards until an air flow rate greater than 250 lb/hr was used. Therefore, the code underpredicted the air flow rate corresponding to the flooding onset by 20%. Moreover, as shown in Figure 2.6.2, the code did not predict a situation where some of the injected water may flow up while the rest may continue to flow down.

The underprediction of air flow rate at the flooding onset could be caused by a higher interfacial shear as well as a higher liquid entrainment rate. In order to study these parameters separately, the entrainment rate (or ratio) in TRAC-PD2 was set to zero and the test series were recomputed. However, contrary to the force balance, the code did not predict a liquid flow reversal even for the air flow rate of 1000 lb/hr. On further investigation, an error was discovered in the code which inadvertently used the following expression for the interfacial shear coefficient in the annular-mist regime:

$$c_i = \left[\frac{0.01(1+300\delta/D)(1-E)}{D} + \frac{3c_D}{4d} E \right] \rho_g (1-\alpha) \qquad (2.6.1)$$

where c_i is the coefficient of interfacial shear, δ, D, d, c_D and E are the film thickness, hydraulic diameter, droplet diameter, droplet drag coefficient and the entrainment fraction, respectively. The above expression does not reduce to the correct shear coefficient for the pure annular flow. The correct expression should have been:

$$c_i = \left[\frac{0.01\ (1 + 300\ \delta/D)(1 - E)}{D} + \frac{3c_D(1 - \alpha)E}{4d} \right] \rho_g \qquad (2.6.2)$$

After this correction was implemented in TRAC-PD2 at BNL, the code was rerun with no entrainment, and now the liquid flow reversed at an air flow rate of approximately 310 lb/hr which was 24% higher than the experimental value of air flow rate at the flooding onset. The calculated results are shown by the open triangles in Figure 2.6.2.

The TRAC-PD2 entrainment model was reactivated and the code was rerun with the above-mentioned BNL correction. Since the correct expression for the interfacial shear coefficient, i.e., Equation (2.6.2), represents a higher value of interfacial friction than Equation (2.6.1) the liquid flow reversed at an air flow rate which was lower than the original TRAC-PD2 prediction. This is shown by the open diamonds in Figure 2.6.2. The last calculation also indicates that the TRAC-PD2 entrainment model predicts a much larger entrainment ratio than in the test. This is confirmed through a comparison of TRAC-PD2 prediction of liquid film and droplet upward flows with the data in Figure 2.6.3. The data at the exit of the test set up shows that, as expected, first the droplets started going up with the air and at slightly higher air flow rate some liquid film also started flowing up. As the air flow rate is increased further, the film flow rate goes up faster than the droplet flow rate. However, this same figure also shows that TRAC-PD2 computes much higher entrainment ratio which results in depletion of the liquid film flowing upwards. This figure also shows that TRAC-PD2 not only computes higher entrainment ratio but also earlier inception.

Figure 2.6.4 shows a comparison of entrainment ratios computed by the TRAC-PD2 model and, Ishii-Mishima (1981) model coupled with the Ishii-Grolmes (1975) inception criterion. The TRAC-PD2 model predicts a much earlier inception of entrainment and much larger values of entrainment ratio than the Ishii-Mishima-Grolmes model. Furthermore, TRAC-PD2 predicts the beginning of co-current upflow at a higher air flow rate than the entrainment inception point as shown in this figure. This can be explained in terms of the TRAC formulation for the liquid phase. The code has only one liquid field and as long as the net force on the liquid phase is in the downward direction the liquid will keep flowing down, even though the entrainment model predicts an existence of droplets. So for the range of air flow rate between the inception of entrainment and the beginning of co-current flow, the code predicts downflow of liquid film along with the droplets. Obviously this is not correct from a physical viewpoint. Two liquid fields, namely the film and the droplets are necessary to rectify this situation. Furthermore, it should be noted that the air flow rate for the entrainment inception according to the Ishii-Mishima-Grolmes model is slightly higher than the data, though closer to the data than the TRAC-PD2 model.

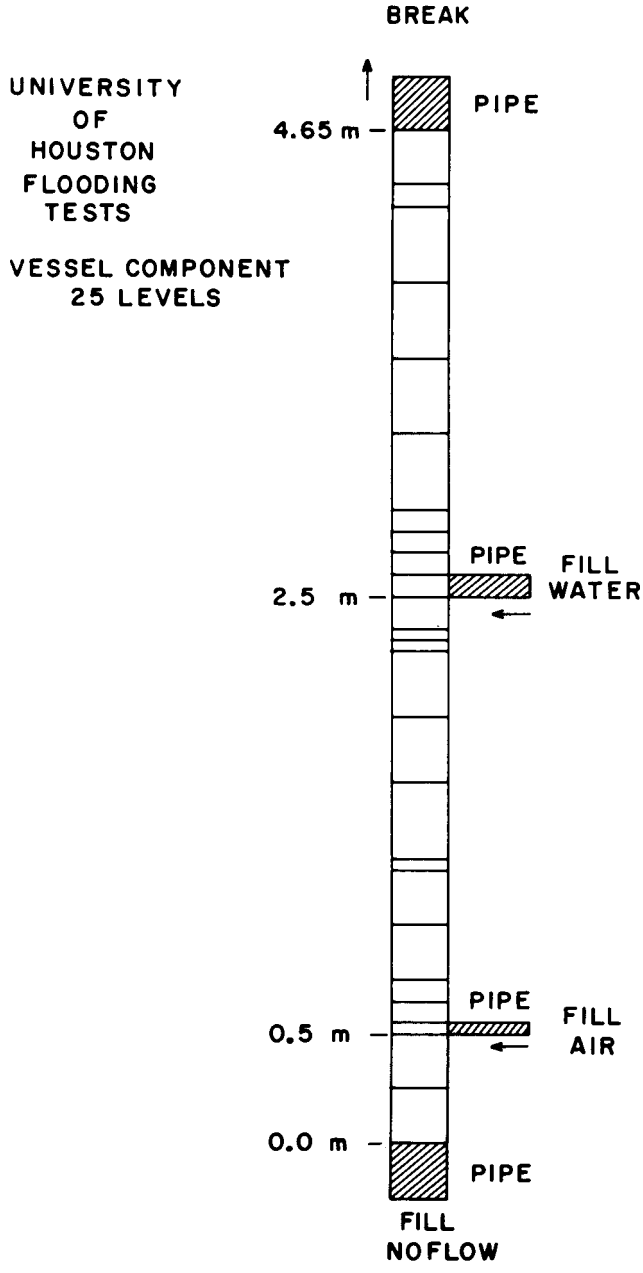

Figure 2.6.1 TRAC Nodalization of the University of Houston Test Section. (BNL Neg. No. 2-894-82)

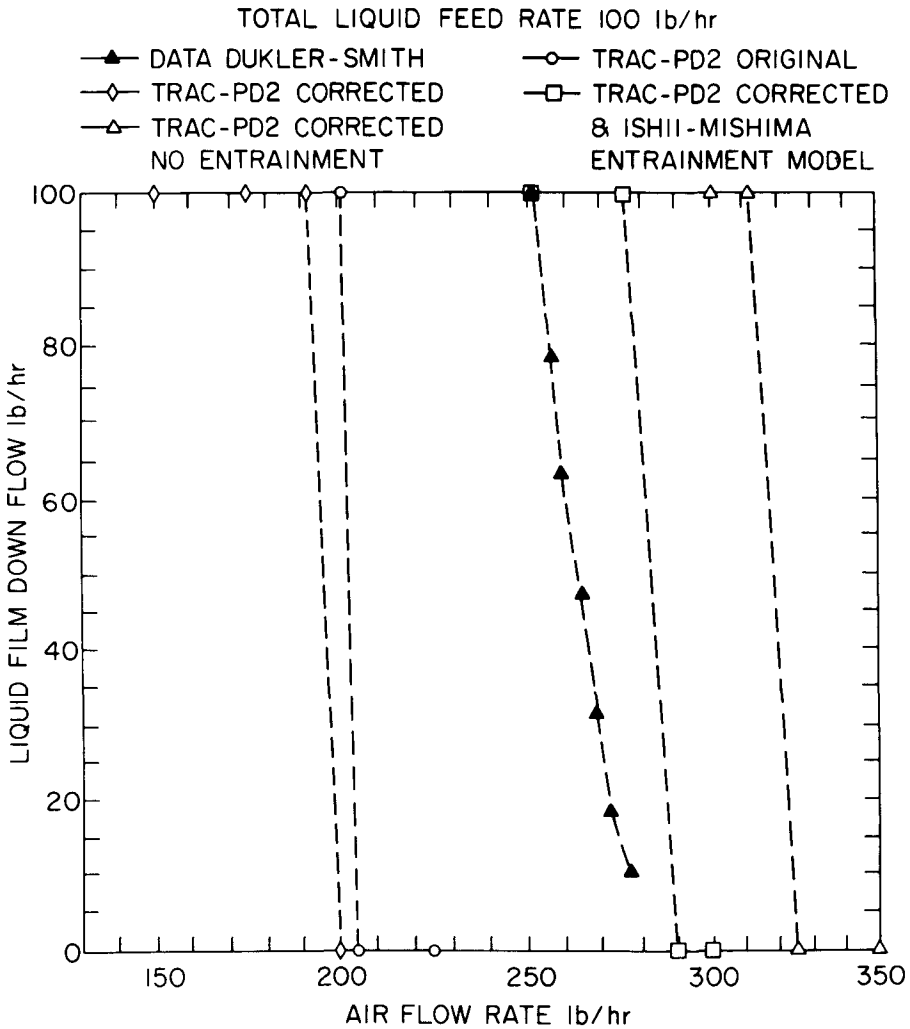

Figure 2.6.2 Comparison Between the Measured and Predicted Water Downflow Rates vs. Various Air Flow Rates for Water Feed Rate of 100 lb/hr. (BNL Neg. No. 6-1298-81)

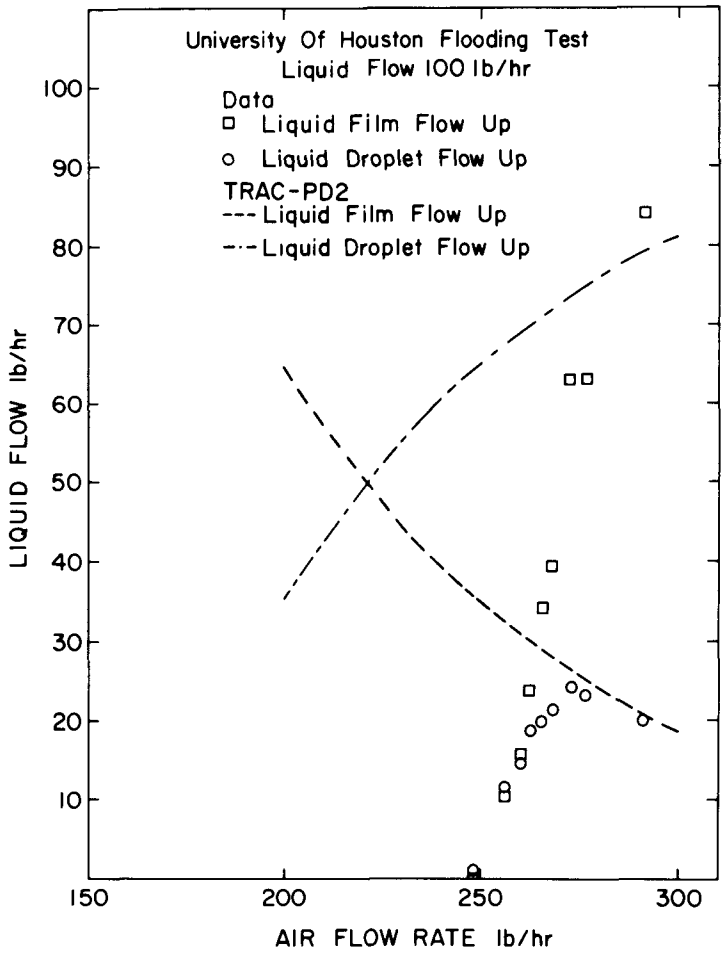

Figure 2.6.3 Comparison Between the Measured and Predicted Upflow of Liquid Film and Droplets. (BNL Neg. No. 3-636-82)

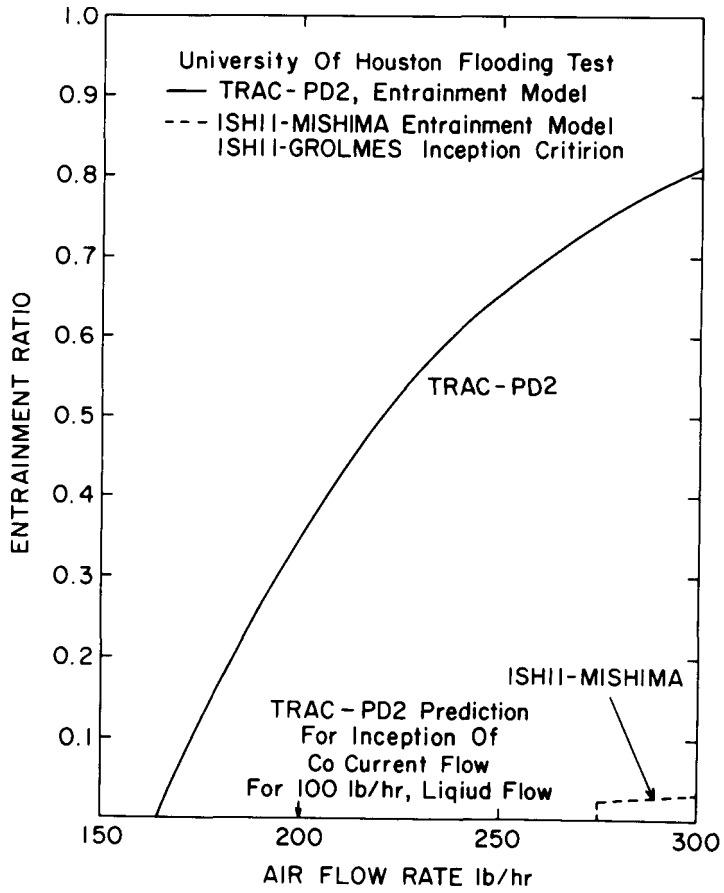

Figure 2.6.4 Comparison Between the TRAC-PD2 and Ishii-Mishima Entrainment Models for Water Feed Rate of 100 lb/hr. (BNL Neg. No. 3-637-82)

Finally, the Ishii and Mishima (1981) model for the entrainment ratio and the Ishii and Grolmes (1975) model for the inception of entrainment for rough films were incorporated in the BNL-corrected TRAC-PD2. As expected, the code now reversed the liquid flow at an air flow rate of approximately 275 lb/hr which is 10% higher than the experimental value of 250 lb/hr. The results of this calculation are shown by open squares in Figure 2.6.2. This and previous calculations show the importance of using an accurate entrainment model for the prediction of flooding phenomenon.

2.6.4.2 Water Feed Rate of 1000 lb/hr

Calculations with the BNL-corrected TRAC-PD2 were attempted for the water feed rate of 1000 lb/hr. The code produced stable solutions for the cases of no air flow and 100 lbs/hr (0.012583 kg/s) air flow rate. In both these cases, all the liquid flowed down. For the case of zero air flow, the void fraction obtained from the film thickness measurement at 146 cm below the water injection point (station A) near the bottom of the test section had a mean value of 0.95 and a minimum value of 0.87. The code predicted a void fraction of 0.98875, which indicates a higher liquid film velocity than in the experiment. Similarly for 100 lb/hr air flow rate, the interpolated mean and minimum values of void fraction were 0.95 and 0.85, respectively. The predicted values for the void fraction were between 0.9731 and 0.9878 for 5 seconds of transient calculation except at 4.5 seconds, when it computed a low value of 0.6645, probably a numerical artifice. As the air flow rate was increased to 200 lb/hr (0.025166 kg/s), the code failed to produce a stable solution. The predicted exit flow rate oscillated in the range of -0.0077 kg/s to 1.898 kg/s whereas the time-averaged experimental value was 0.0943 kg/s. The computed void fraction at station A varied between 0.8775 to 0.99197 during the 4.5 seconds of transient calculation, while the void fraction interpolated from the data had a mean value of 0.95 and minimum value of 0.85 at this position. It should be noted that this air flow rate of 200 lb/hr was larger than the air flow rate at the flooding point, i.e., 130 lb/hr, and TRAC-PD2 did predict some liquid upflow with the air.

From the above calculations, it can be concluded that the code always predicted a thinner liquid film which might be due to the way the code assigns the wall friction to the liquid and vapor phase. For a void fraction greater than 0.95, the code assigns the entire wall friction to the vapor phase and nothing to the liquid even though a liquid film exists on the wall. This has probably resulted in a higher liquid velocity and a thinner film in the above University of Houston test simulations.

Because of budget restrictions, the above calculations were not pursued in FY 1981. However, they will be restarted in FY 1982 with the TRAC-PF1 code (Liles, 1981b).

2.6.5 Discussion

The flooding phenomenon is controlled by the interfacial shear, wall shear, gravity, and the onset and rate of liquid entrainment. TRAC-PD2 calculates the interfacial shear on the liquid film by using the Wallis (1970) correlation, which may be on the lower side as indicated by Bharathan (1979). However, no direct assessment of this parameter was done by using the University of Houston tests.

Regarding the wall shear, the two-fluid model of TRAC-PD2 assigns the entire wall friction to the gas or vapor phase if the void fraction is greater than 0.95. This is not correct at least for the present tests where the void fraction was greater than 0.95 but a liquid film existed on the wall. However, an assessment of this "error" has not been made.

The TRAC-PD2 entrainment model is inadequate for predicting the present flooding tests. The model initiates entrainment at a lower air flow rate and calculates much higher entrainment rate than that observed in the experiment and calculated from the Ishii and Mishima (1981) model. The code developers at LANL stated (Liles, 1981a, p. 50) that the TRAC-PD2 entrainment model appeared to provide reasonable results for the FLECHT reflood tests. However, the situations in the University of Houston tests are completely different from the FLECHT tests where thermal and hydrodynamic effects were coupled. An agreement between the TRAC-PD2 predictions and the FLECHT tests does not guarantee the accuracy of the entrainment model. It is worth mentioning that TRAC-PD2 uses a static entrainment ratio, which is the fraction of liquid as droplets in a cell. However, all the entrainment correlations available in the literature provide the fraction of liquid flow rate in the droplet field and could be called dynamic entrainment ratio. These are generally obtained from the co-current flow data and can be converted to the static entrainment ratio if the liquid and gas velocities along with the relative velocity of the droplets are available. However, this transformation may not be valid for the counter-current flow. Furthermore, as TRAC-PD2 uses only one liquid velocity, i.e., the same velocity for the liquid in the film and as droplets, the dynamic and static entrainment ratio is the same. However, it is well-known that the liquid film and the droplets may move with different velocities and even in opposite directions.

2.6.6 Conclusions

The following conclusions can be drawn from the TRAC-PD2 simulation of the University of Houston flooding tests:

a) TRAC-PD2 underpredicted the air flow rate at the flooding onset. This was primarily caused by the early initiation and high rate of entrainment calculated by the code. More accurate entrainment correlation based on basic experiments seems to be needed for a better prediction.

b) A coding error in the interfacial shear coefficient for the annular-mist flow regime was discovered, and it was corrected at BNL. However, the correction did not change the code prediction significantly.

c) The partitioning of wall friction between the liquid and the gas phase should be done on a more physical basis. The present practice of assigning the entire wall friction to the gas phase when void fraction is greater than 0.95 may not agree with the reality for many situations.

d) Two liquid fields, namely the film and the droplets, should be used instead of one to calculate the annular-mist regime, particularly for the counter-current flow situations.

2.7 FRIGG-Loop Experiments

2.7.1 Objective

The FRIGG-Loop forced circulation tests (Nylund, 1968) were simulated with the TRAC-PD2 code in order to assess the code's capability to predict the steady-state axial void distribution in a heated rod bundle. Since subcooled water entered the bundle, these tests also provide data to verify the code's subcooled boiling model.

2.7.2 Test Description

FRIGG Tests (Nylund, 1968) were performed in a steam-water loop with a test section simulating the Marviken boiling heavy water reactor fuel assembly. The test section included a vertical electrically heated rod bundle with uniform radial and axial energy distributions mounted in a 0.159 m diameter shroud. The heated length of the bundle was 4.37 m; it contained 36 rods whose outside diameters were 0.0138 m. In the test series under consideration, subcooled water was introduced at the bottom of the test section. During the experiment, the pressure at the upper end of the rod bundle, mass flux and power were kept constant. Three-dimensional void fraction distributions in the bundle were measured with multi-beam gamma densitometers which provided approximately six percent accuracy for the area-averaged void fraction data.

Two forced circulation tests were simulated with TRAC-PD2. These were Run Nos. 313020 and 313007. The operating conditions of these tests are shown in Table 2.7.1.

Table 2.7.1 FRIGG-Loop Tests Simulated with TRAC-PD2

Test No.	Power (Q, kW)	Mass Flux (kg/m^2s)	Pressure (bar)	Inlet Subcooling (°K)	Exit Quality
313020	4155	1159	49.7	22.4	0.096
313007	1500	1110	50.0	11.7	0.022

2.7.3 TRAC Input Model Description

The test section was modeled by using the one-dimensional VESSEL module of TRAC-PD2. It was divided into 23 levels with one cell in each level. The axial lengths of the cells varied from 0.1 to 0.3 m such that the center of the computational cells coincided with the void measurement locations. The mass flow rate and fluid temperature boundary conditions at the entrance of the test section were provided by a FILL component, whereas a BREAK component was

employed at the test section exit to provide the pressure boundary condition. The nodalization is shown in Figure 2.7.1. Heat transfer in the rods was modeled using five radial nodes. However, no comparison of rod temperatures was made due to lack of experimental data.

Steady-state solutions were obtained by transient relaxation of the code. Unlike TRAC-P1A which did not produce a steady-state for FRIGG tests (Neymotin, 1980b), the TRAC-PD2 code yielded steady-states without any difficulty. This indicates that TRAC-PD2 has a better two-fluid computational algorithm than that of TRAC-P1A. Typical calculation took approximately 50 CPU seconds in the BNL CDC-7600 computer.

It should be mentioned that the three-dimensional VESSEL module could have been used to model the test section. However, it would be much more expensive than the one-dimensional representation. Furthermore, the one-dimensional calculation yielded sufficient information to evaluate the code's subcooled boiling model and the interfacial shear correlation.

2.7.4 Code Prediction and Comparison with Data

Figures 2.7.2 and 2.7.3 show the comparison between the predicted and the measured area-averaged void fraction distributions for Run Nos. 313020 and 313007, respectively. The dashed curves are the original TRAC-PD2 (Version 26.0) predictions which show significant underprediction of void fraction. This prompted a review of the code's constitutive package and the corresponding FORTRAN listing. A logic error was discovered in the subroutine TF3DE which inadvertently assigned the interfacial shear coefficient corresponding to the annular flow to the bubbly and bubbly-slug flow regimes when heated structures were present. Consequently, the original TRAC-PD2 calculated a much higher value of relative velocity and a much lower value of void fraction for the bubbly and bubbly-slug regimes.

The above error was corrected at BNL and both the tests were recomputed using the corrected version of TRAC-PD2. The predicted area-averaged void fractions are indicated by the chain-dotted curves in Figures 2.7.2 and 2.7.3. It is clear that TRAC-PD2 now predicts the high void fraction data very accurately. Also, the computed relative velocity for Run 313020, as shown in Figure 2.7.4, indicates reasonable agreement with the relative velocity calculated from the drift-flux models. As such, the interfacial shear coefficients of TRAC-PD2 appear to be adequate for predicting the high void fraction data where bulk boiling occurs. However, it is also clear from Figures 2.7.2 and 2.7.3 that TRAC-PD2, even with BNL corrections, is inadequate at the low void fraction region where subcooled boiling persists. This initiated a review of the TRAC's subcooled boiling model.

The principal features of the subcooled boiling model as implemented in TRAC-PD2 are depicted in Figure 2.7.5. Subcooled boiling occurs if $T_{liquid} \leq T_{sat}$, $T_{wall} \geq T_{sat}$ and the void fraction is less than 0.1. If this is the case, a condensation rate based upon twice the wall-to-liquid heat transfer area, liquid subcooling and a condensation heat transfer coefficient based on Stanton number, St, equal to 0.02 is calculated. The net amount of heat transferred from the wall to the fluid is then split into two parts: a) heat received by the liquid through laminar or turbulent forced

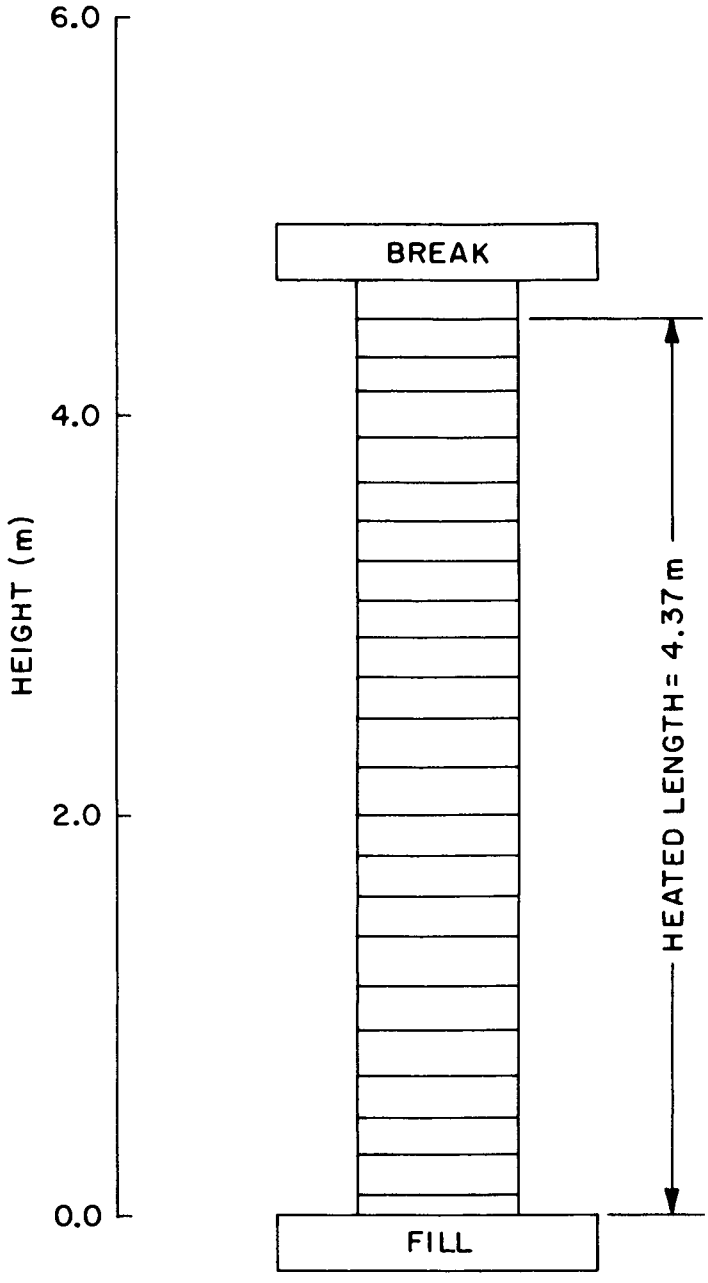

Figure 2.7.1 TRAC Nodalization of the FRIGG-Loop Test Section. (BNL Neg. No. 2-889-82)

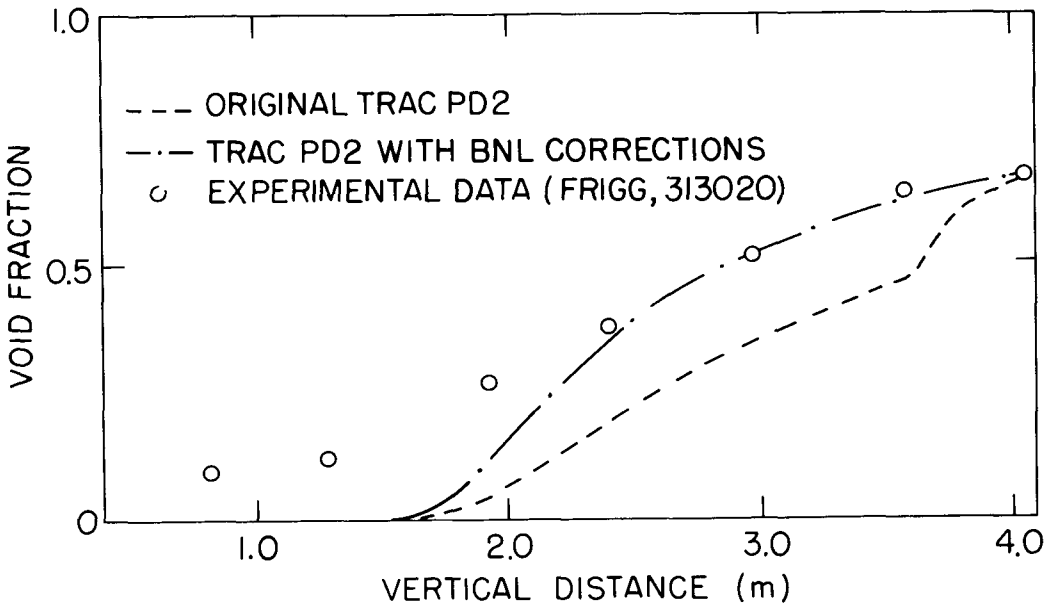

Figure 2.7.2 Comparison Between the Measured and Predicted Area-Averaged Axial Void Distribution for FRIGG Run 313020. (BNL Neg. No. 1-716-81)

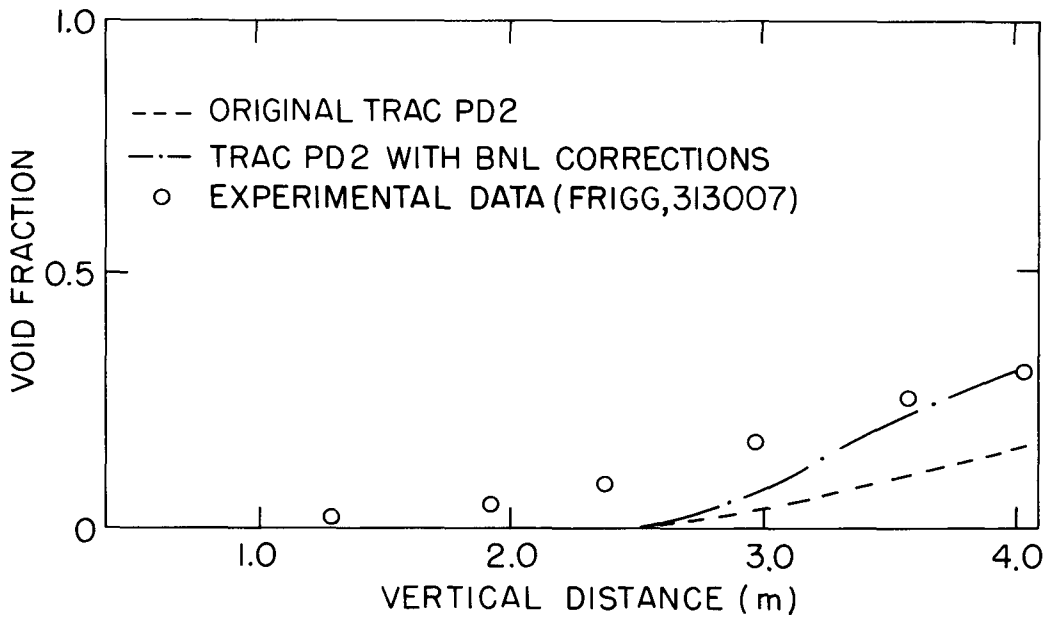

Figure 2.7.3 Comparison Between the Measured and Predicted Area-Averaged Axial Void Distribution for FRIGG Run 313007. (BNL Neg. No. 1-718-81)

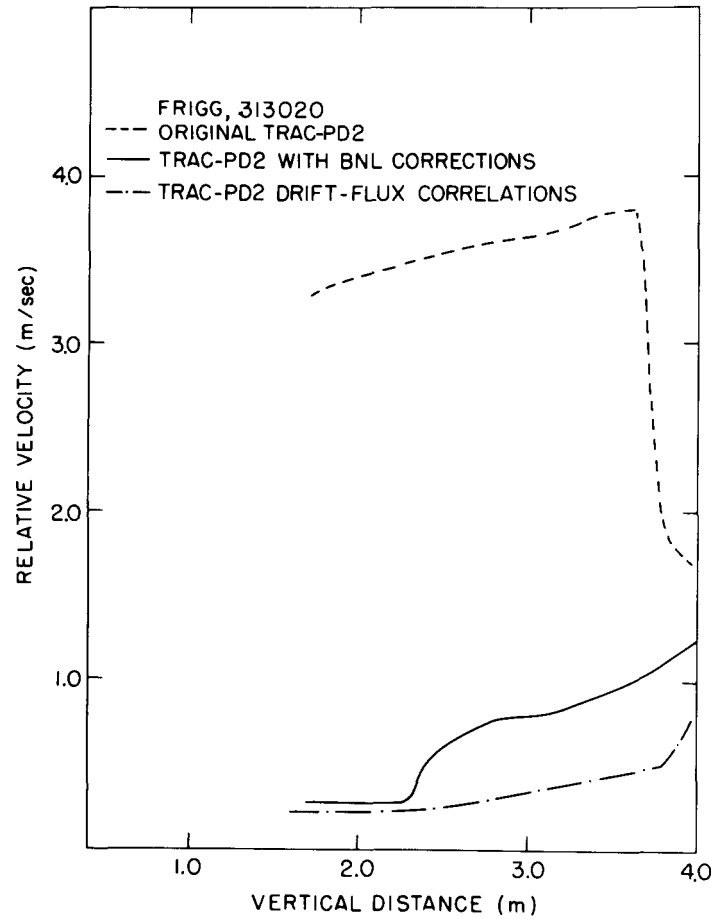

Figure 2.7.4 Comparison Between the Calculated Relative Velocities From TRAC-PD2 Two-Fluid and Drift-Flux Models. (BNL Neg. No. 3-793-82)

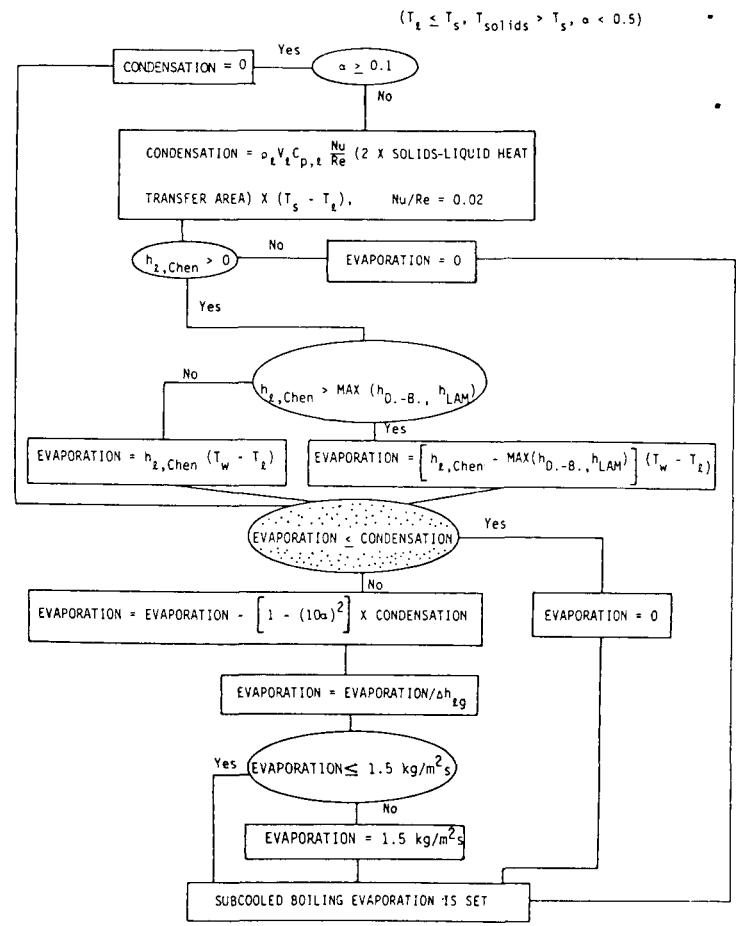

Figure 2.7.5 Principal Features of the TRAC-PD2 Subcooled Boiling Model. (BNL Neg. No. 2-881-82)

convection, and b) heat transmitted through the mechanism of nucleate boiling. The splitting is done using the Chen correlation (Liles, 1981a). The nucleate boiling heat transfer and the condensation rate are compared at this point (dotted area of Figure 2.7.5). If condensation prevails, no net vapor generation is assumed. Otherwise, the net vapor generation rate is calculated as the difference between the nucleate boiling vapor generation rate and the condensation rate. During the calculation a coefficient of $1 - (10\alpha)^2$ is used, with the apparent reason of driving the condensation rate to zero at α = 0.1. Also, an artificial upper limit of 1.5 kg/(m^2s)is set for the net vapor generation rate per unit of heated surface area.

It is clear from the model description that the condensation rate has a significant impact on the predicted net vapor generation rate in the subcooled boiling regime. It also affects the onset of net vapor generation. An overestimation of the condensation rate not only shifts the onset point towards the location where the equilibrium quality, X_{eq}, is equal to zero, but also lowers the rate of vapor generation. An underestimation of the condensation rate has the reverse effect.

The correlation for condensation rate used in the subcooled boiling model, i.e., Stanton number equal to 0.02, was obtained from a number of experiments on condensation of vapor on subcooled liquid jets and is not appropriate for condensation of vapor bubbles in subcooled liquid. Sensitivity studies revealed that a reduction in the condensation rate improves the predictions at the low void fraction region significantly. A value of 0.0018 for the Stanton number produced results which were in very good agreement with the data of Run 313020. This is shown by the solid curve in Figure 2.7.6. It should be stressed, however, that this value of the Stanton number (0.0018) was found to produce excellent result for a particular run, but it is not recommended for general use. Instead, a mechanistic condensation heat transfer coefficient applicable for bubble collapse in subcooled liquid should be used.

2.7.5 Discussion

The original TRAC-PD2 (Version 26.0) predictions were in poor agreement with the area-averaged void fraction data of both the FRIGG tests simulated at BNL. However, after a coding error was corrected, the code gave excellent results for the high void fraction region. This implies that the interfacial shear relations used in the code are most likely adequate for the bulk boiling regime. However, the subcooled boiling model of the code is very poor and needs improvement. A possible course of action would be to use a correlation for the point of net vapor generation and then use a "mechanistic" or "profile-fit" model for the rate of vapor generation in subcooled boiling region. Such a model has been recommended by BNL (Saha, 1981) for inclusion in the future version of TRAC.

2.7.6 Conclusions

The following conclusions can be drawn from the simulation of two FRIGG tests with TRAC-PD2:

a) The BNL corrected version of TRAC-PD2 produced excellent results for the area-averaged void fraction in the upper part of the bundle. Therefore, it may be inferred that the interfacial shear coefficients of TRAC-PD2 are adequate in the bulk boiling regime.

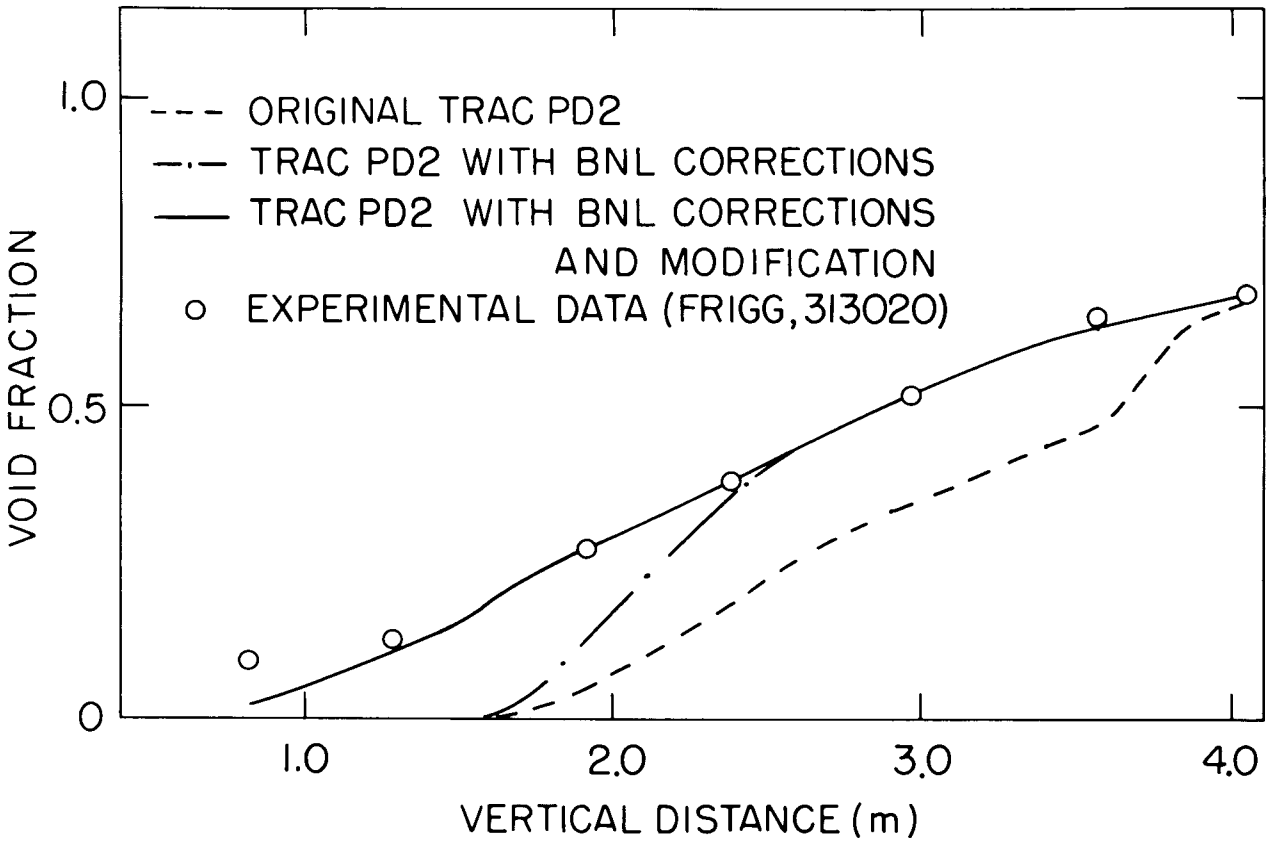

Figure 2.7.6 Comparison Between the Computed and the Measured Area-Averaged Void Fraction Data for the FRIGG-Loop Test 313020 (BNL Neg. No. 1-715-81)

b) The subcooled boiling model of TRAC-PD2 is very poor. The main reason for this seems to be the use of a very high value of Stanton number for condensation calculation. Moreover, the condensation model used in the code is inappropriate for bubble condensation.

c) A better agreement may be obtained at low void fraction region by reducing the effect of condensation. Alternatively, a correlation for the point of net vapor generation along with a "mechanistic" or "profile-fit" model for actual vapor generation may be used.

2.8 B&W Steam Generator Tests

2.8.1 Objective

The B&W steam generator tests (Loudin, 1976) were simulated with TRAC-PD2 in order to assess the code's capability to predict the performance of Integral Economizer Once-Through Steam Generators (IEOTSG) during load changes. An accurate prediction of the steam generator thermal performance is crucial for the best-estimate analysis of PWR's during a small-break or a plant transient situation. In the present simulation, the once-through STEAM GENERATOR component of TRAC-PD2 was exercised.

2.8.2 Test Description

The test apparatus was a laboratory steam generator which was a single-pass, counter-current, vertically oriented shell and tube heat exchanger. It consisted of 19 tubes, 5/8 inch in nominal diameter (with 0.628 inch in outside diameter and 0.0365 inch in wall thickness), spaced on a triangular pitch of 7/8 inch-centers. The tube bundle was enclosed in a hexagonal shell 3.935 inches across flats and was held in place by 16 tube support plates spaced at approximately 3 feet intervals. The distance between the lower and the upper tube sheets was 52 feet and 1-3/8 inches. To simulate the standard B&W Once-Through Steam Generators (OTSG), a steam bleed line was installed at an elevation of 32' - 3/8" from the lower tube sheet. Thus some steam from the bundle region could mix with feedwater and raise its temperature close to saturation. On the other hand, by simply closing the valve in the bleed line one could simulate the Integral Economizer Once-Through Steam Generators (IEOTSG).

A variety of transient experiments were conducted in both the OTSG and IEOTSG configurations. Since the OTSG component of TRAC-PD2 did not include models for the aspirator (or, the steam bleed line), only the IEOTSG configuration has been simulated. Specifically, two test series have been simulated at BNL. These are:

a) Series 68-69-70 where the load was increased from 15% to 25% by stepping up the steam valve opening, and

b) Series 74-75-76 where the load was increased from 55% to 65% by stepping up the feedwater valve opening.

In both cases, the operating pressures and temperatures were representative of the full-scale plant conditions, and all the pertinent variables at the primary and secondary sides were measured. These included the pressure, flow rate, inlet and exit fluid temperature at the primary side, and the feedwater

flow rate and temperature, steam pressure and temperature, and differential pressure at the secondary side. The data are proprietary to B&W and the measurement uncertainties were not available in the data report (Loudin, 1976).

2.8.3 TRAC Input Model Description

The test apparatus was modeled by using the once-through option of STEAM GENERATOR component of TRAC-PD2. The thermohydraulics of the primary and secondary sides are based on the one-dimensional drift-flux model similar to that used in the PIPE component, and the heat transfer from one side to the other takes place through radial conduction in the tube wall.

Three different nodalizations were studied for each test series. In all cases, the primary side had two more cells than the secondary side to represent the inlet and outlet plena. This is required by TRAC. The number of active nodes in the primary and secondary sides were increased from 10 to 20 to 40. In all cases the cell lengths were uniform and the active length of the steam generator was 15.9 m. Four radial nodes were employed in the tube wall for heat conduction calculations.

The boundary conditions were imposed by a set of FILL and BREAK components at the inlet and exit of the primary and secondary sides. A steady-state was established for each test series. The transient was then initiated by changing the boundary conditions.

For the simulation of both of the test series, the flow rate, inlet temperature and exit pressure at the primary side were specified as functions of time. The feedwater flow rate and temperature were also specified. In addition, for test series 68-69-70, the steam flow rate at the exit of the secondary side was specified and the pressure at the secondary side was calculated by the code. For test series 74-75-76, however, two types of boundary conditions were applied at the exit. In one case, the steam flow rate was specified and the secondary side pressure was computed. This was similar to the simulation of the test series 68-69-70. In the other case, the pressure at the exit of the secondary side was specified and the exit steam flow rate was computed. Thus both types of boundary conditions were studied.

The CPU time required for these calculations was highly dependent on the number of cells employed. Table 2.8.1 shows the CPU time required for the test series 74-75-76 in the BNL CDC-7600 computer. The computing time for the test series 68-69-70 was close to the numbers shown in Table 2.8.1.

Table 2.8.1 Summary of Computer Time for TRAC-PD2 Calculation of B&W Steam Generator Test

Series No.	No of Cells	Steady-State		Transient	
		Problem Time (s)	CPU Time (s)	Problem Time (s)	CPU Time (s)
74-75-76	10	60	30	50	40
	20	60	40	50	50
	40	60	120	50	130

2.8.4 Code Prediction and Comparison with Data

Figures 2.8.1(a) through 2.8.1(c) show the TRAC-PD2 results for Series 68-69-70 for various nodalizations. The experimental data for the primary exit water temperature, secondary exit steam temperature and the secondary side pressure are also shown in these figures. However, the vertical scales are withheld because the data are B&W proprietary. It can be seen that the TRAC results are highly dependent on nodalization, and as expected, the prediction approached the data as the number of cells was increased. The magnitude of oscillation in the calculated variables also decreased as the number of cells increased. Although there were some discrepancies between the data and the calculation with 40 nodes in each side of the steam generator, the prediction with 40 nodes may be considered as satisfactory. It is worth mentioning that because of poor resolution, there was some error in reading the data from the B&W report.

Figures 2.8.2(a) through 2.8.2(c) show the comparison for the Series 74-75-76. In this calculation the secondary side exit pressure was used as a boundary condition. Therefore, the code calculated the exit steam flow rate. The prediction for this series shows the same trend as the Series 68-69-70. The magnitude of oscillation decreased as the number of cells was increased and, in general, the agreement with data was better for the 20 or 40 node calculations than the 10 node calculation.

Figures 2.8.3(a) through 2.8.3(c) show the results of the second TRAC calculation with 40 nodes for Series 74-75-76. Here the secondary side exit steam flow rate was specified and the code calculated the secondary side pressure which is shown in Figure 2.8.3(c). It can be seen that although the primary side water temperature and the secondary side steam temperature were predicted well, the secondary side pressure was underpredicted to some extent. Also, significant oscillations were present even in the 40 node calculation.

2.8.5 Discussion

The results presented in Section 2.8.4 show that TRAC-PD2 is capable of predicting the trend of the flow variables during load changes. However, the steam generator must be nodalized very finely to obtain accurate results. Even in that situation, the calculation may show significant fluctuations in the computed variables. These oscillations seem to be caused by the fluctuating heat transfer. A detailed check of the TRAC results shows that the selection of heat transfer regime is very sensitive to the steam quality in the low and high quality regions, and the heat transfer coefficient vary widely. A fine nodalization limits this abrupt change of heat transfer to a smaller value and, thus, tends to limit the magnitude of oscillations. It is worth noting that even with 40 cells in each side, the present calculations show some oscillations.

One possible way to resolve the above problem might be to track the two-phase mixture level through the fixed mesh nodalization scheme of TRAC. Alternatively, a number of fine cells may be inserted in the coarse mesh cell where the two-phase mixture level would be expected to reside at a given time. This is similar to the fine mesh rezoning technique used in the fuel conduction model during reflood.

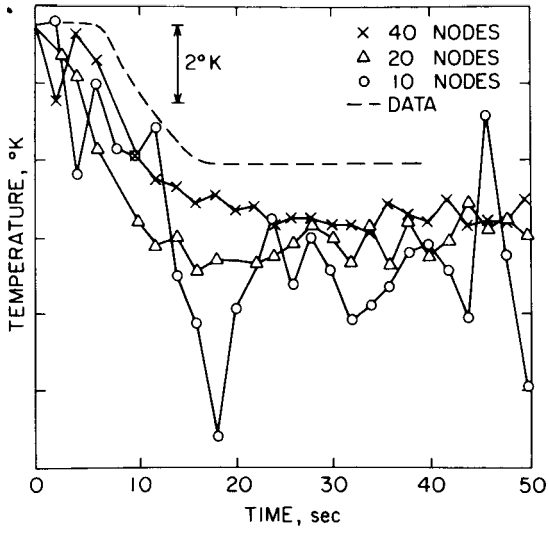

(a) Primary Side Exit Water Temperature vs. Time. (BNL Neg. No. 7-580-81)

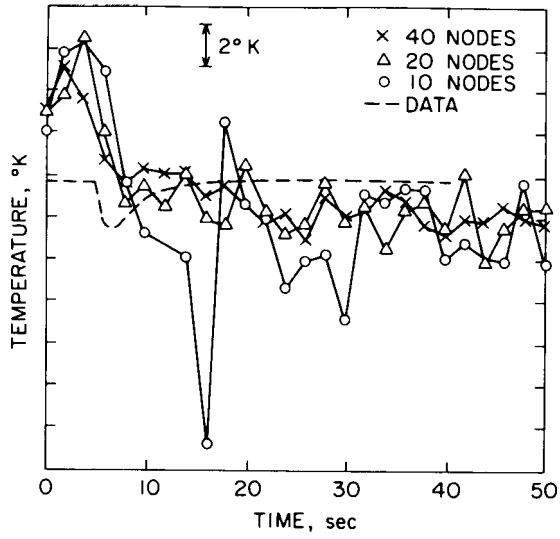

(b) Secondary Side Exit Steam Temperature vs. Time. (BNL Neg. No. 7-578-81)

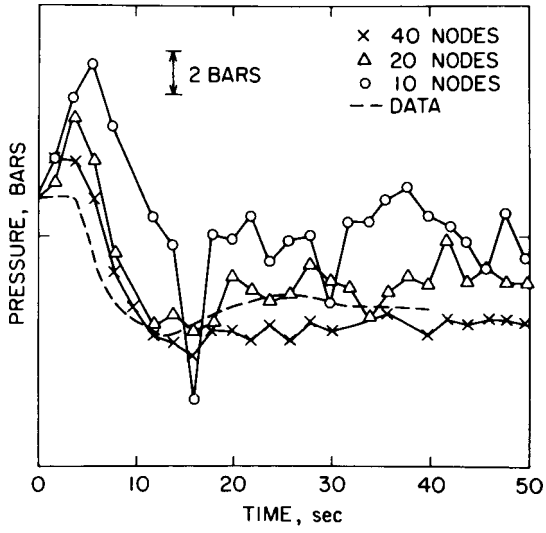

(c) Secondary Side Exit Steam Pressure vs. Time. (BNL Neg. No. 7-581-81)

Figure 2.8.1 Comparison Between the Data and TRAC-PD2 Predictions for Test Series 68-69-70.

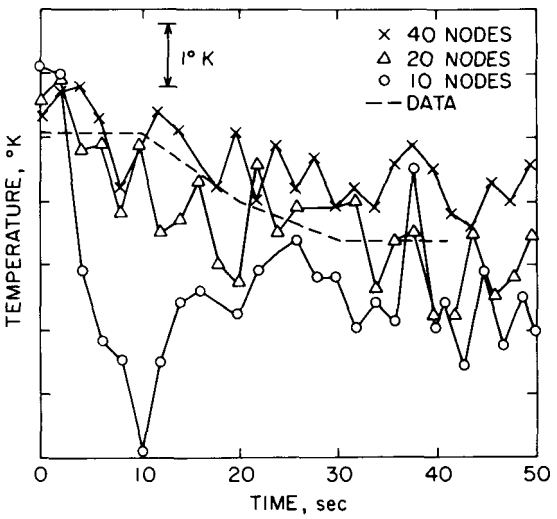

(a) Primary Side Exit Water Temperature vs. Time. (BNL Neg. No. 7-579-81)

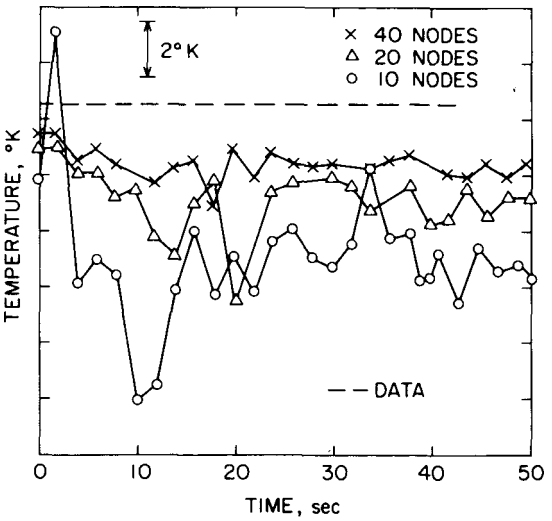

(b) Secondary Side Exit Steam Temperature vs. Time. (BNL Neg. No. 7-576-81)

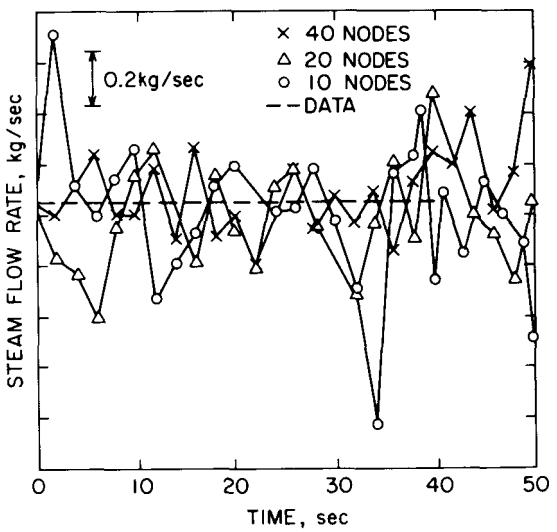

(c) Secondary Side Exit Steam Flow Rate vs. Time. (BNL Neg. No. 7-577-81)

Figure 2.8.2 Comparison Between the Data and TRAC-PD2 Predictions for Test Series 74-75-76(with Secondary Side Exit Pressure Boundary Condition).

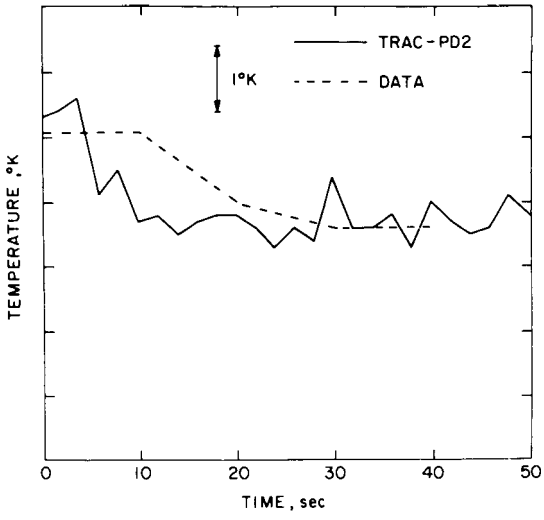

(a) Primary Side Exit Water Temperature vs. Time. (BNL Neg. No. 2-875-82)

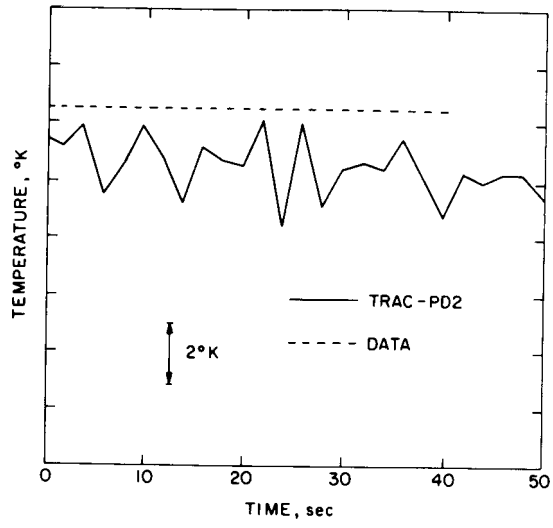

(b) Secondary Side Exit Steam Temperature vs. Time. (BNL Neg. No. 2-876-82)

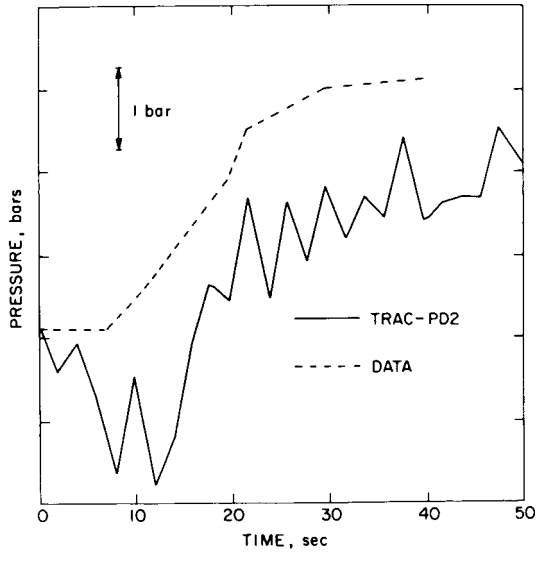

(c) Secondary Side Exit Steam Pressure vs. Time. (BNL Neg. No. 2-877-82)

Figure 2.8.3 Comparison Between the Data and TRAC-PD2 Prediction for Test Series 74-75-76 (with Secondary Side Exit Steam Flow Rate Boundary Condition).

2.8.6 Conclusions

The following conclusions may be drawn from the simulation of the B&W Steam Generator tests with TRAC-PD2:

a) The code can predict the trends during the load following transients. The prediction improves as a finer nodalization is used.

b) The code can accept either a pressure or a steam flow rate boundary condition at the exit of the secondary side.

c) Significant oscillations were observed in TRAC calculations even with a fine nodalization. This problem should be resolved by the code developers. Possible courses of action have been suggested.

2.9 FLECHT-SEASET Bottom Reflood Experiment

2.9.1 Objective

The FLECHT-SEASET bottom reflood test No. 31504 was simulated with TRAC-PD2 in order to assess the code's capability to predict the reflood stage of a hypothetical large break LOCA. A two-dimensional conduction model with a fine-mesh rezoning technique, similar to that in the COBRA code (Thurgood, 1981), is used in TRAC-PD2 to determine the quench front location during reflood. This represents a major change from the reflood model of TRAC-P1A.

Since the quench front propagation is affected by channel hydrodynamics, wall heat transfer as well as rod heat conduction, this simulation will assess the combined effects of many thermohydraulic models used in the code during a bottom reflood situation.

2.9.2 Test Description

The FLECHT-SEASET reflood experiments (Hochreiter, 1978) have been performed in a vertically oriented cylindrical vessel of 0.194 m in inside diameter and approximately 4.5 m in height. A 161-rod bundle installed in the vessel included an electrically heated section of 3.66 m in length with a cosine axial power distribution. The maximum power region extended from approximately 1.6 m to the 2.0 m elevation. The outside diameter of the heated rods was 0.0095 m. The experiment was initiated with a bottom injection of cold water into the steam-filled initially preheated rod bundle. The bundle exit pressure was maintained at constant value during the transient. Electrical power was varied with time according to the ANS Standard + 20% of Decay Power. The specific conditions of the simulated Run 31504 were as follows: water injection rate = 0.0254 m/s, ΔT_{sub} = 79°K, P_{exit} = 0.277 MPa, initial power = 0.79 MWt, initial maximum clad temperature = 1126°K.

The experiment under consideration lasted for approximately 600 seconds until all the rods were quenched. During the course of transient, a 256 channel data acquisition system was used to record rod surface temperatures at 19 elevations throughout the bundle. Pressure, differential pressure as well as fluid, steam and structure temperatures were also recorded at different rod bundle locations and in out-vessel test components.

2.9.3 TRAC Input Model Description

The one-dimensional option of the TRAC-PD2 VESSEL component with 17 axial levels (nodes) was used for this simulation. The hydraulic mesh sizes varied from 0.2 m to 0.6 m and the nodalization is shown in Figure 2.9.1. At the beginning of reflood, according to the code calculational logic each heat conduction cell was subdivided into a number of fine permanent meshes (from three to six for different cells) in order to get desirable initial and transient rod surface temperature and axial power distribution representation. During the calculation additional transitory fine nodes are inserted for a better resolution of the rod surface temperature in the quench front vicinity. The total number of axial rod conduction nodes was prescribed not to exceed 150. Nine radial nodes were used in the rod heat conduction calculations. For the stable minimum film boiling temperature the homogeneous nucleation temperature option was chosen.

The boundary conditions were provided by using a FILL to provide constant mass flow rate from the lower plenum and a BREAK to specify a constant pressure at the vessel top.

TRAC-PD2 with BNL corrections, as discussed in Section 2.7.4, was used to perform the calculation. The calculation was terminated when the rods were quenched up to a specified elevation above the maximum power generation region. The trend of the calculation was clear at this point and further computation could not be justified in view of limited computer budget. The calculation took 12800 CPU seconds in the BNL CDC-7600 computer for 422 seconds of transient.

2.9.4 Code Prediction and Comparison with Data

The calculated rod surface temperatures at different elevations are compared to the experimental data in Figures 2.9.2 through 2.9.5. The shaded areas show the experimental scatter for the maximum ($\langle T_m \rangle$) and quench ($\langle T_q \rangle$) temperatures as well as for the corresponding moments of transient ($\langle t_m \rangle$ and $\langle t_q \rangle$) whenever the maximum temperature at a particular elevation was encountered (turn around time) or quenching occurred.

Figure 2.9.2 shows the comparison between the predicted and the measured surface temperature at the 0.3 m (1 ft) level. Needless to say that the TRAC-PD2 prediction is in poor agreement with the data. However, it should be emphasized that the length of the first hydraulic cell was 0.6 m. Since TRAC does not track the mixture level within a cell, the predicted thermohydraulic condition at the 0.3 m level, i.e., the average condition in the first cell, was quite different from what was experienced by the thermocouple at 0.3 m level. This is probably the reason for the severe underprediction of surface temperature and quench time. The prediction would most likely improve if several hydraulic cells were used at the bottom part of the test section.

Figure 2.9.3 shows the comparison between the predicted and the measured surface temperature at 1.22 m (4 ft) elevation. Good agreement between the prediction and data was obtained, although the predicted surface temperature showed some oscillations. Reasonable agreement was also obtained at the maximum power region as shown in Figure 2.9.4 where the predicted surface temperature has been compared with the data at 1.98 m (6 ft 6 inch) elevation.

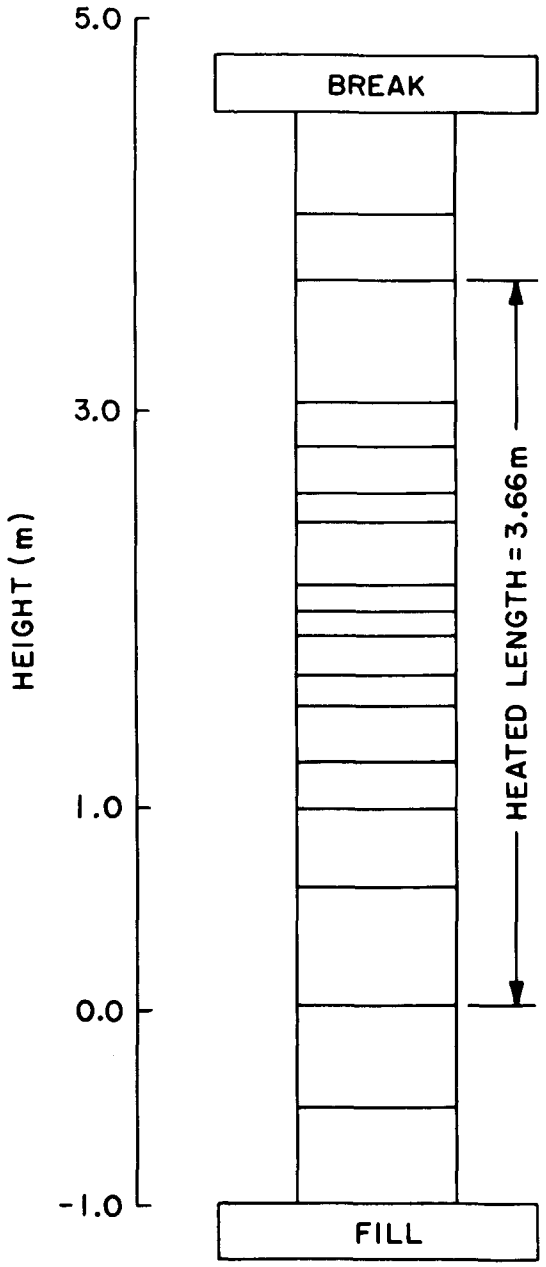

Figure 2.9.1 TRAC Nodalization of the FLECHT-SEASET Reflood Test Section. (BNL Neg. No. 2-892-82)

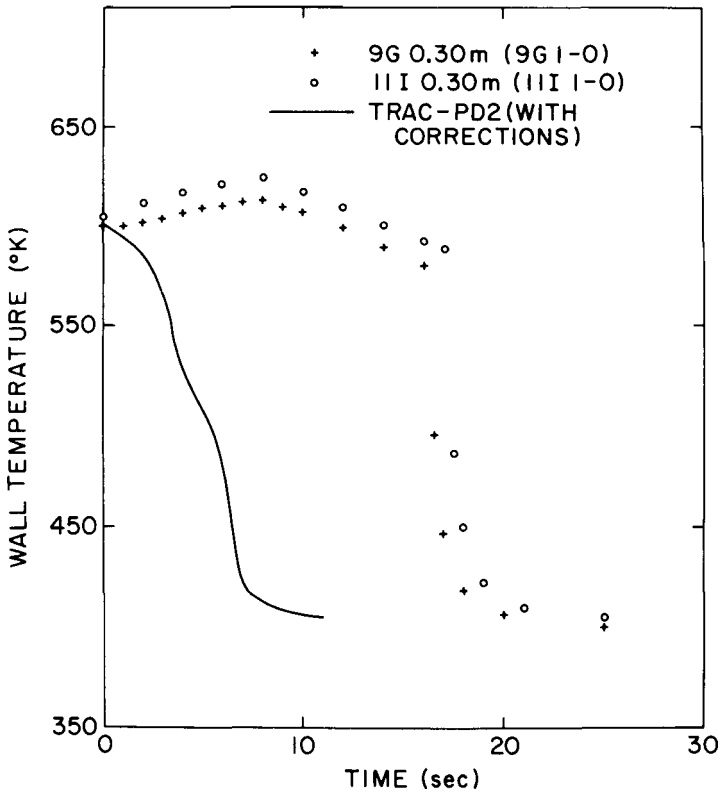

Figure 2.9.2 Comparison Between the Measured and Predicted Rod Surface Temperature at 0.3 m Elevation. (BNL Neg. No. 2-882-82)

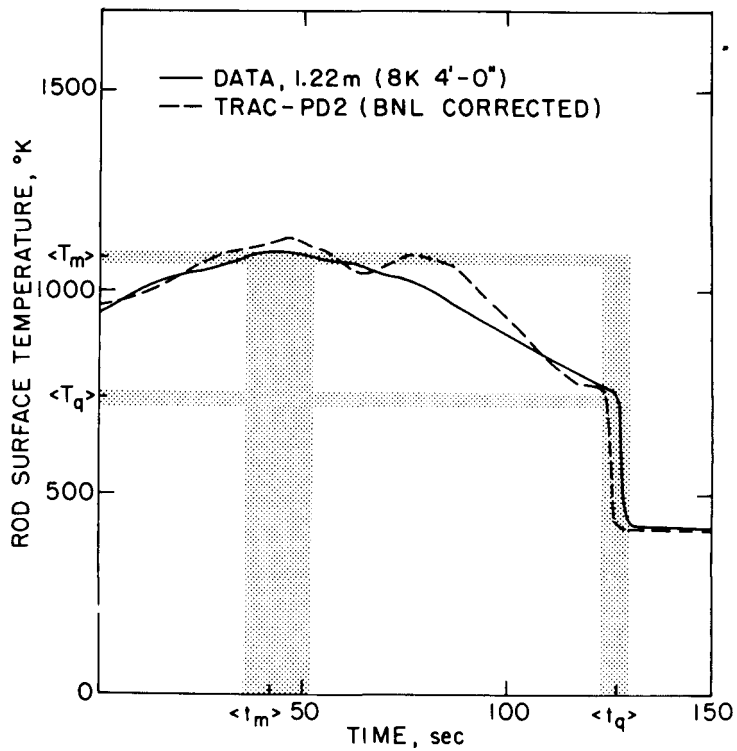

Figure 2.9.3 Comparison Between the Measured and Predicted Rod Surface Temperature at 1.22 m Elevation. (BNL Neg. No. 5-1162-81)

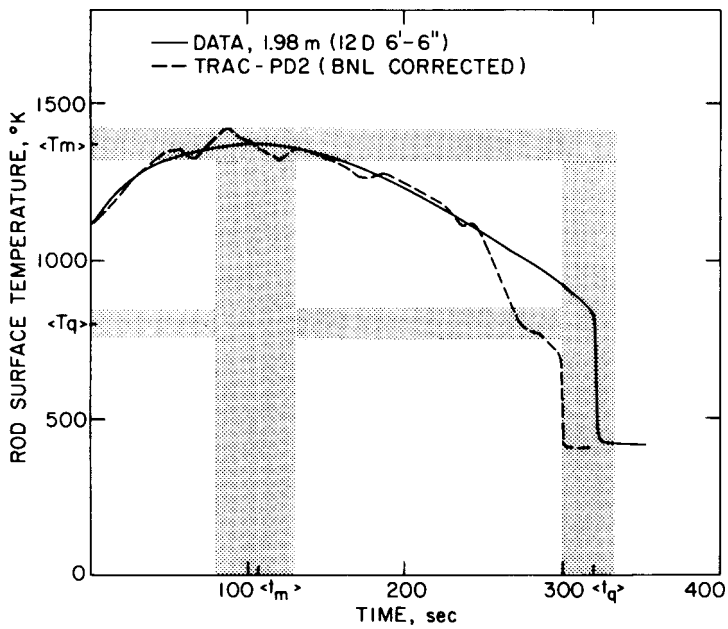

Figure 2.9.4 Comparison Between the Measured and Predicted Rod Surface Temperature at 1.98 m Elevation.(BNL Neg. No. 5-1163-81)

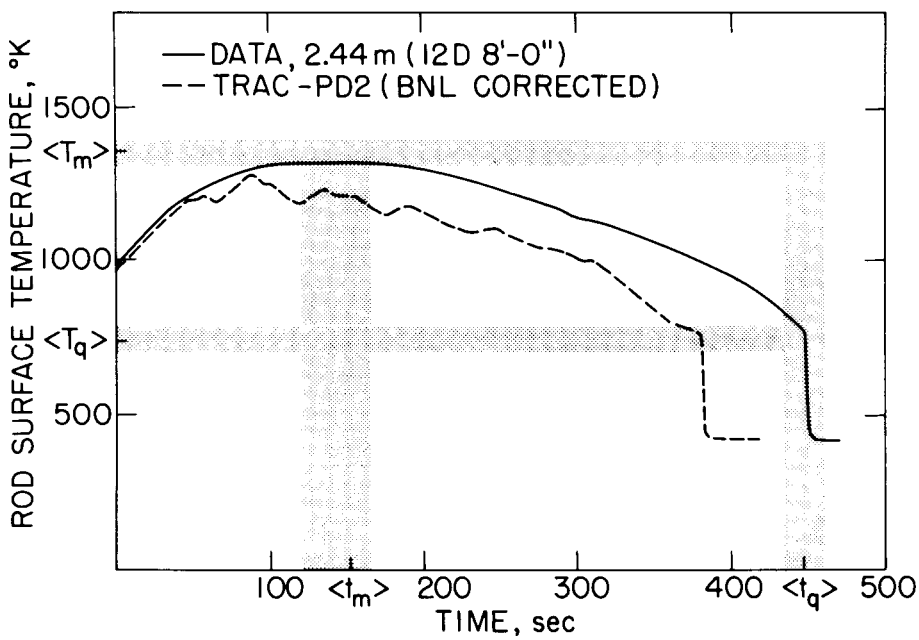

Figure 2.9.5 Comparison Between the Measured and Predicted Rod Surface Temperature at 2.44 m Elevation.(BNL Neg. No. 5-1165-81)

However, from this elevation and up, the code started to underpredict the quench time. This is depicted in Figure 2.9.5 where the predicted surface temperature has been compared with the data at 2.44 m (8 ft) elevation.

The above figures show that TRAC-PD2 (with BNL corrections) predicted the peak cladding temperature quite well. However, the predicted surface temperatures displayed some oscillations not observed in the experiment. The oscillations were mainly due to sharp changes in the heat transfer coefficients which were associated with two-phase slugs moving up and, sometimes down the bundle. The slugs were surrounded by high void fraction regions (or mixtures) with relatively low wall-to-fluid heat transfer characteristics. In addition, oscillations of other field variables such as liquid and vapor velocities, vapor temperature, outflow mass rate and some others were found in the calculations.

2.9.5 Discussion

From the results presented in the earlier section, it is clear that TRAC-PD2 with the BNL correction has predicted the surface temperature at the low-to-middle part of the rod bundle quite well. The poor agreement at the bottom part (0.3 m level) is probably due to the large hydraulic cell employed, and a finer hydraulic nodalization would probably improve the prediction. However, the reason for underprediction of surface temperature in the upper part of the bundle is not that clear.

Several factors may have contributed to the underprediction of quench time in the upper part. First, the interfacial shear package of TRAC-PD2 may underpredict the relative velocity for low mass-fluxes. This idea is supported by TRAC's overprediction of the Battelle-Frankfurt level swell test (see Section 2.5). An underprediction of relative velocity can cause the "mixture level" to rise faster than in the experiment and eventually quench the rods earlier. Secondly, early quench at a particular elevation may also enhance the precursory cooling at a higher elevation. This is accomplished through a higher steam flow rate and a lower steam superheat at the higher elevation. Figure 2.9.5 tends to support this notion. Here the predicted surface temperature had been significantly lower than the data long before the quench front arrived. Finally, the overprediction of entrainment rate as indicated in Section 2.6 also contributes to the underprediction of rod surface temperature.

2.9.6 Conclusions

The following conclusions may be drawn from the simulation of FLECHT-SEASET Test No. 31504 with the BNL-corrected version of TRAC-PD2:

a) The peak cladding temperature at the maximum power region was predicted quite well.

b) The code underpredicted both the surface temperature and the quench time at the bottom and the upper part of the bundle.

c) A finer nodalization at the bottom part would most probably improve the code prediction for the lower region.

d) The discrepancy at the upper region is most likely caused by the enhanced precursory cooling.

e) Oscillations in flow variables were observed in the TRAC calculation. These have caused some oscilation in the predicted surface temperature. However, these oscillations did not significantly affect the predicted peak cladding temperature and quenching time.

2.10 RPI (1x3) Phase Separation Experiment

2.10.1 Objective

The RPI (1x3) steady-state phase separation tests (Lahey, 1978) were simulated with TRAC-PD2 in order to assess the code's capability in predicting the lateral and axial void migration (or separation) in a two-dimensional air-water system. The phase separation phenomenon is governed by the combination of phasic inertia, gravity, interfacial shear, turbulent mixing, wall shear and the pressure gradient. Thus, the code's performance in predicting these tests depends on the combined effects of the interfacial and wall shear models built into the code. It should be noted that TRAC-PD2 does not include the effect of turbulent mixing in either the liquid or the vapor (or gas) phase.

2.10.2 Test Description

The test apparatus consisted of a vertically oriented rectangular channel with 0.914 m (3 ft) in height, 0.3 m (1 ft) in width and 0.0127 m (1/2-inch) in depth. A mixing tee was connected at the bottom through which an air-water mixture entered the channel via a 0.0508 m x 0.00953 m rectangular opening. Also, two horizontal pipes were attached near the top of the channel through which the two-phase mixture left the test section. The schematic of the RPI test apparatus is shown in Figure 2.10.1.

There was a provision for inserting 24 vertical rods of 0.00635 m (1/4 inch) outside diameter with equal spacing of 0.0127 m (1/2-inch) inside the test vessel. Some tests were conducted with the rods in the test channel and the rest were performed without them. In some tests both the exit pipes were open, and in the remaining tests only one exit pipe was operational. The air and water flow rates and their temperatures were measured individually at the entrance to the mixing tee. The pressure was measured only at the center of the test channel. In all the tests, the system pressure was near-atmospheric. The void migration, i.e., the phase separation, was determined by measuring the line-average void fraction at 20 locations (four rows with five stations in each row) by a gamma densitometer. The void fraction measurement locations are also shown in Figure 2.10.1. The duration of sampling period was chosen to yield better than 1% accuracy from the point of view of count statistics. However, from a repeatability study, the void fraction data should be considerd to be accurate within a few percent ($\sim$ 5%).

Tests were performed with low (0.257%) and high (1.09%) quality air-water mixtures. In the current assessment effort, three tests with rods inside the channel box were simulated. The operating conditions of these tests are shown in Table 2.10.1.

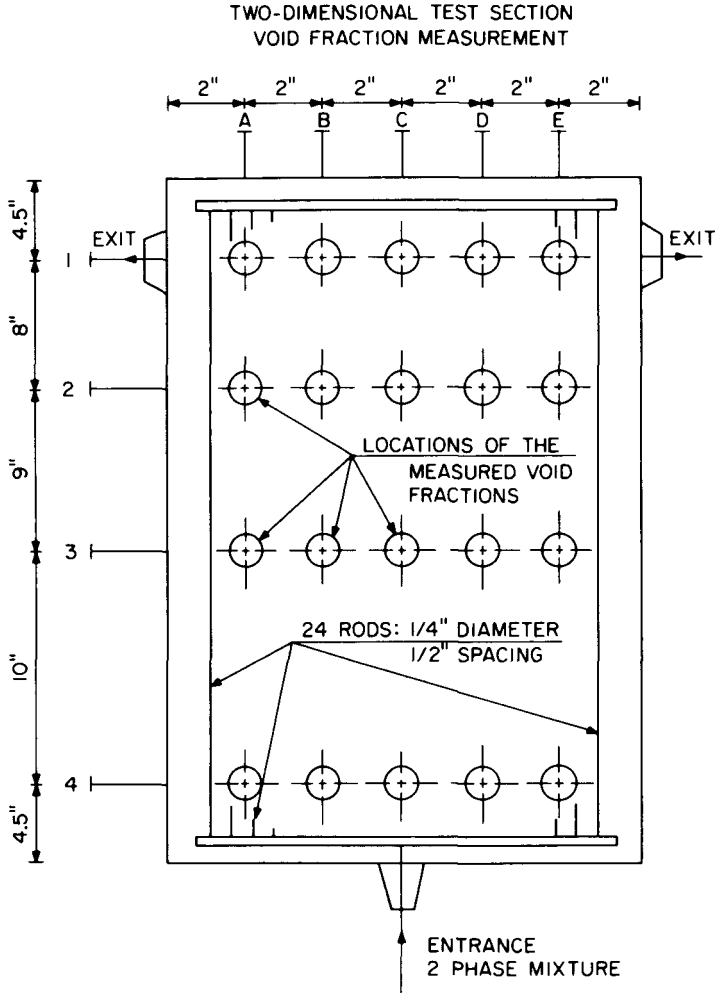

Figure 2.10.1 Schematic of the RPI (1 x 3) Test Section (BNL Neg. No. 3-73-82)

TABLE 2.10.1 Operating Conditions of RPI Tests Simulated

Test No.	No. of Exits	Rods in/out	System Pressure (bar)	Water Flow Rate (kg/s)	Air Flow Rate (kg/s)	Quality
8	2	In	1.289	1.5574	0.00399	0.00257
6	1	In	1.496	1.5574	0.00399	0.00257
18	2	In	1.358	2.404	0.02643	0.0109

2.10.3 TRAC Input Model Description

The test channel was modeled by using the two-dimensional (radial and axial) option of the TRAC VESSEL module. It was divided into six axial levels and seven radial or lateral columns. The top faces of the axial levels were located at the 0.228 m (9-inch), 0.508 m (20-inch), 0.686 m (27-inch), 0.74 m (29-inch), 0.861 m (34-inch) and 0.914 m (36-inch) elevation from the bottom of the test channel. On the other hand, the right hand faces of the lateral columns were located at the distance of 0.025 m (1-inch), 0.075 m (3-inch), 0.125 m (5-inch), 0.175 m (7-inch), 0.225 m (9-inch), 0.275 m (11-inch) and 0.3 m (12-inch) from the left hand side of the channel. This nodalization was chosen so that all the void fraction measurement stations coincided with the individual cell centers, and still maintained a reasonable number (42) of hydraulic nodes.

The mixing tee at the bottom of the test channel was modeled with a TEE component. The vertical primary pipe of the TEE was divided into 15 equal size cells each of 0.1778 m in length, and a small 0.0762 m long cell. Water entered at the bottom of this primary pipe and the flow rate boundary condition was provided by a FILL component. Air was introduced through the horizontal secondary pipe which was connected to the vertical primary pipe at 2.578 m from the bottom of the test channel. This horizontal pipe was divided into two small cells and another FILL component was attached to the free end of this pipe to provide the air flow rate boundary condition.

The exit pipes near the top of the test channel were modeled by two PIPE components with two cells each. Two BREAK components were attached to the free ends of these PIPE components to supply the pressure boundary condition. The system pressure, measured at the center of the channel, was used for this purpose. This would affect the air density slightly, but would not alter the overall solution to any significant extent.

Steady-state solutions were sought by transient relaxation of the code. A stable solution was obtained for Test No. 8. However, for Test Nos. 6 and 18 the solutions showed oscillatory behavior for a long time, and the calculations were terminated. The calculation for Test No. 8 took 450 CPU seconds in

the BNL CDC-7600 for 16.9 seconds of transient, while the calculation for Test No. 6 took 766 CPU seconds for 10.16 seconds of transient. Simulation of Test No. 18 was attempted in two ways. With the TEE at the entrance, the calculation took 511 CPU seconds for 5 seconds of transient, whereas with a PIPE component at the entrance it took 1022 CPU seconds for 16 seconds of the transient.

2.10.4 Code Prediction and Comparison with Data

As mentioned earlier, only the simulation of Test No. 8 produced a solution which was very close to a steady-state with symmetric flows through the exits. The history of predicted exit mass flow rates is shown in Figure 2.10.2. This is a significant improvement over the results obtained with TRAC-P1A which produced an asymmetric solution for symmetric boundary conditions (Rohatgi, 1980c).

Figures 2.10.3 and 2.10.4 show the comparison between the predicted and the measured lateral void fraction distribution at various axial levels for Test No. 8. The levels shown in these figures correspond to the TRAC VESSEL levels; Level 1 being at the bottom and Level 5 being at the flow exit level. It can be seen that although TRAC-PD2 predicts the void fraction distribution reasonably well at the bottom and top levels, i.e., Levels 1 and 5, it does not perform well at the intermediate levels, i.e., Levels 2 and 3. At these levels, TRAC-PD2 predicts a more rapid lateral void migration than the data indicate. Addition of a turbulent mixing model may improve the code prediction as suggested by some COBRA-TF calculations (Crowell, 1980). Finally, the predicted water and air flow directions of Test No. 8 are shown in Figure 2.10.5. It should be noted that TRAC-PD2 did predict a recirculation pattern as observed in the test.

The code failed to yield even near steady-state solutions for Test Nos. 6 and 18. The computed exit mass flow rate for Test No. 6 (with one exit) is shown in Figure 2.10.6. The code results oscillated around the expected value and did not settle down. It is not known whether oscillations of similar magnitude prevailed during the test since only the inlet flow rates were reported (Lahey, 1978). Therefore, it is not clear whether the predicted oscillations are due to the code numerics or these might have some physical basis.

Figures 2.10.7 through 2.10.9 show the comparison between the calculated lateral void fraction distibution at various axial level and the time-averaged data for Test No. 6. The spreads in the calculated void fractions between t = 7.16 s and t = 10.16 s are also shown in these figures. Notice that at Level 1, i.e., at the bottom, the fluctuation in the calculated void fraction is rather small and the void distribution looks reasonable. At the intermediate level, i.e., Level 3, the fluctuations are stronger (particularly at the left hand side) and the calculated void distribution is rather flat. This is consistent with the TRAC results for Test No. 8 (see Figure 2.10.4). Finally, at the exit pipe level, i.e., Level 5, the calculation exhibited enormous oscillation near the closed end and the prediction was rather poor compared to the data. It seems that according to the calculation, air collects in the upper left hand corner of the test section and after the flow regime changes to the annular-mist regime, the phasic velocities change direction and the void fraction starts to decrease. The reverse happens when the void fraction approaches zero. This persists throughout the calculation. The pressure

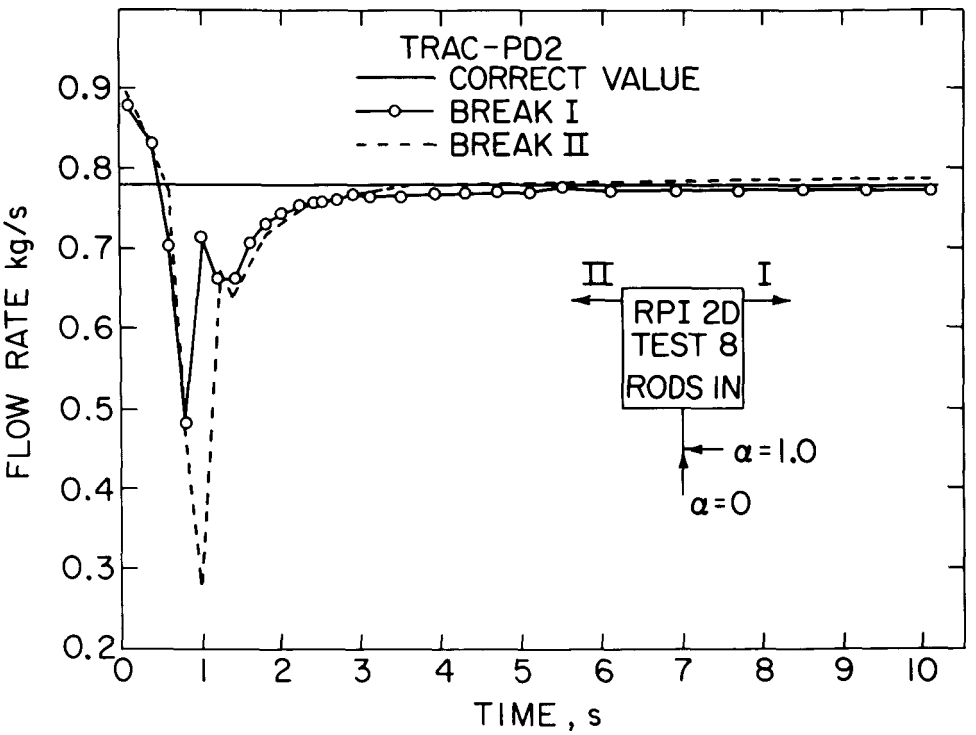

Figure 2.10.2 The Predicted Exit Mass Flow Rates for RPI Test No. 8 (BNL Neg. No. 1-826-81)

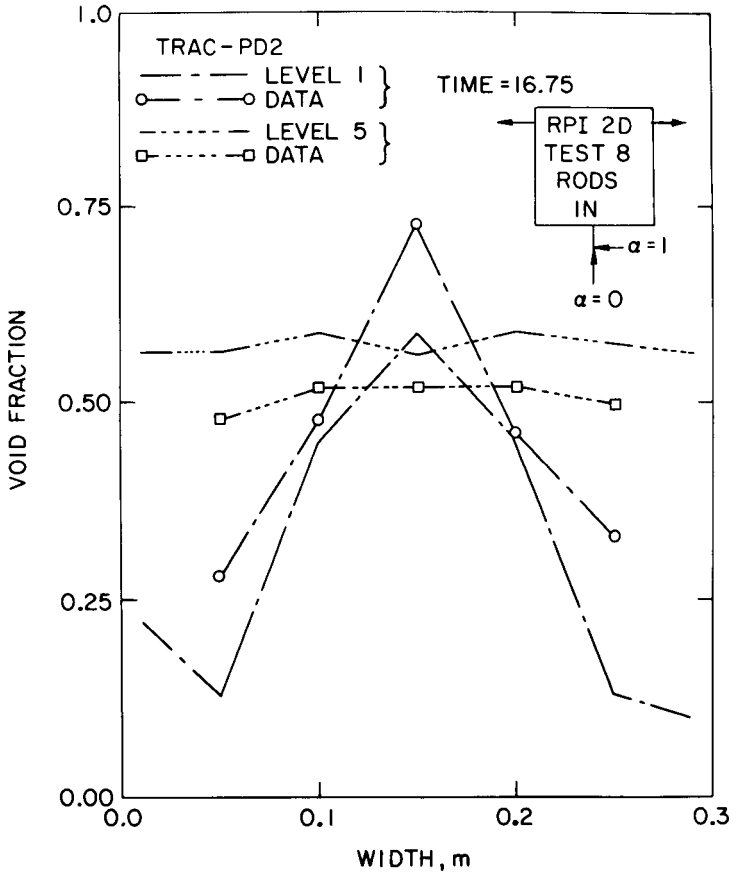

Figure 2.10.3 Comparison Between the Measured and Predicted Lateral Void Distribution at the Bottom and Exit Pipe Levels for RPI Test No. 8. (BNL Neg. No. 1-827-81)

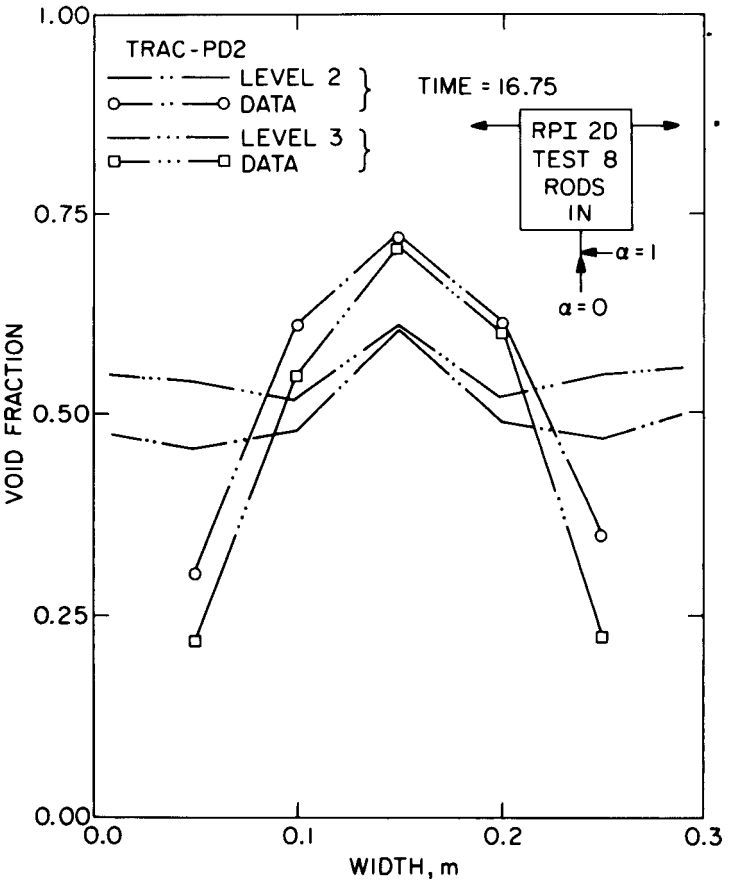

Figure 2.10.4 Comparison Between the Measured and Predicted Lateral Void Distribution at Intermediate Levels for RPI Test No. 8. (BNL Neg. No. 3-72-82)

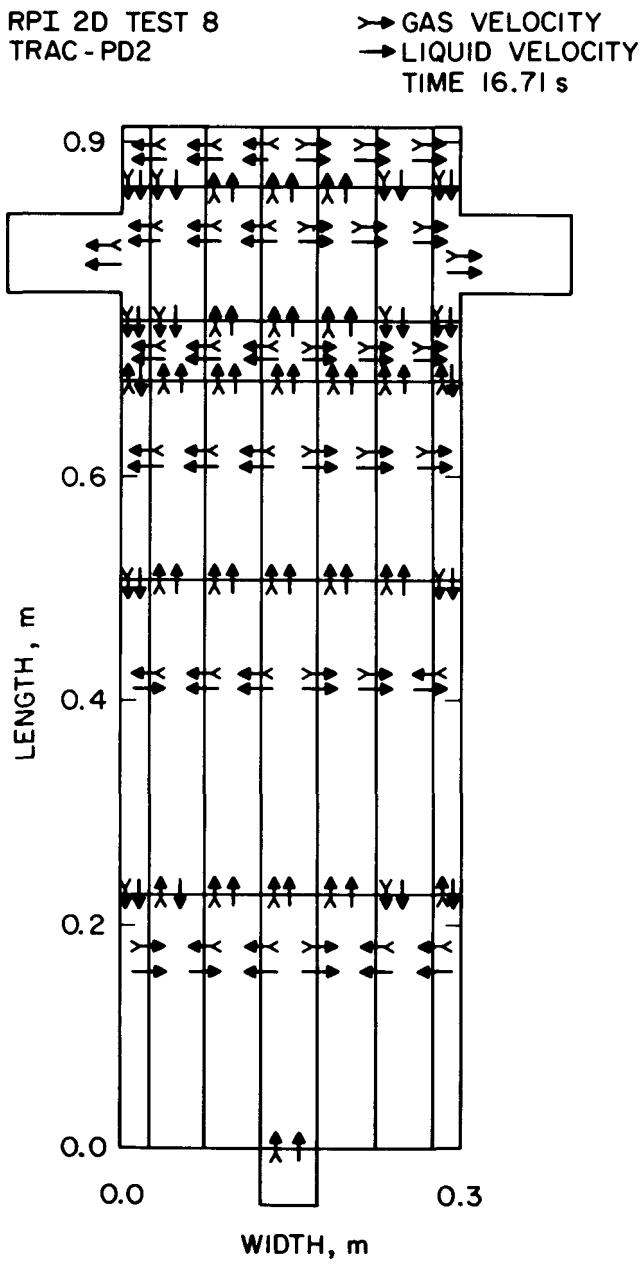

Figure 2.10.5 Predicted Water and Air Flow Directions for RPI Test No. 8. (BNL Neg. No. 2-893-82)

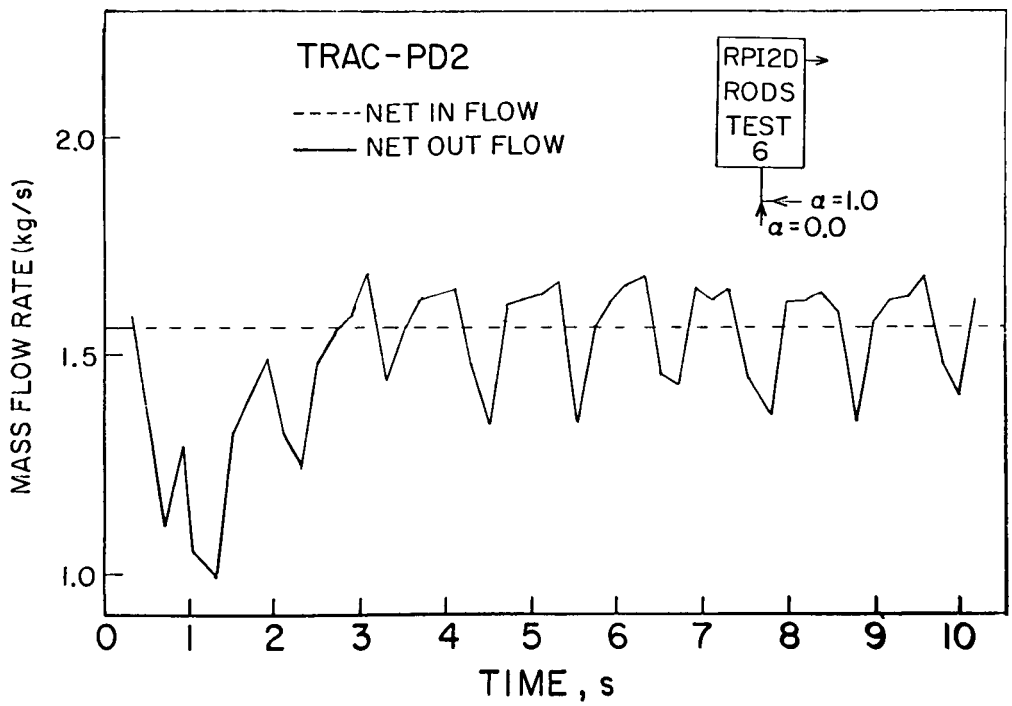

Figure 2.10.6 Predicted Inflow and Outflow for RPI Test No. 6.(BNL Neg. No. 4-510-81)

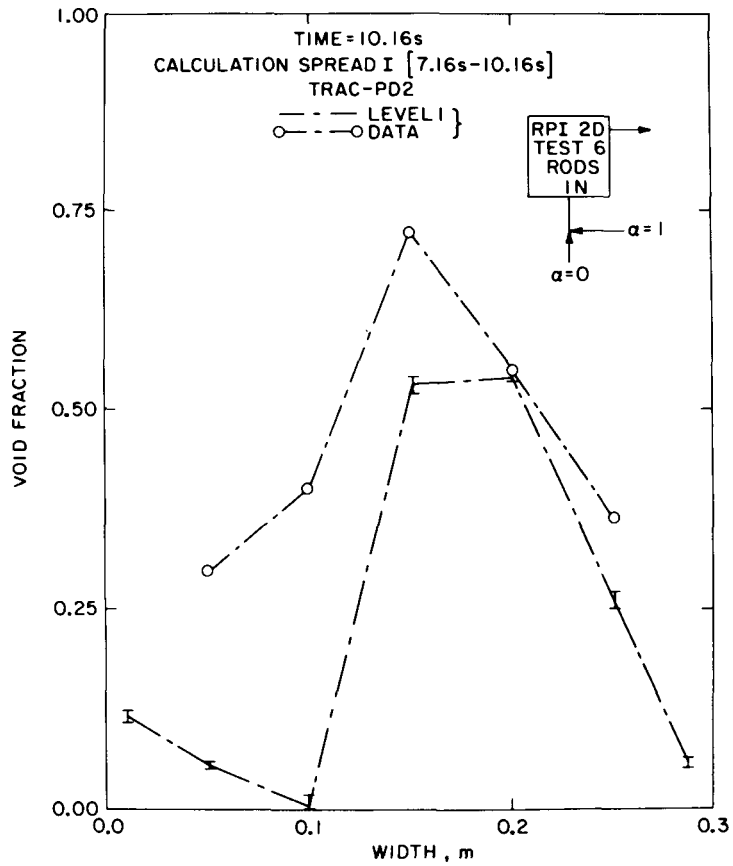

Figure 2.10.7 Comparison Between the Calculated and Measured Lateral Void Distribution at the Bottom Level for RPI Test No. 6. (BNL Neg. No. 2-878-82)

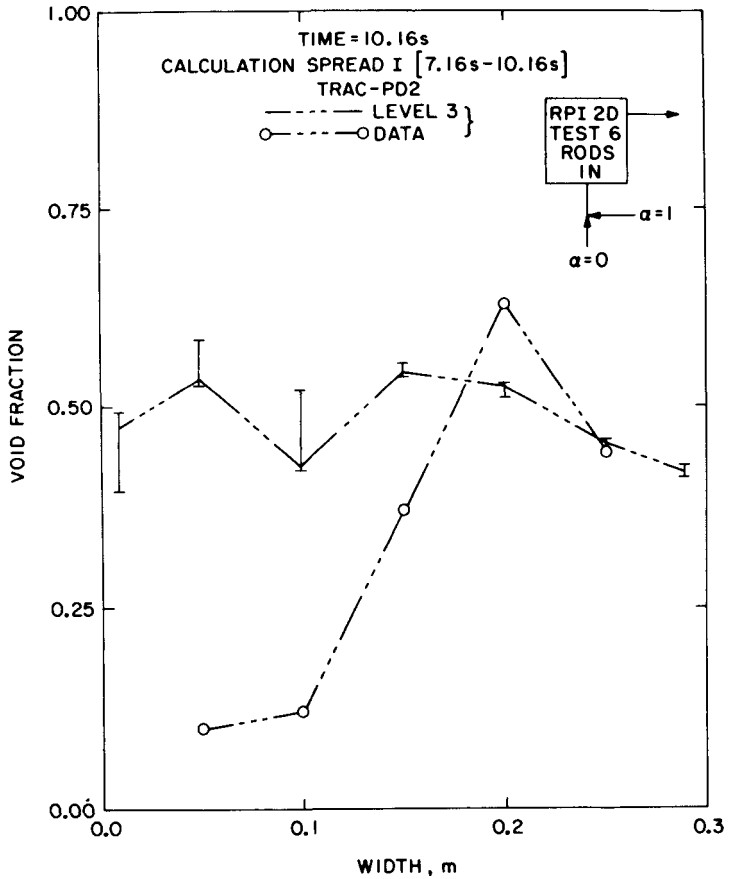

Figure 2.10.8 Comparison Between the Calculated and Measured Lateral Void Distribution at an Intermediate Level for RPI Test No. 6. (BNL Neg. No. 2-880-82)

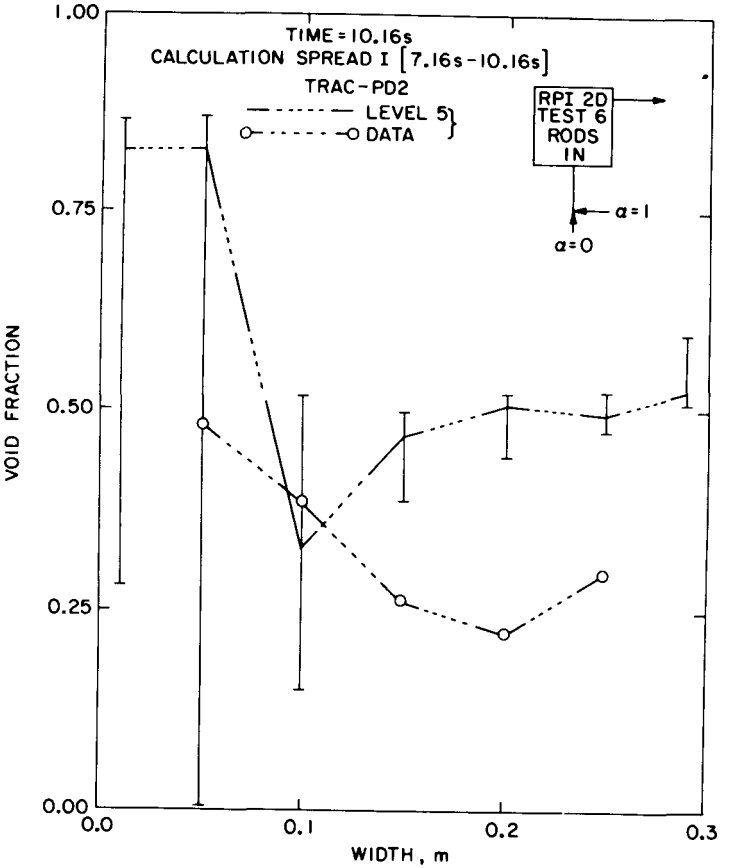

Figure 2.10.9 Comparison Between the Calculated and Measured Lateral Void Distribution at the Exit Pipe Level for RPI Test No. 6. (BNL Neg. No. 2-879-82)

also shows similar oscillations. This phenomenon did not occur in Test No. 8 calculation as the two outlets prevented any accumulation of air in the upper corners.

The test with high inlet void fraction, i.e., Test No. 18, was simulated by two ways. First, a TEE component was used at the entrance like the other test simulations. The code did not produce a stable solution and large magnitude oscillations in void fraction were observed even at the vessel entrance. In the second calculation, the TEE component was replaced with a PIPE component and a two-phase mixture with a void fraction of 0.7 was introduced at the inlet of this pipe. Even in this case the void fraction at the exit of this pipe, i.e., at the vessel entrance, did not stabilize. On the contrary, the magnitude of oscillations increased as shown in Figure 2.10.10. This suggests that before any simulation of the RPI high quality tests can be performed, the relative velocity model or numerical algorithm for the PIPE component must be improved. Note that a flow rate or pressure boundary condition cannot be imposed on the TRAC VESSEL module directly; it has to be through a PIPE or a TEE component.

2.10.5 Discussion

Of the three test simulations attempted with TRAC-PD2, only the calculation for Test No. 8 (low quality with two exits) reached a near steady-state solution. The code did predict a recirculation pattern and the lateral void distributions at the lower and upper axial levels were in reasonable agreement with the data. However, the predicted void distributions at the intermediate levels were not in good agreement with the data. The lack of a turbulent mixing model, i.e., the Reynolds stress term, in TRAC may be a possible reason.

Large magnitude oscillations in void fraction were calculated at the upper closed corner for Test No. 6. It is not clear whether these oscillations were caused by the numerics or they might be representing some physical phenomena.

Finally, the drift-flux model as implemented in TRAC-PD2, seems to have a convergence problem at high void fraction regime. This was probably the reason for the unstable solution obtained for Test No. 18. This test should be recomputed with the recently released TRAC-PF1 since this new code is entirely based on the two-fluid formulation.

2.10.6 Conclusions

The following conclusions may be drawn based on the TRAC-PD2 calculations of the three RPI tests:

a) The code predicted an almost steady-state condition for the low quality test with rods in and two exits (Test No. 8). This was an improvement over the TRAC-P1A prediction for the same test.

b) The code did not predict stable solution either for the low quality, one exit test (Test No. 6) or for the high quality, two exit test (Test No. 18). Although the reason for the former calculation is not clear, the latter calculation is believed to be caused by a convergence problem in TEE or PIPE component of TRAC-PD2 for high void fractions.

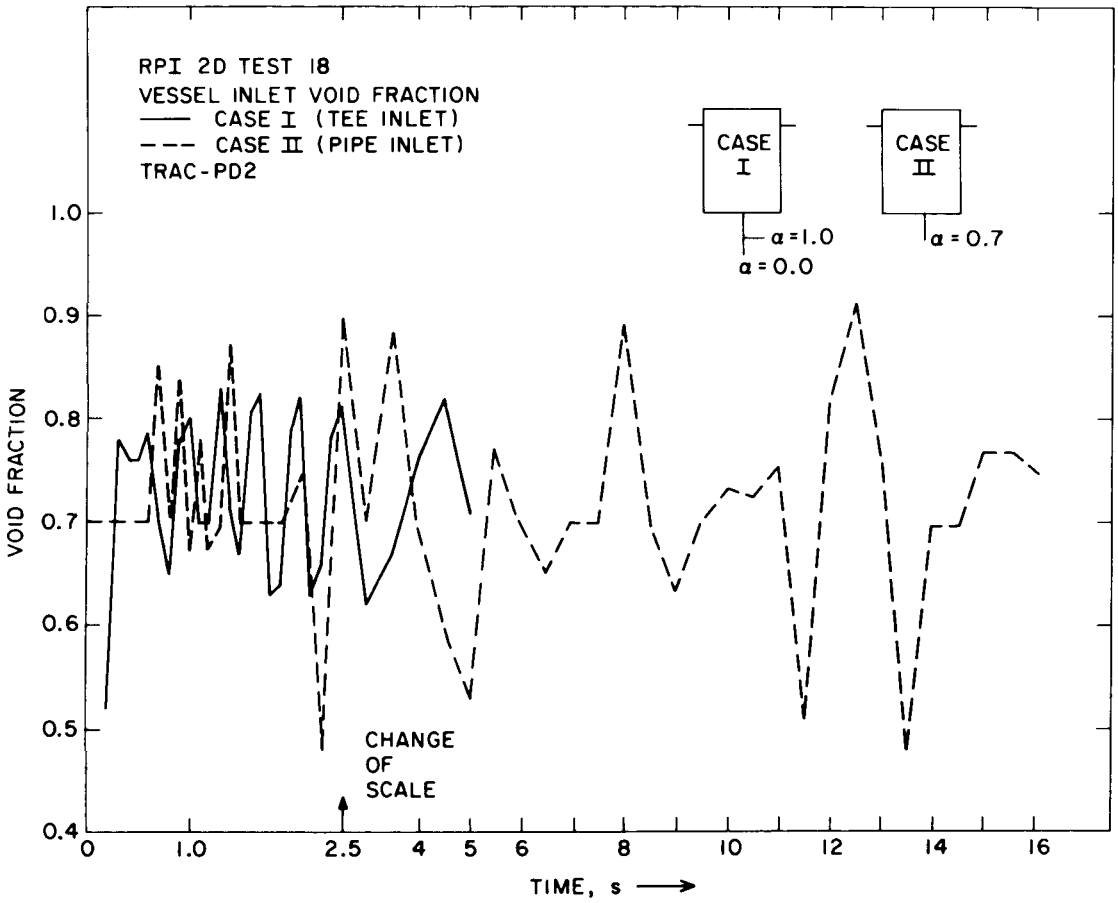

Figure 2.10.10 Calculated Vessel Inlet Void Fraction for RPI Test No. 18 with Two Different Inlet Components. (BNL Neg. No. 7-741-81)

c) The code, in general, overpredicts the lateral void migration. Additional modeling efforts including the Reynolds stress terms seem to be needed to improve this situation.

2.11 Rancho Seco Overcooling Transient

2.11.1 Objective

The loss of feedwater and the subsequent overcooling of the reactor vessel which occured at the Rancho Seco Nuclear Power Plant on March 20, 1978 was analyzed by using an updated version of TRAC-PD2 to assess the code's capability to simulate this type of transient. Recently the overcooling transient is receiving great attention because of its potential to create undue thermal stresses in the reactor pressure vessel and thus challenge the vessel integrity.

2.11.2 Transient Scenario

The transient scenario employed for the TRAC calculation was mainly based on the information obtained from the memorandum to Paul S. Check from Richard Lobel of NRC-DOR dated July 31, 1978 (Lobel, 1978) and the FSAR of Rancho Seco Plant (SMUD, 1971). However, since a number of critical boundary conditions and details were uncertain or missing, some assumptions had to be made.

The Rancho Seco plant consists of a B&W pressurized water reactor with two once-through steam generators. The transient of March 20, 1978 was triggered by the loss of main feedwater to the steam generators when the plant was operating at 72% of full load. This loss of feedwater caused the reactor coolant temperature and pressure to increase sharply. This in turn tripped the reactor and the turbine. Since the PORV on the pressurizer was gagged (Taylor, 1980) one of the two safety valves opened to reduce the primary side pressure. This valve was known to remain partially open ("simmer") during the remainder of the transient, although the extent of actual openning was not known.

Shortly after the reactor trip, the High Pressure Injection System (HPIS) was initiated by the operator. At about 8 minutes after the reactor trip the Auxiliary Feedwater (AFW) was actuated in one steam generator. This initiated overcooling of the primary side which was aggravated a few minutes later when the main feedwater pumps were turned on. The scenario or assumption used in the present calculation is summarized in Table 2.11.1.

2.11.3 TRAC Input Model Description

The Rancho Seco Plant is a B&W lower loop plant with two hot legs, four cold legs and two once-through steam generators (OTSGs). An updated version of TRAC-PD2, received from LANL in February 1981, was used for the present calculation. The update was necessary to model the safety valve at the top of the TRAC PRESSURIZER component and to inject the auxiliary feedwater into the upper part of the TRAC STEAM GENERATOR component.

The system nodalization is shown in Figure 2.11.1. The reactor vessel modeled by the VESSEL module was divided into 6 axial, 2 radial and 2 azimuthal sectors. Each steam generator had 12 cells in the primary side and 10

TABLE 2.11.1. Boundary Conditions or Assumptions for BNL Calculation of Rancho Seco Overcooling Transient

Time or Trigger Pressure	Event	Remarks
-1 Min	Steady-State	72% of full load, core power constant until reactor trip.
0	Feedwater Trip	Flow rate ramped down to 10 kg/s (from 525 kg/s) in 60 sec. Feedwater temperature remained constant.
2355 psig (163.4 bar)	Reactor and Turbine Trip	Core power vs. time taken from the decay heat curve of FSAR (See Figure 2.11.2).Turbine isolation closed in 1 sec. Steam bypass valve open (Trigger pressure and flow rate from FSAR-see Table 2.11.2).
2400 psig (166.5 bar)	Pressurizer safety valve fully open	Code calculates the discharge flow rate
2100 psig (145.8 bar)	Pressurizer safety valve partially closed	10% open until 4 mins when pressure starts to rise. Thereafter, valve 100% open.
60 sec	HPI Actuation	One HPIS initiated. Flow rate from FSAR (See Figure 2.11.3). Temperature assumed to be 32°C. Flow rate equally split to both loops.
480 sec	AFW Actuation in one loop	Flow rate: 49 kg/s Temperature: 32°C Injection in Loop A steam generator only.

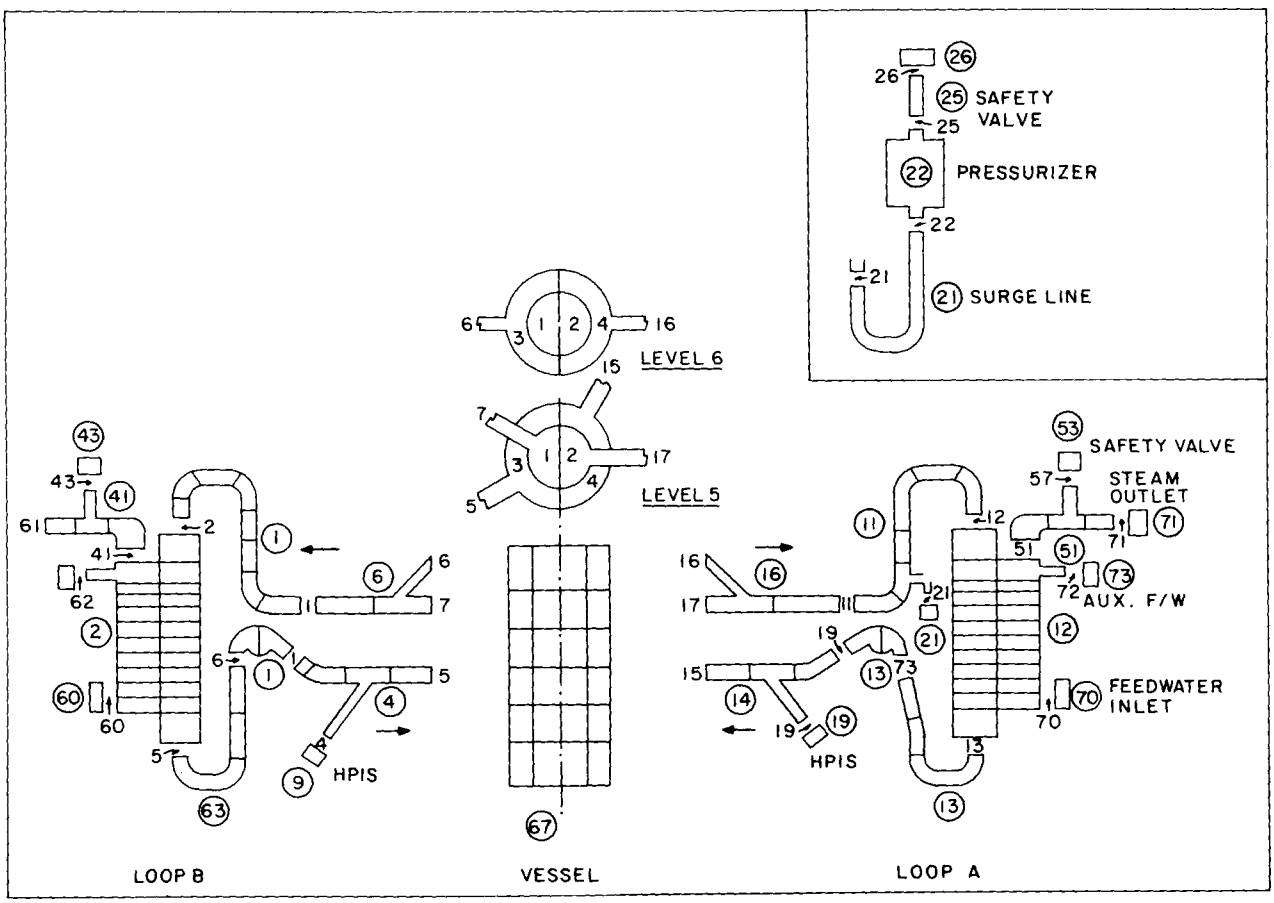

Figure 2.11.1 TRAC Nodalization of the Rancho Seco Reactor System. (BNL Neg. No. 4-691-81)

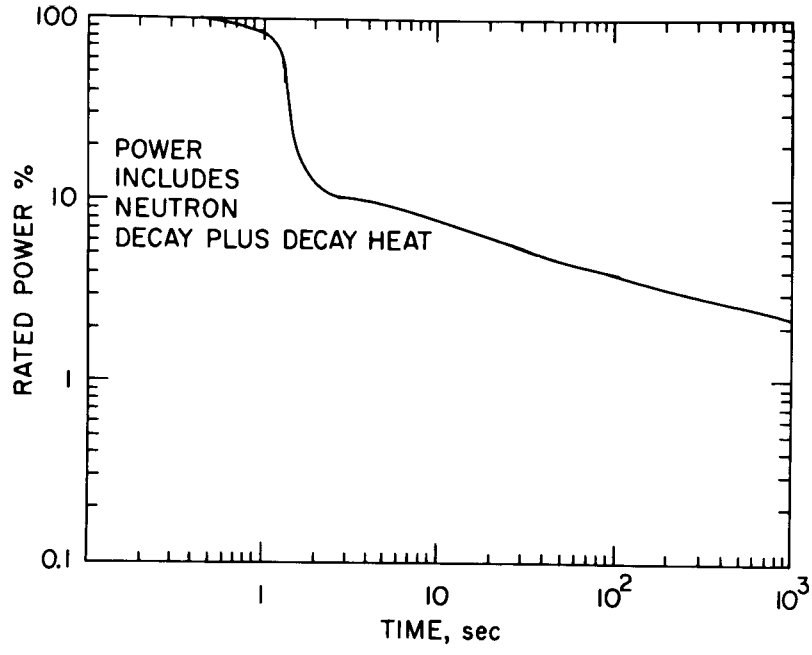

Figure 2.11.2 Core Power vs. Time After Reactor Trip.
(BNL Neg. No.2-885-82)

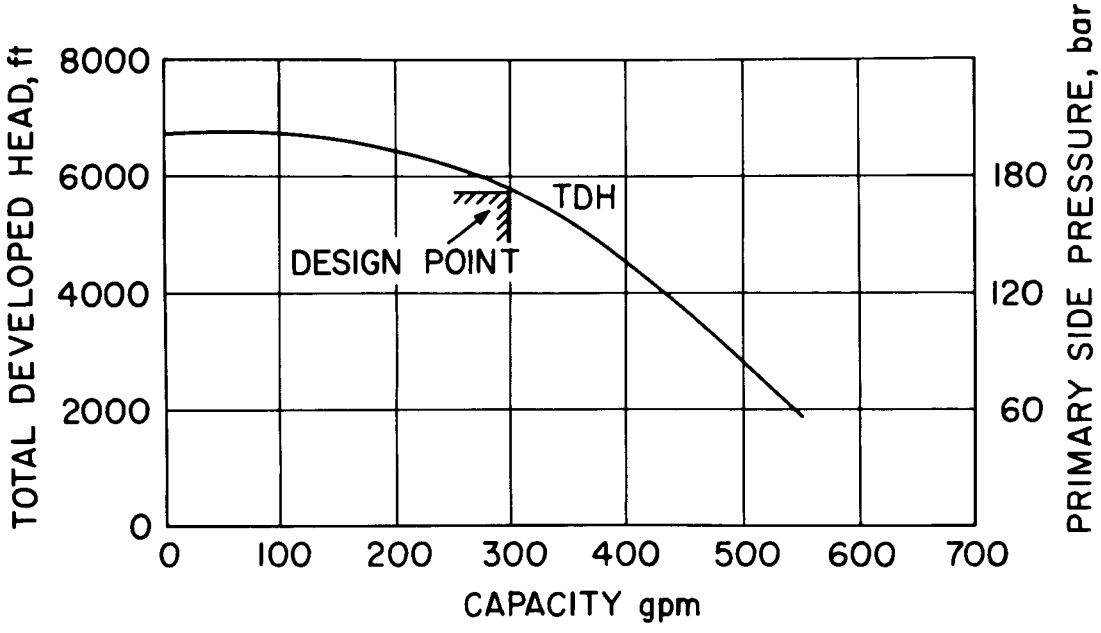

Figure 2.11.3 Flow-Head Characteristic of the HPI Pump.
(BNL Neg. No. 2-887-82)

TABLE 2.11.2. Trigger Pressure and Capacity of Steam Bypass and Relief Valves for Rancho Seco Calculation

Valve	Pressure (psig)	Capacity (lb/hr)
Steam Bypass Valve to Condenser	925	918,000
Atmospheric Vent Valve	985	1,530,000
Relief Valve	1050	1,692,000
Relief Valve	1070	1,692,000
Relief Valve	1090	2,013,000
Relief Valve	1102.5	1,692,000

cells in the secondary side. The standard once-through STEAM GENERATOR component of TRAC-PD2 was used. Notice that this component does not have the models for aspirator and downcomer which are, of course, present in the actual B&W once-through steam generators. (The impact of not having these models will be discussed later.) Two cold legs in each loop were combined into a single leg for the sake of simplicity and some reduction in the computer running time. In total, the system was modeled with 150 cells.

The steady-state calculation was performed by replacing the pressurizer subassembly with a BREAK component where the pressure boundary condition (148.8 bar) was imposed. However, during the transient calculation, the surge line, pressurizer and the safety valve were connected to the hot leg of the primary loop. The boundary conditions used for the transient calculation are described in Table 2.11.1. It should be added that a separate calculation was performed to determine the appropriate additive loss coefficient across the pressurizer safety valve to yield the design flow rate at design pressure. The same loss coefficient was used for the entire transient.

The calculation took approximately 175 CPU seconds in the BNL CDC-7600 for 30 seconds of transient to reach a steady-state, and approximately 5000 CPU seconds for 600 seconds of transient.

2.11.4 Code Prediction and Comparison with Data

The result of the steady-state calculation is shown in Table 2.11.3 which indicates a generally excellent agreement with the actual plant conditions. Several trial runs were needed to obtain the result. The initial water level in the steam generator secondary side and the reactor coolant pump speed were the main parameters which were varied. For the final run, the pump speed used was 129.25 rad/sec which is slightly higher than the rated value of 124 rad/sec. The predicted secondary steam flow rate and temperature showed some discrepancies and were slow to reach a steady condition. However, the errors were considered to be acceptable and the transient calculation was started.

Figures 2.11.4 and 2.11.5 show the hot and cold leg temperatures and the primary side pressure during the transient, as measured and calculated by the updated TRAC-PD2. The calculation was terminated at 10 minutes, shortly after the auxiliary feedwater injection, when the calculated primary side pressure and temperatures started to decrease as observed in the actual data. (One of the objectives of this calculation was to demonstrate this behavior.) Furthermore, there was considerable uncertainty in the operator action after 10 minutes with respect to the main and auxiliary feedwater injection rates.

The following observations can be made by comparing the calculated results with the actual plant data:

1. The increase of the primary side pressure in the calculation before the reactor trip appeared to be somewhat slower than the data (see Figure 2.11.6). Initially it was suspected that the unknown steam flow rate in the secondary side of the steam generator between the time of feedwater trip and the turbine trip might be the reason. Therefore, several trial runs were made with various formulae to calculate the steam flow rate. These formulae were:

TABLE 2.11.3. TRAC-PD2 Steady-State Calculation for Rancho Seco

Variable	Plant Conditions	Prediction	Error/Comment
Power	1.996×10^9W	1.996×10^9W	Imposed
Coolant Temperature Rise in Core	20°K	19.9°K	0.1°K
Cold Leg Temperature	586.6°K	586.6°K	0.0°K
Hot Leg Temperature	588.6°K	588.5°K	0.1°K
Primary Pressure	148.8 bar	148.8 bar	Imposed
Primary Flow Rate	17375 kg/s	17415 kg/s	0.2%
Feedwater Temperature	506.9°K	506.9°K	Imposed
Feedwater Flow Rate	525.4 kg/s	525.4 kg/s	Imposed
Secondary Side Exit Pressure	63.8 bar	63.8 bar	Imposed
Steam Exit Temperature	590°K	581.6°K	8.4°K
Steam Flow Rate	525.4 kg/s	536.0 kg/s	2.0%

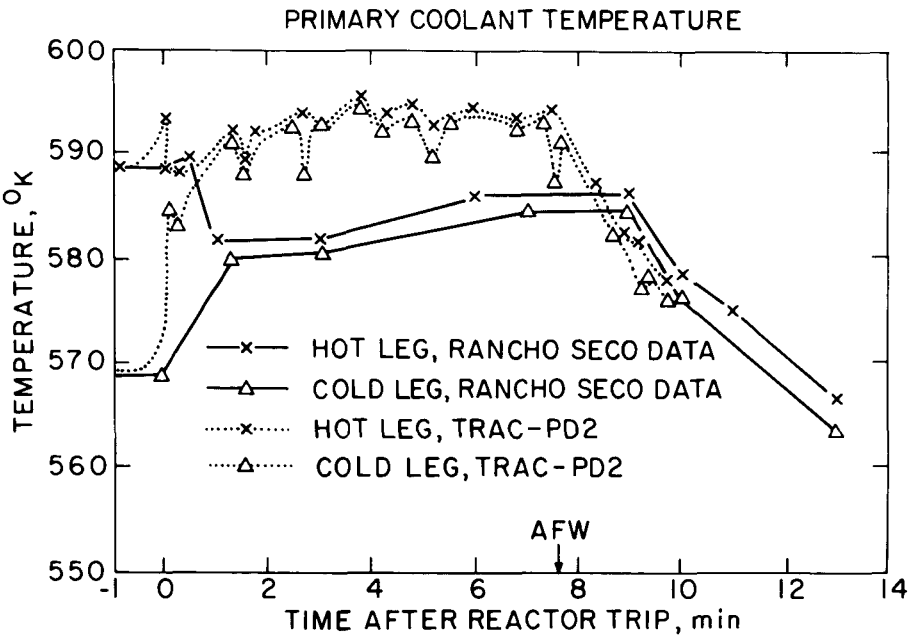

Figure 2.11.4 Comparison Between the Predicted and Measured Hot and Cold Leg Temperatures.(BNL Neg. No. 4-689-81)

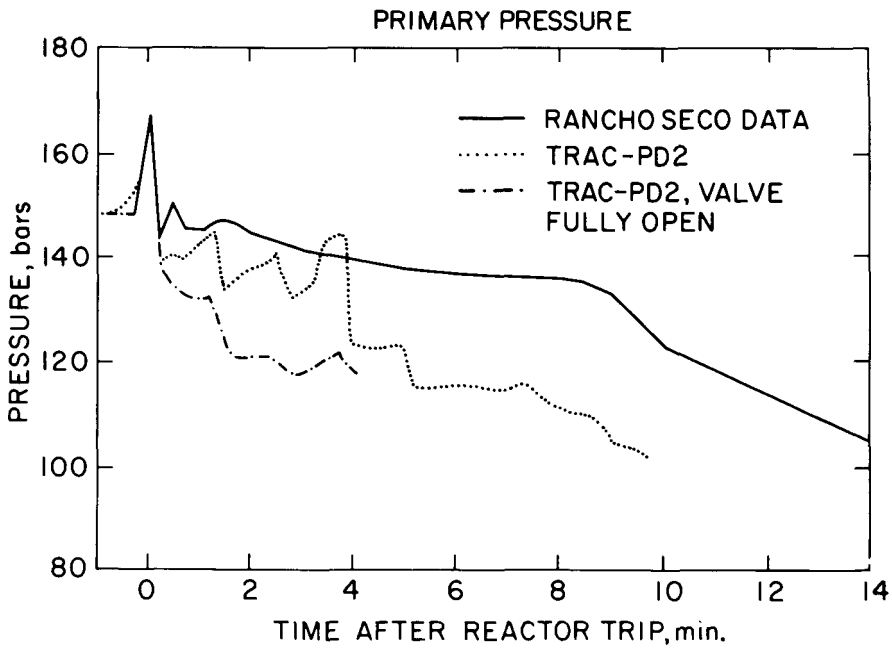

Figure 2.11.5 Comparison Between the Predicted and Measured Primary Side Pressure. (BNL Neg. No. 4-687-81)

a) A constant flow rate as in the steady-state,

b) $W_{steam} = k_1 \sqrt{P_{secondary}}$, with k_1 calculated from the steady state conditions,

c) $W_{steam} = k_2 \ P_{secondary}$, with k_2 calculated from the steady state conditions.

Both formulae (b) and (c) assume that $P_{secondary} >> P_{condenser}$, which is perfectly valid. Moreover, formula (b) assumes that the steam density remains at the steady-state value whereas formula (c) assumes the steam density to be proportional to the secondary pressure. However, the primary side pressures, calculated using the above three formulae, did not show any significant differences. Therefore, the apparent discrepancy could be due to the inconsistency in the presentation of the original data (Lobel, 1978), where the primary side pressure started to rise and the steam generator water level started to drop much sooner than the feedwater trip.

2. The average primary coolant temperature shortly after the feedwater trip was significantly higher than the data. It is believed that this is due to the lack of the aspirator and the downcomer in the once-through steam generator (OTSG) component of TRAC. In the B&W OTSG, the downcomer holds a substantial amount of water which is available for additional cooling in the case of a loss of feedwater transient. Since the current version of TRAC does not have these features, the additional cooling effect was lost and, hence, a higher average primary temperature was calculated.

3. Immediately after the reactor trip, the temperature difference across the core decreased faster than the actual data. Since the primary purpose of the present calculation was to assess the thermal-hydraulic capabilities of TRAC, no neutronic calculation was performed; instead, a reactor power versus time curve from the FSAR of Rancho Seco was used. Apparently, the reactor power during the transient remained higher than the power provided from the FSAR.

4. The calculated primary side pressure, after the reactor trip, is lower than the data. One of the major uncertainties in this transient was the behavior of the safety valve on the pressurizer. It was known that the safety valve was opened below its design pressure of 2500 psig (173.4 bar) and was simmering during the remainder of the transient. During the TRAC calculation the valve was opened fully when the pressure reached 2400 psi (166.5 bar). However, since the valve closing characteristic was unknown, several runs were performed with varying degree of valve opening when the primary pressure reached 2100 psig (145.8 bar). This set point was chosen because the plant data showed that the pressure was sharply increasing at this value. Figure 2.11.6 shows the sensitivity of the primary side pressure to various valve openings.

When the valve was fully closed, i.e., 0% opening, the primary pressure started to increase like the data. However, while the actual pressure leveled off in about 20 seconds, the calculated pressure kept

climbing. On the other hand, when the valve was left fully open, the pressure continued to drop until it leveled off at a substantially lower value than the data indicated. After several trial runs, it appeared that a 10 percent opening of the valve would yield the best agreement with the data. However, at about 4 minutes into the transient, the calculated primary pressure started to increase again. At this point, the valve was fully opened. As a result, the primary pressure suddenly dropped to a level which would have been reached even if the valve was fully opened 3 minutes earlier, as shown in Figure 2.11.5.

5. The primary pressure and the hot and cold leg temperatures showed considerable oscillations at about the same frequencies. It was noticed that these oscillations were accompanied with sudden changes in the heat transfer rate in the cell containing the mixture level in the secondary side of the steam generator. Similar behavior was also observed in the simulation of stand-alone B&W steam generator tests discussed in Section 2.8. A finer nodalization of the steam generator component would have probably reduced the magnitude of these oscillations.

6. A large difference in the fluid temperature in two adjacent azimuthal cells in the same level of the upper plenum was observed after the auxiliary feedwater was injected into one steam generator only. This is shown in Figure 2.11.7. It is not clear whether this is physically correct or it is due to inadequate mixing predicted by the code because of the lack of a turbulent mixing model. Further investigation is needed to resolve this issue.

2.11.5 Discussion

The present calculation has demonstrated that TRAC-PD2, with some modification or updates, is capable of calculating a loss-of-feedwater transient with subsequent overcooling of the primary side. The calculation has also indicated the importance of providing the "correct" boundary conditions as illustrated through the sensitivity study of the pressurizer safty valve opening. This is very important when one attempts to simulate a plant incident or an experiment where some of the pertinent information were not recorded.

It is clear from the present calculation that the TRAC once-through STEAM GENERATOR component should include the models for aspirator and downcomer which play a significant role during the loss-of-feedwater transient. If these models are not included in future versions of TRAC, the user should connect various TRAC components (e.g., two once-through STEAM GENERATOR components, TEE's, PIPE's, etc.) to represent the actual flow paths in a B&W once-through steam generator. Such a scheme has been devised at BNL and it is working (Jo, 1981).

The present calculation, like the TRAC-PD2 simulation of the B&W steam generator experiments discussed in Section 2.8, showed the effect of nodalization with regard to the steam generator behavior. It was suggested in Section 2.8 that either the two-phase mixture level be tracked or fine transitory meshes be inserted in the secondary side of a steam generator to obtain better and smoother results.

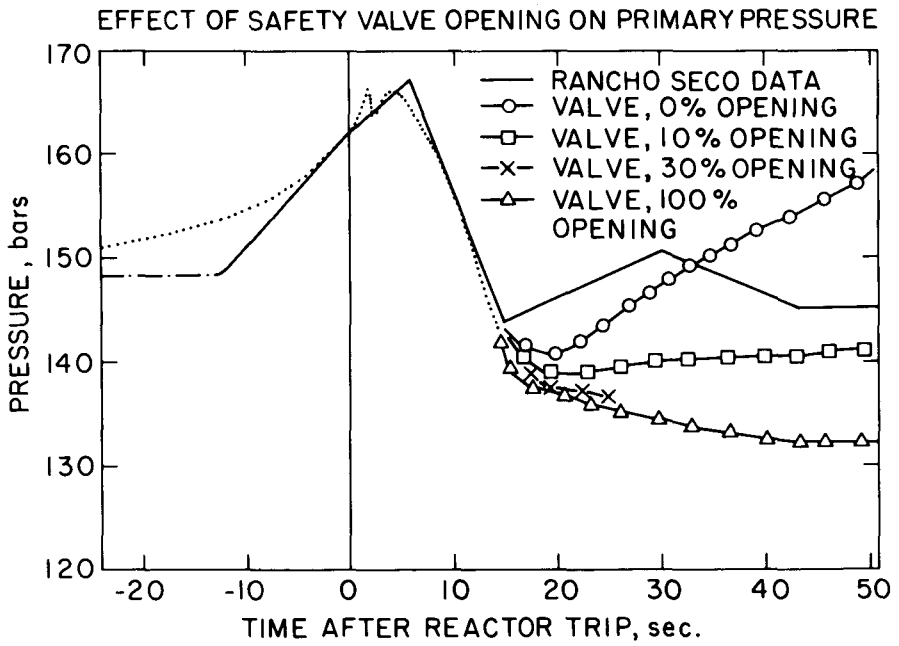

Figure 2.11.6 Comparison Between the Measured and Calculated Primary Side Pressure for Various Pressurizer Safety Valve Openings. (BNL Neg. No. 4-688-81)

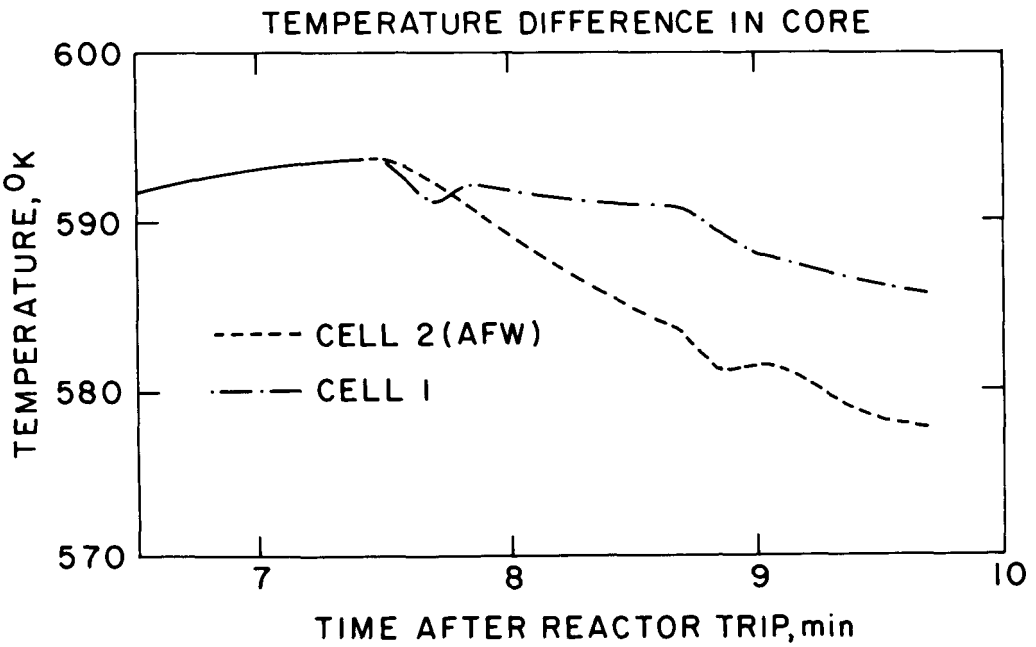

Figure 2.11.7 Calculated Fluid Temperatures at the Two Halves of the Core Exit. (BNL Neg. No. 4-690-81)

Another interesting feature revealed through this calculation was the "incomplete" mixing in the core when the loop conditions were asymmetric due to injection of auxiliary feedwater in one steam generator only. A one-dimensional code would, of course, mix the two incoming streams completely and would predict a single value for water temperature in each axial level in the core and upper plenum. In reality, the streams may not mix completely because of high resistance to cross-flow, and the TRAC results may be more representative of the correct trend. However, comparison with pertinent test data must be performed to make a quantitative assessment of this item.

2.11.6 Conclusions

The following conclusions may be drawn from the simulation of the Rancho Seco overcooling transient with an updated version of TRAC-PD2:

a) The code is capable of calculating a loss-of-feedwater transient with subsequent overcooling of the primary side.

b) Knowledge of "correct" boundary condition is important as shown through the code sensitivity of the pressurizer safety valve opening.

c) The TRAC once-through STEAM GENERATOR component should include models for the aspirator and downcomer. Alternatively, the user should connect various TRAC components to model the flow paths of a B&W OTSG.

d) A finer nodalization of the steam generator secondary side would probably be needed to suppress the pressure and temperature oscillations found in the present calculation.

e) An asymmetric loop condition would yield an asymmetric fluid temperature condition in the core and upper plenum. This may be more realistic than a one-dimensional calculation which mixes the fluid completely in the radial and azimuthal directions.

3. RELAP5/MOD1 ASSESSMENT CALCULATIONS

This chapter presents the RELAP5/MOD1 assessment calculations performed at BNL during FY 1981. Three tests were simulated with Cycle 1 of the code (Ransom, 1980) released in November, 1980. These were: (i) Marviken Critical Flow Test 24, (ii) FRIGG-Loop Test 313020, and (iii) B&W Steam Generator Test Series 74-75-76. These tests were also simulated with the TRAC-PD2 code, and the results have been discussed in Sections 2.4, 2.7, and 2.8, respectively. This chapter, therefore, provides a unique opportunity for one-to-one comparison between the TRAC-PD2 and RELAP5/MOD1 code results.

Since the objectives and the test descriptions for the above experiments were presented in the appropriate sub-sections of Chapter 2, each section of this chapter will be divided into: (i) RELAP5/MOD1 input model description, (ii) code prediction and comparison with data, (iii) discussion, and (iv) conclusions.

3.1 Marviken Critical Flow Test

3.1.1 RELAP5/MOD1 Input Model Description

Only Test 24 with the shortest nozzle was simulated. As one of the objectives of the present calculation, besides assessing the RELAP5/MOD1 code, was to provide a comparison between the RELAP5 and TRAC-PD2 results, an effort was made to maintain the same nodalization as was used for the TRAC-PD2 calculation. The test vessel and the discharge pipe were modeled with a RELAP5/MOD1 PIPE component with 40 volumes having the same axial lengths as used for the TRAC-PD2 calculation and shown in Figure 2.4.1. However, the test nozzle was modeled differently since RELAP5 has a separate choking model and does not require a fine nodalization near the exit or break. Moreover, a fine nodalization in the high velocity region such as break would be detrimental to RELAP5's running speed as the time step is controlled by the material Courant limit because of the semi-implicit numerical scheme. Therefore, the test nozzle was initially modeled with a two-volume PIPE component. Even so, the calculation was rather time-consuming and finally a one-volume PIPE was used for the nozzle.

The no flow boundary condition at the top of the test vessel was automatically assumed by the code since no junction was provided at that location. The pressure boundary condition of 1 bar was provided at the nozzle exit through a set of JUNCTION and TIME DEPENDENT VOLUME. Also, the choking option was used in all junctions.

The calculation with the one-volume nozzle took 173 CPU seconds in the BNL CDC-7600 computer for 60 seconds of transient. This was somewhat faster than the TRAC-PD2 calculation which took 269 CPU seconds for 70 seconds of transient, but used 40 volumes in the nozzle. However, the running time for RELAP5/MOD1 increased dramatically when the test nozzle was modeled by two volumes. In that case, the code took 251 CPU seconds for only 10.5 seconds of transient.

3.1.2 Code Prediction and Comparison with Data

Figures 3.1.1 and 3.1.2 show the comparison between the predicted and the

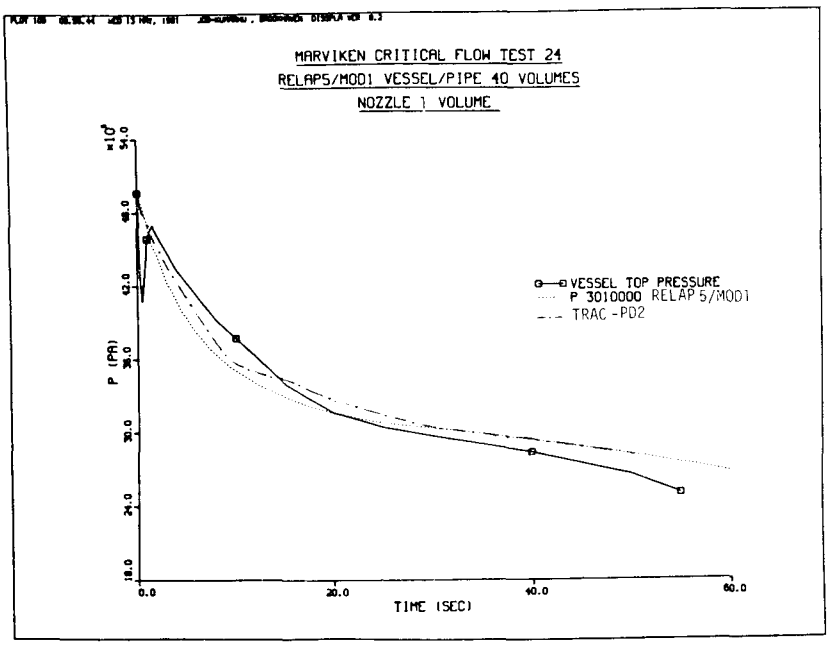

Figure 3.1.1 Comparison Between the Measured and Predicted Vessel Top Pressure.(BNL Neg. No. 7-743-81)

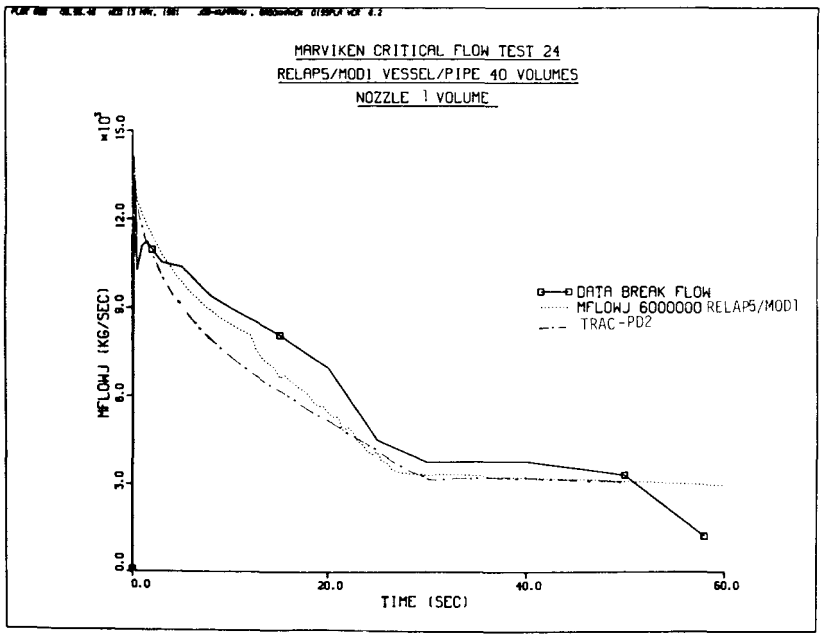

Figure 3.1.2 Comparison Between the Measured and Predicted Discharge (Break) Flow Rate. (BNL Neg. No. 7-742-81)

measured values of pressure at the top of the vessel and the exit mass flow rate, respectively. The results for both the RELAP5/MOD1 calculation with one-volume nozzle and the TRAC-PD2 calculation with 40-cell nozzle are shown in these figures. The mass flow rate prediction of RELAP5/MOD1 is in better agreement with the data than that of TRAC-PD2. However, the vessel top pressure prediction of RELAP5 is in poorer agreement with the data than that of TRAC-PD2. It should be noted that although these codes have different models for computing the interfacial mass and momentum transfer and the break flow rates, the calculated mass flow rate and the vessel top pressure are both underpredicted during the first 15 seconds of the transient.

3.1.3 Discussion

As indicated earlier, the computer running time for RELAP5/MOD1 can depend highly on the nodalization employed in the test nozzle, i.e., the high fluid velocity region. Fortunately the results of RELAP5/MOD1 with one- and two-volume nozzles were not very different so that the calculation with the one-volume nozzle was continued and it can be considered as the RELAP5/MOD1 prediction for Marviken Test 24. Although the code (RELAP5/MOD1) prediction for exit mass flow rate was in better agreement with data than the TRAC-PD2 prediction, the vessel top pressure was not predicted well by RELAP5/MOD1. This lack of acceptable agreement with both the mass flow rate and pressure data seems to be a general problem for both the RELAP5/MOD1 and TRAC (PD2 and P1A) codes. Further studies are clearly needed to resolve this issue.

3.1.4 Conclusions

The following conclusions may be drawn from the RELAP5/MOD1 calculation of Marviken Test 24:

a) The user should avoid small-length cells near the break or in the high velocity region. Otherwise, the computing cost could be very high.

b) The code (RELAP5/MOD1) prediction for the exit mass flow rate, although lower than the data, was in better agreement than the TRAC-PD2 prediction. However, the RELAP5/MOD1 prediction for vessel top pressure was in poorer agreement with the data than that of TRAC-PD2.

c) Like TRAC-P1A and TRAC-PD2, RELAP5/MOD1 also shows an inherent discrepancy between the prediction and the test data. During most of the subcooled blowdown period, the code underpredicted both the vessel top pressure and the exit mass flow rate. This should be investigated further.

3.2 FRIGG-Loop Test

3.2.1 RELAP5/MOD1 Input Model Description

The FRIGG-Loop forced circulation Run Number 313020 (Nylund, 1968) was simulated with the RELAP5/MOD1 (Cycle 1) code using the same axial nodalization and boundary conditions used for the TRAC-PD2 calculations discussed in Section 2.7.3. A PIPE component with heat structures was used to model the

test section, and the appropriate RELAP5 components such as TIME DEPENDENT VOLUME, JUNCTION and SINGLE JUNCTION were used to provide the flow rate boundary condition at the entrance and the pressure boundary condition at the exit.

The calculation was run for 40 seconds of real time with fixed boundary conditions until the results indicated an almost steady-state condition. It took approximately 120 CPU seconds in the BNL CDC-7600 computer.

3.2.2 Code Prediction and Comparison with Data

Figure 3.2.1 shows the RELAP5/MOD1 prediction for the area-averaged axial void fraction distribution along with the data and the prediction of TRAC-PD2. Since RELAP5 does not have a subcooled boiling model, the void fraction prediction is poor in the lower part of the bundle. Moreover, vapor generation in RELAP5 is assumed to begin at a certain liquid superheat. This assumption, appropriate for the flashing phenomenon, is not valid for flows in heated channels where subcooled boiling can occur.

In the upper part of the bundle where bulk boiling occurs, the code predicted slightly lower values of void fraction than the data. This, along with the fact that the bulk boiling was computed to occur at essentially saturated conditions implies that the interfacial shear was underpredicted by the code. This led to a higher relative velocity and consequently a lower void fraction in the upper part of the bundle.

3.2.3 Discussion

Since RELAP5/MOD1 does not include a subcooled boiling model, it was not surprising to see a poor agreement between the measured and the predicted values of area-averaged void fraction at the lower part of the bundle. The model recommended for the future versions of TRAC (Saha, 1981) may also be used in the future versions of RELAP5.

The discrepancy in the upper part of the bundle is most probably due to the interfacial shear correlations used in the RELAP5/MOD1 code. Simulation of more experiments is needed to determine if the interfacial shear package of RELAP5/MOD1 should be modified.

3.2.4 Conclusions

The following conclusions may be drawn from the simulation of FRIGG Test 313020 with the RELAP5/MOD1 code:

a) A subcooled boiling model should be included in RELAP5/MOD1 if the code is to be used to accurately calculate the two-phase mixture behavior in heated channels.

b) The interfacial shear package of RELAP5/MOD1 may need modifications to be able to predict the void fraction in the bulk boiling regime more accurately. However, more simulations should be carried out first to determine this need.

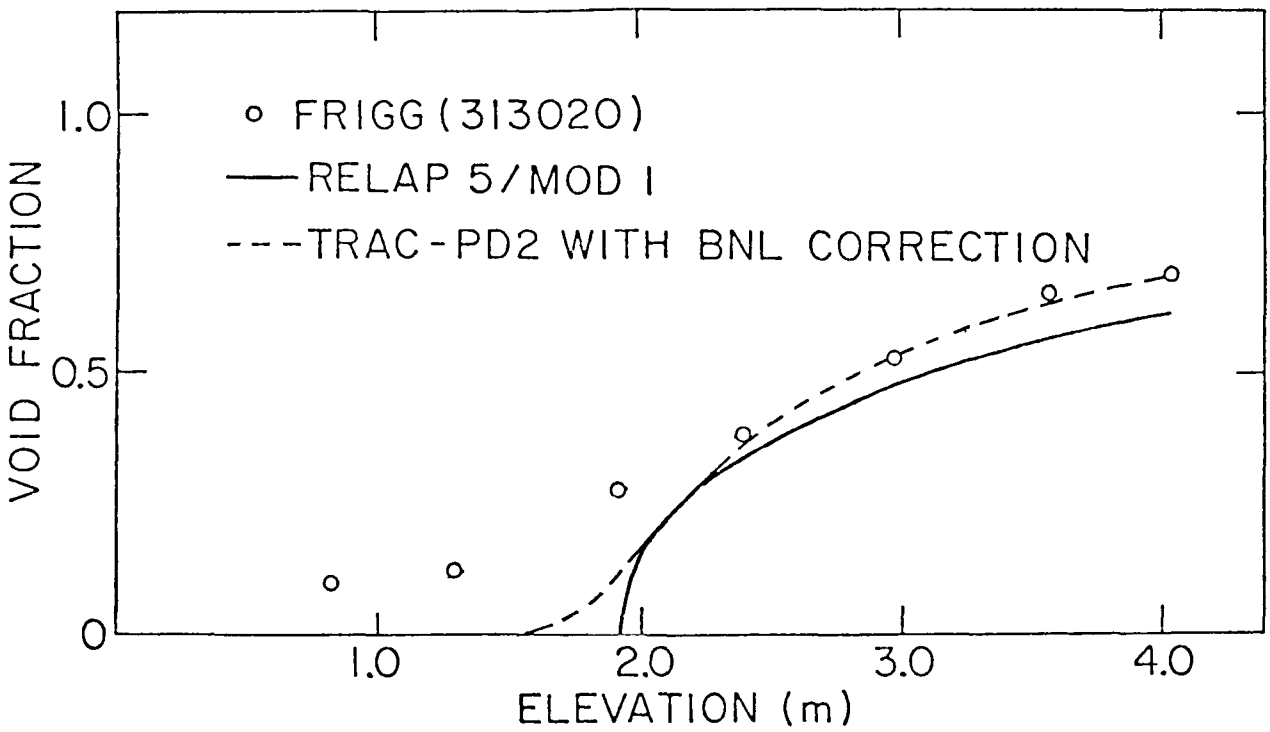

Figure 3.2.1 Comparison Between the Computed and Measured Area-Averaged Axial Void Distribution for the FRIGG-Loop Test 313020. (BNL Neg. No. 7-754-81)

3.3 B&W Steam Generator Test

3.3.1 RELAP5/MOD1 Input Model Description

The test series 74-75-76 for B&W IEOTSG (Loudin, 1976) were simulated by RELAP5/MOD1 (Cycle 1) using two PIPE components, one to represent the primary and the other to represent the secondary side of the model steam generator, HEAT STRUCTURE to represent the tube wall, and TIME DEPENDENT VOLUMES and JUNCTIONS to provide the appropriate boundary conditions. Identical boundary conditions as in the TRAC-PD2 calculation discussed in Section 2.8 were used. The flow rates and temperatures at the inlets and pressures at the exits were specified for both the primary and secondary sides.

As in the TRAC-PD2 simulation, the number of active nodes in each side of the steam generator were varied from 10 to 20 to 40. Four radial nodes were used for the heat conduction calculation.

The computer time for the calculation was approximately half of that of the TRAC-PD2 calculation for the same number of nodes as shown in Table 3.3.1. As the number of nodes increased the calculation time increased more than linearly. The same trend was observed in the TRAC-PD2 calculation.

Table 3.3.1 Summary of Computer Time for RELAP5/MOD1 Calculation of B&W Steam Generator Test

Series No.	No. of Cells	Steady State		Transient	
		Problem Time (s)	CPU Time (s)	Problem Time (s)	CPU Time (s)
74-75-76	10	60	10	50	10
	20	60	20	50	20
	40	60	80	50	55

3.3.2 Code Prediction and Comparison with Data

Figures 3.3.1(a) through 3.3.1(c) show the RELAP5 calculation results along with the data. The vertical scales are withheld because the data are B&W proprietary. These results indicate similar oscillations observed in the TRAC-PD2 calculation, but with a somewhat different trend.

While the accuracy, i.e., the agreement with the data, was improved as the number of nodes was increased, the magnitude of oscillation did not decrease with the increasing number of nodes as in TRAC-PD2. In some cases the magnitude of the oscillations became larger as the number of nodes were increased, which is a disturbing trend. Generally the agreement with the data was poorer in the calculations done with 10 or 20 nodes when compared with the corresponding TRAC-PD2 calculations. However, the results, with the exception of oscillations, improved significantly in the 40-node calculation.

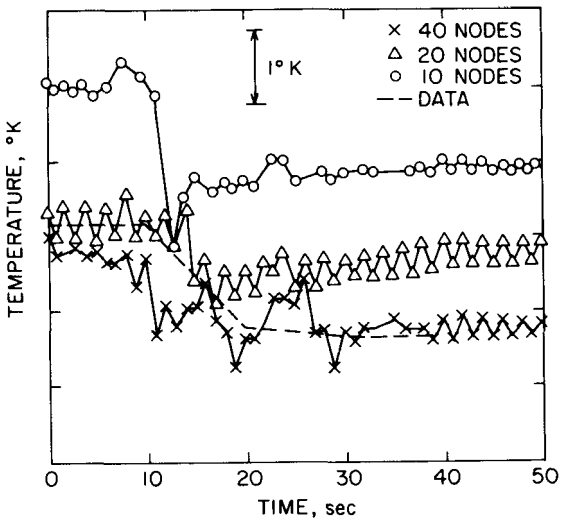

(a) Primary Side Exit Water Temperature vs Time. (BNL Neg. No. 7-582-81)

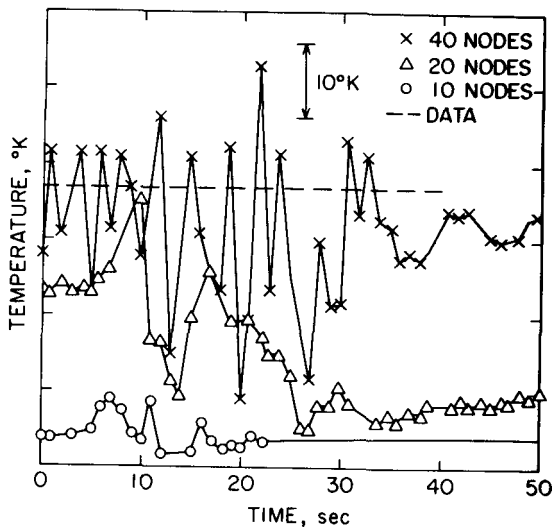

(b) Secondary Side Exit Steam Temperature vs. Time. (BNL Neg. No. 7-575-81)

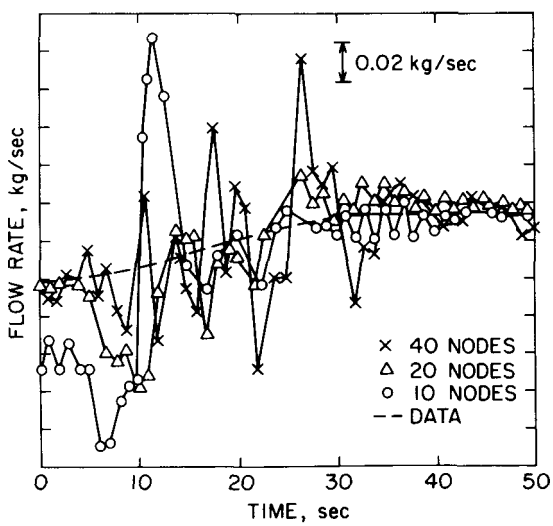

(c) Secondary Side Exit Steam Flow Rate vs. Time. (BNL Neg. No. 7-583-81)

Figure 3.3.1 Comparison Between the Data and the RELAP5/MOD1 Predictions for Test Series 74-75-76.

In the calculations using 10 or 20 nodes, even the prediction for steady-state and, in particular, the secondary-side steam temperature, was in poor agreement with the data. It seems that the oscillation was caused by the fluctuations in the heat transfer calculations as in the TRAC calculations. However, it is not clear why the magnitude of oscillations for some parameters, e.g., steam temperature, increased with an increase of the number of nodes.

3.3.3 Discussion

The results indicate that RELAP5/MOD1 can simulate the trend of the steam generator behavior for load change transients. However, it required 40 nodes in each side for a reasonable accuracy, but still showed substantial oscillations. The cause of the oscillations and the possible courses of action are the same as indicated in Section 2.8.5.

3.3.4 Conclusions

The following conclusions may be drawn from the simulation of the B&W steam generator test with RELAP5/MOD1:

a) The code can predict the trends during the load following transients. The average value of the prediction improves as a finer nodalization is used.

b) Significant oscillations may be expected in RELAP5 calculations even with a fine nodalization. This problem should be resolved by the code developers. Possible courses of action have been suggested in Section 2.8.5.

4. SUMMARY AND CONCLUSIONS

A large variety of separate-effects and basic thermohydraulic tests have been simulated at BNL with the TRAC-PD2 code in FY 1981. These include experiments dealing with (i) steady-state and transient critical flow, (ii) level swell during depressurization, (iii) countercurrent flow limitation (CCFL) and entrainment, (iv) flow boiling in a heated rod bundle, (v) integral economizer once-through steam generator (IEOTSG) performance during load changes, (vi) bottom reflood, and (vii) two-dimensional phase separation of two-phase mixtures. In addition, the early part of an overcooling transient which occurred at the Rancho Seco nuclear power plant on March 20, 1978 was also simulated with an updated version of TRAC-PD2.

In general, TRAC-PD2 behaved more smoothly than its predecessor, TRAC-P1A. In several cases where TRAC-P1A had failed to reach a steady-state, TRAC-PD2 was able to yield at least a near steady-state solution. Only the RPI phase separation test with high inlet quality was an exception. In addition, for the cases where one-to-one comparisons between the TRAC-P1A and TRAC-PD2 predictions were performed, the TRAC-PD2 code was generally found to yield slightly better results than TRAC-P1A. Therefore, TRAC-PD2 is a definite improvement over the TRAC-P1A code.

The RELAP5/MOD1 (cycle 1) code, on the other hand, received only a limited review at BNL during FY 1981. Experiments dealing with (i) transient critical flow, (ii) flow boiling in a heated rod bundle, and (iii) steam generator (IEOTSG) performance during load change, were simulated with this code. The results were comparable to the TRAC-PD2 results, and no clear technical superiority of either code emerged. The computer running times for the two codes were also comparable (see Table 4.1). Further assessment of RELAP5/MOD1 is, of course, needed.

The major conclusions drawn from the BNL assessment calculations are listed below. They are arranged according to the phenomenon studied.

a) Critical Flow: TRAC-PD2, in general, underpredicts the critical flow rate when a subcooled liquid condition exists upstream of a nozzle or pipe. RELAP5/MOD1 appears to do slightly better in a similar situation.

b) Level Swell: TRAC-PD2 appears to overpredict the rate of level swell during a depressurization. Lack of a flashing delay model, along with a possibly higher interfacial shear, is believed to be the reason. (RELAP5/MOD1 was not applied to similar situations).

c) CCFL and Entrainment: TRAC-PD2 appears to underpredict the gas velocity at the onset of entrainment, and overpredict the entrainment ratio. As a result the gas velocity at the flooding onset is underpredicted by TRAC-PD2. (RELAP5/MOD1 was not applied to similar situations.)

TABLE 4.1. Comparison of TRAC-PD2 and RELAP5/MOD1 Computer Running Times

Transient Test	Ratio of CPU to Problem Time	
	TRAC-PD2	RELAP5/MOD1
1. Marviken CFT 24	3.84[a]	2.88[b] 23.90[c]
2. B&W Steam Generator Generator Test 74-75-76 (40 cells in each side of steam generator)	2.60[d]	1.10[d]
	CPU Time (s)	
Steady-State Test	TRAC-PD2	RELAP5/MOD1
1. FRIGG Test 313020 (23 cells)	50[e]	115[f]

(a) 40 cells in the nozzle; transient was run up to 70 seconds.
(b) 1 cell in the nozzle; transient was run up to 60 seconds.
(c) 2 cells in the nozzle; transient was run up to 10.5 seconds.
(d) Based on 50 seconds of transient.
(e) Took 2.7 seconds of real time to reach the steady-state.
(f) Took 38.2 seconds of real time to reach the steady-state.

5.3 Recommendations for Future Code Assessment

The code assessment activity in the past has concentrated on simulating tests pertinent to the large break loss-of-coolant accident (LBLOCA). Assessment of future versions of TRAC-PWR (starting with TRAC-PF1) and RELAP5 should continue with some of these tests until the questions raised during the present assessment are resolved satisfactorily. Examples of such separate-effects tests are:

a) Subcooled critical flow tests, i.e., Marviken, CANON, Super-CANON, Moby-Dick, Super Moby-Dick, BNL nozzle tests.

b) CCFL and entrainment tests, such as University of Houston and Dartmouth College tests.

c) Reflood tests, such as FLECHT-SEASET, CCTF, and NRU tests.

However, more emphasis should be given to the tests dealing with phenomena pertinent to the small break loss-of-coolant accident (SBLOCA) and plant transients. Examples of separate-effects tests that should be simulated are:

a) Boil-off tests conducted in THTF, FLECHT-SEASET, TLTA, etc.

b) Level swell tests such as GE large and small vessel, Battelle-Frankfurt, THETIS, etc.

c) Steam generator tests, i.e., B&W and FLECHT-SEASET tests.

d) Safety and relief valve tests, i.e, KWU, CE/EPRI, NPETC (Japan) tests.

e) Two-phase pump tests, i.e., CE/EPRI, INEL, B&W, LOBI tests.

f) Two-phase natural circulation tests, i.e., FRIGG, PKL, Semiscale, FLECHT-SEASET tests.

In addition, the integral tests conducted in LOFT, Semiscale, LOBI, etc. should continue to be simulated. Efforts should be made to include the full-scale plant tests and actual transients in the overall assessment matrix. However, only the tests or transients with known boundary conditions should be considered. Otherwise, the code assessment activity would degenerate to a code "tune-up" exercise.

Finally, the overall code assessment activity should include an independent assessment of the numerical technique(s) used in the codes. Attempts should be made to determine and recommend the "optimum" nodalization for a given phenomenon or accident sequence. And, last but not the least, a code acceptance criterion should be developed.

6. REFERENCES

Abuaf, N., et al.,(1981), "A Study of Nonequilibrium Flashing of Water in a Converging-Diverging Nozzle," NUREG/CR-1864, BNL-NUREG-51317, June 1981.

Bharathan, D.,(1979), "Air-Water Countercurrent Annular Flow," EPRI NP-1165, September 1979.

Crowell, K. R., (1980), "Preliminary Two-Fluid Viscous Stress, Reynolds Stress, and Turbulent Heat Flux Models for COBRA-TF," Battelle Pacific Northwest Laboratory Report FATE-80-115, December 1980.

Dukler, A.E., and Smith, L., (1979), "Two-Phase Interactions in Counter-Current Flow: Studies of the Flooding Mechanism," NUREG/CR-0617, January 1979.

Ericson, L., et al., (1979), "Marviken Critical Flow Tests," Joint Reactor Safety Experiments in Marviken Power Stations, MXC-224, September 1979.

Hochreiter, L.E., et al., (1978), "PWR FLECHT-SEASET Unblocked Bundle, Forced and Gravity Reflood Task: Task Plan Report," NRC/EPRI/Westinghouse Report No. 3, March 1978.

Holzer, B., et al., (1977), "Specification of OECD Standard Problem No. 6: Determination of Water Level and Phase Separation Effects during the Initial Blowdown Phase," Battelle-Institute of Frankfurt (Main) Report, February 1977.

Ishii, M., and Grolmes, M.A., (1975), "Inception Criteria for Droplet Entrainment in Two-Phase Concurrent Film Flow," AIChE Journal, Vol. 21, pp. 308-318, 1975.

Ishii, M., and Mishima, K., (1981),"Correlation for Liquid Entrainment in Annular Two-Phase Flow of Low Viscous Fluid," ANL/RAS/LWR 81-2, March 1981.

Jo, J. H., (1981), "B&W Once-Through Steam Generator Tests," in Safety Research Programs Sponsored by Office of Nuclear Regulatory Research, Quarterly Progress Report, July 1-September 30, 1981, Section 7.1.2., NUREG/CR-2331, BNL- NUREG-51454, Vol. 1, No. 3.

Knight, T.D., et al., (1980),"TRAC-P1A Independent Assessment-1979," Los Alamos National Laboratory Draft Report, 1980.

Lahey, R. T., (1978),"Two-Phase Flow Phenomena in Nuclear Reactor Technology," Quarterly Progress Report 8, March-May 1978, NUREG/CR-0418, 1978.

Liles, D. R., et al, (1981a), "TRAC-PD2: An Advanced Best-Estimate Computer Program for Pressurized Water Reactor Loss-of-Coolant Accident Analysis," NUREG/CR-2054, LA-8709-MS, April 1981.

Liles, D. R., et al., (1981b), "TRAC-PF1: An Advanced Best-Estimate Computer Program for Pressurized Water Reactor Analysis," LANL Draft Report, November 1981.

Lobel, R., (1978),"Summary of Meeting Held at Rancho Seco Nuclear Power Plant on June 10, 1978 to Discuss a Recent Cooldown Event," USNRC Memorandum for Paul S. Check, July 31, 1978.

Loudin, G. W., and Oberjohn, W. J., (1976), "Transient Performance of a Nuclear Integral Economizer Once-Through Steam Generator," Alliance Research Center Report 4679, January 1976.

Minogue, R. B., (1981), "Research Information Letter No. 115; Independent Assessment of TRAC-P1A Computer Code," USNRC Memorandum for Harold R. Denton, February 25, 1981.

Neymotin, L., (1980a), "TRAC-P1A Predictions of the Battelle-Frankfurt Top Blowdown Test," ANS Transactions, Vol. 35, pp. 330-332, November 1980.

Neymotin, L., (1980b), "FRIGG-Loop Forced and Natural Circulation Tests," in Water Reactor Safety Research Division Quarterly Progress Report for January 1 - March 31, 1980, NUREG/CR-1506, BNL-NUREG-51218, Section 4.8, June 1980.

Nylund, O., et al., (1968), "FRIGG Loop Project: Hydrodynamic and Heat Transfer Measurements on a Full-Scale Simulated 36-rod Marviken Fuel Element with Uniform Heat Flux Distribution," FRIGG-2, R4-447/RTL-10007, Sweden, 1968.

Ransom, V. H., et al., (1980), "RELAP5/MOD1 Code Manual," NUREG/CR-1826, EGG-2070, November 1980.

Reocreux, M., (1977), "Contribution to the Study of Critical Flow Rates in Two-Phase Water-Vapor Flow," Translation Series, NUREG-tr-0002, August 1977.

Riegel, B., (1979), "Experience Super-CANON," TT/SETRE/79-2-B/BR, February 1979.

Rohatgi, U. S. and Sanborn, Y., (1980a), "Independent Assessment of TRAC-P1A with Marviken Critical Flow Tests," ANS Transactions, Vol. 35, pp. 304-306, November 1980.

Rohatgi, U. S., (1980b), "University of Houston Counter-Current Flow Test," in Water Reactor Safety Research Division Quarterly Progress Report for April 1-June 30, 1980, NUREG/CR-1618, BNL-NUREG-51255, Section 4.2, August 1980.

Rohatgi, U. S., (1980c), "RPI Phase Separation Tests," in Water Reactor Safety Research Division Quarterly Progress Report for January 1-March 31, 1980, NUREG/CR-1506, BNL-NUREG-51218, Section 4.7, June 1980.

Rohatgi, U. S., Jo, J., and Neymotin, L., (1982), "Constitutive Relations in TRAC-PD2," BNL-NUREG Report, in press.

Rousseau, J. C., et al., (1976),"Void Fraction Measurements during Blowdown by Neutron Absorption or Scattering Methods," Paper presented at the OECD/NEA/-CSNI Specialist's Meeting on Transient Two-Phase Flow, Toronto, Canada, August 1976.

Saha, P., (1979), "Moby-Dick Steam-Water Experiments," in Water Reactor Safety Research Division Quarterly Proress Report for April 1-June 30, 1979, NUREG/CR-1035, BNL-NUREG-51081, Section 3.2, September 1979.

Saha, P. and Sanborn, Y., (1980), "Independent Assessment of TRAC-P1A with Super-CANON Blowdown Tests," ANS Transactions, Vol. 35, pp. 306-307, November 1980.

Saha, P., (1981), "A Simple Subcoled Boiling Model," ANS Transactions, Vol. 39, pp. 1058-1060, November-December 1981.

SMUD (Sacramento Municipal Utility District), (1971), Rancho Seco Nuclear Generating Station Final Safety Analysis Report, May 1971.

Taylor, M. A., (1980), "Insights on Overcooling Transients in Plants with the B&W NSSS," USNRC Memorandum for S. Fabic, October 29, 1980.

Thurgood, M. J., et al., (1981), "COBRA-TF Equations and Constitutive Models," Battelle Pacific Northwest Laboratory Report FATE-81-16, June 1981.

Van der Welle, R., (1981), "A Numerical Procedure for Vertical One-Dimensional Two-Phase Flow," Nuclear Engineering and Design, Vol. 65, pp. 113-130, 1981.

Wallis, G. B., (1970), "Annular Two-Phase Flow, Part 1, A Simple Theory," Journal of Basic Engineering, ASME, Vol. 92, pp. 59-72, March 1970.

DISTRIBUTION

USNRC

O. E. Bassett
J. Guttmann
C. Kelber
W. C. Lyon
R. B. Minogue
F. Odar
D. F. Ross
B. Sheron
L. M. Shotkin
L. H. Sullivan
L. S. Tong
N. Zuber

BNL

W. Y. Kato
H. J. C. Kouts
DNE Associate Chairmen
NSP Division Heads & Group Leaders
LWR CAAG Personnel
Nuclear Safety Library (2)

External

J. Jackson, LANL
D. R. Liles, LANL
T. D. Knight, LANL

F. Aguilar, INEL
V. H. Ransom, INEL
T. R. Charlton, INEL
A. C. Peterson, INEL

D. Majumdar, DOE/Idaho

M. Ishii, ANL

S. Thompson, SNL

B. S. Shiralkar, GE

L. Agee, EPRI
R. B. Duffy, EPRI
G. S. Lellouche, EPRI
W. B. Loewenstein, EPRI
G. S. Srikantiah, EPRI

R. T. Fernandez, YAEC

I. Brittain, Winfrith (U. K.)